Pergamon

Prog. Part. Nucl. Phys., Vol. 35, pp. 423–503, 1995

0146–6410/95 $29.00

0146-6410(95)00045-3

Enhancement of Parity and Time-Invariance Violating Effects in Compound Nuclei

V. V. FLAMBAUM and G. F. GRIBAKIN

School of Physics, University of New South Wales, Sydney 2052, NSW, Australia

ABSTRACT

Effects of weak interactions: parity nonconservation and time-invariance violation, can be enhanced up to 10^6 times in compound nuclei. This factor is produced by (i) "simple" kinematical enhancement (ratio of the s-wave to the p-wave neutron capture amplitudes), and (ii) very large density of compound resonances (dynamical enhancement). The latter phenomenon should be generic to many complex many-body systems (rare-earth atoms, atomic clusters, quantum dots in solids, etc.), and is strongly related to the problem of quantum chaos. This review is devoted to the theoretical aspects of the problem. Statistical theory is used to calculate the r.m.s. value and the distribution of matrix elements of the weak perturbations between compound states. The behaviour of effects upon averaging over many compound resonances is studied. It is shown that the effects, though of random sign, are not suppressed by such averaging. Valence mechanism, rotational doublet states, doorway states are considered as possible sources of regular contributions to the effect. The renormalization of weak interaction by the strong interaction and its relation to the problem of π-mesons in nuclear matter is discussed.

KEYWORDS

Weak interactions, parity nonconservation, compound nuclei, quantum chaos.

Contents

1 Introduction

Huge enhancement of parity nonconserving effects (as well as any weak interaction) in compound nuclei is a remarkable physical phenomenon. It contains a number of different physical aspects in it. First of all, these effects are produced by the fundamental weak interactions, and thus can be viewed as a probe for their investigation. Secondly, this phenomenon is strongly influenced by the nuclear dynamics. So, the measured effects reveal details of the nuclear structure and the role of the strong interaction, which renormalizes the weak interaction in the nuclear matter. Thirdly, measuring weak interaction effects in the region of compound resonances one encounters the problem of quantum chaos: the nuclear spectrum and the structure of nuclear eigenstates are chaotic, and the system itself gives a particular example of the generic quantum chaotic system.

Therefore, the study of effects produced by the weak interaction in compound nuclei contributes to several areas of physics. On the other hand, the complexity of the problem makes interpretation of experimental data and the process of extracting basic information from the results of measurements very difficult. There is a great demand for a theory which could describe different aspects of the problem (weak, nuclear, chaotic). This makes the whole problem very challenging for theorists. Even the most precise experimental data cannot be fully appreciated and used without a good and reliable theory (which in case of "chaotic" states should be a statistical theory).

The relative strength of the parity nonconserving (PNC) weak interaction in nuclei (the ratio of the weak to the strong interaction) can be estimated as

$$F \sim Gm_\pi^2 = 2 \times 10^{-7}, \tag{1}$$

where G is the Fermi constant and m_π is the π-meson mass. Accordingly, the estimates of effects in neutron optics made in the pioneering works of Michel (1964), Stodolsky (1974), Karl and Tadic (1977), and others were very small. However, in 1980 it was suggested (Sushkov and Flambaum 1980) that in heavy nuclei one can observe PNC effects enhanced up to 10^6 times, i.e., at a level of about 10% (see also Karmanov and Lobov 1969, Lobov 1970, Forte 1978, Stodolsky 1980, Sushkov and Flambaum 1982, Bunakov and Gudkov 1981, 1983). There are two main factors of enhancement of PNC effects in nuclei, which give roughly equal contributions ($\sim 10^3$) to the total enhancement factor. The first one (*kinematical*) results from admixing large amplitudes to the small ones by means of the weak interaction (e.g., the s-wave to the p-wave in neutron capture). The second factor (*dynamical*, or *statistical*) arises due to a high level density of compound states, which provides mixing of opposite parity levels at very small energy separations. To estimate this enhancement factor accurately one has to evaluate the weak interaction matrix element coupling these states. The latter is noticeably suppressed because of a complex structure of the compound states, which makes the dynamical enhancement proportional to $D^{-1/2}$ rather than D^{-1}, where D is the mean level spacing (Haas *et al* 1959, Blin-Stoyle 1960, Shapiro 1968). In some cases, such as PNC effects in nuclear fission and some effects in the (n, γ) reaction, there can be another, resonance enhancement up to D/Γ times, where Γ is the compound state width. Dynamical enhancement must be a general feature in various many-body systems with dense spectra and complex eigenstates (nuclei, rare-earth atoms, molecules, clusters, quantum dots in solids, etc.). One may consider this enhancement as a manifestation, or a signature of quantum chaos in a system.

It can be compared with the known enhancement of perturbations in classical chaotic systems, which results from exponential divergence of trajectories. Besides PNC effects, the two factors (kinematical and dynamical) enhance time and parity violating (P,T-odd) effects (Kabir 1982, Stodolsky 1982, Bunakov and Gudkov 1983). Note that there could be also T-odd P-even effects. The possibility of their enhancement was considered by Ericson (1966), Mahaux and Weidenmüller (1966), Moldauer (1968) [see also detailed calculations by French *et al* 1988, Bunakov *et al* 1990, and the books Tests of Time Reversal Invariance in Neutron Physics (1987) and Time Reversal Invariance and Parity Violation in Neutron Reactions (1994) for more recent developments]. The physics of these effects is quite different and we do not consider them in the present review.

At present there is a large amount of experimental data on various PNC effects in nuclei. Values of $\sim 10^{-4} - 10^{-3}$ were obtained for the asymmetry of γ quanta emission with respect to the neutron spin in the (n,γ) reaction (Abov and Krupchitskii 1976, Benkoula *et al* 1977) ($\mathbf{k}_\gamma \cdot \boldsymbol{\sigma}$ correlation, where $\mathbf{k}_\gamma$ is the momentum of the γ-quantum, and $\boldsymbol{\sigma}$ is the neutron spin). There were also measurements of the circular polarization of γ-quanta in reactions with unpolarized nuclei. Among the most surprising results was the discovery of large ($\sim 10^{-4}$) PNC effects in nuclear fission by polarized neutrons (Danilyan *et al* 1977, Vodennikov *et al* 1978, Andreev *et al* 1978, Petukhov *et al* 1979, Vesna *et al* 1980). The correlation measured is $\mathbf{p}_f \cdot \boldsymbol{\sigma}$, where $\mathbf{p}_f$ is the momentum of the light fragment. Forte *et al* (1980) measured the PNC rotation of neutron spin by unpolarised nuclei. The record values of PNC effects have been observed in polarized neutron capture. The relative difference of the cross sections for neutrons with positive and negative helicities ($\mathbf{k} \cdot \boldsymbol{\sigma}$ correlation; $\mathbf{k}$ is the neutron momentum) is $10^{-2} - 10^{-1}$ (Alfimenkov *et al* 1981, 1983, Alfimenkov 1984, Masuda *et al* 1989, Bowman *et al* 1990, Frankle *et al* 1991). All these effects are orders of magnitude greater than the relative strength of the original PNC weak interaction (1). Therefore, predictions of very strong enhancement have been confirmed experimentally. Experimental details can be found in numerous reviews, Bowman *et al* 1993 being the most recent one, and we do not consider any particular experiments in the present work.

The aim of this review is to consider mechanisms of enhancement of PNC effects in compound nuclei at all levels, starting from the nucleon-nucleon weak interaction. Recent experiments by the TRIPLE collaboration (Bowman *et al* 1990, Frankle *et al* 1991) started a systematic study of PNC effects for large sequences of resonances in several nuclei, and measured the root-mean-squared (r.m.s.) values of the weak interaction matrix elements between compound states. On the other hand a considerable progress has been made towards a theory incorporating both dynamical and statistical aspects of the problem of the weak interactions in compound nuclei. This enables one to compare experimental data with the theory and extract the strength of the weak interaction in nuclei.

The review has the following structure. We start from a qualitative consideration of enhancement mechanisms in neutron reactions. In the next section we consider a statistical theory of matrix elements of weak perturbations between compound states, and test this approach with results of numerical experiments on chaotic many-body systems: the atom of Ce and nuclear shell models. Then we consider dynamical aspects of the problem: the renormalization of the weak interaction by the residual strong interaction, which leads to $A^{1/3}$ enhancement of the residual two-body weak interaction between valence nucleons and increases (by a factor of ~ 1.4) the strength of the one-body weak potential of the nucleus.

It is interesting that this problem turns out to be related to the old problems of π-meson behaviour in nuclei (π condensation, etc.) and collective 0^- resonances. Comparison of the theory with experiments yields the strength constant of the weak interaction in nuclei. Its value is in agreement with estimates based on the standard electroweak model and QCD. A surprising result of the TRIPLE collaboration (all 7 statistically significant values of the PNC effect in neutron capture by Th turned out to be positive) initiated the search for regular, non-random mechanisms of enhancement. These mechanisms are critically analysed in sec. 3. In sec. 4 the statistical properties of PNC effects are considered. Surprisingly, some of the PNC and P,T-odd effects in compound nuclei are not necessarily suppressed after averaging over many resonances in spite of their random-sign nature. This result means that one does not need to resolve particular compound resonances to measure large effects, and measurements at higher energies are possible. This possibility can stimulate a new class of experiments in nuclei, as well as in molecules, atomic clusters, chemical reactions, etc. This can be a new approach to the famous problem of asymmetry of biological molecules. An interesting question follows: Is there a limit for enhancement?

1.1 Origin of the Enhancement and Estimates of PNC Effects in Neutron Capture

Let us start off with one of the most impressive and simple examples of PNC effects: the spin asymmetry in neutron capture. The quantity determined experimentally is the relative difference of the cross sections of capture into a p resonance for neutrons with positive and negative helicities:

$$P = \frac{\sigma_p^+ - \sigma_p^-}{\sigma_p^+ + \sigma_p^-} \,. \tag{2}$$

It has been predicted (Flambaum and Sushkov 1980a) and observed experimentally for a number of nuclei [^{81}Br, ^{111}Cd, ^{117}Sn, ^{139}La, ^{238}U and ^{232}Th (Alfimenkov *et al* 1983, Masuda *et al* 1989, Bowman *et al* 1990, Frankle *et al* 1991)] that at neutron energies of 1–100 eV the magnitude of the asymmetry (2) in p resonances reaches 10^{-2}–10^{-1}. One can compare these values with PNC effects in the low-energy p-p and p-α scattering, which are about 3×10^{-7}.

Describing the mechanism which produces these large PNC effects it is convenient to consider the simplest case of a spinless target nucleus of positive parity (see Flambaum and Sushkov 1984 and Appendix A for the general case). Suppose that this nucleus can capture neutrons into a negative parity compound state of spin 1/2. This may happen if the neutron is in the $p_{1/2}$ wave. However, due to the weak interaction the negative parity compound state contains an admixture of positive parity states:

$$|1/2^-\rangle + \sum_\nu \frac{|1/2^+\nu\rangle\langle 1/2^+\nu|W|1/2^-\rangle}{E_- - E_\nu} = |1/2^-\rangle + i\sum_\nu \eta_\nu |1/2^+\nu\rangle \,, \tag{3}$$

where

$$\eta_\nu = \frac{\langle 1/2^+\nu|W|1/2^-\rangle}{i(E_- - E_\nu)} \tag{4}$$

is real, if the state widths are neglected, and i is introduced because the matrix element of the weak interaction W is imaginary for the standard definition of the angular wave functions. The sum in (3) allows neutron capture in the s wave. Let us now consider the wave function of a slow neutron with

momentum k and expand it in terms of the $|ljj_z\rangle$ states with definite angular momentum and helicity (the z axis is along k):

$$e^{i\mathbf{kr}}\chi_\pm \simeq (1+i\mathbf{kr})\chi_\pm = \sqrt{4\pi}\left[Y_{00}(\mathbf{n}) + i\frac{kr}{\sqrt{3}}Y_{10}(\mathbf{n})\right]\chi_\pm$$
$$= \sqrt{4\pi}\left(|0,1/2,\pm 1/2\rangle \mp i\frac{kr}{3}|1,1/2,\pm 1/2\rangle + i\frac{kr\sqrt{2}}{3}|1,3/2,\pm 1/2\rangle\right) , \qquad (5)$$

where $\chi_\pm$ is the spin function. The amplitude of neutron capture from (5) to the state (3) can be written as follows:

$$T = \pm T_p + \sum_\nu \eta_\nu T_{s,\nu}, \qquad (6)$$

where T_p and $T_{s,\nu}$ are the amplitudes of neutron capture from the p and s waves into the $|1/2^-\rangle$ and $|1/2^+\nu\rangle$ states respectively, and the $\pm$ sign corresponds to the capture of neutrons with positive or negative helicity. The interference between the p and s capture amplitudes in (6) results in the difference between the cross sections for different helicities:

$$\sigma_p^\pm \propto |\pm T_p + \sum_\nu \eta_\nu T_{s,\nu}|^2 \simeq T_p^2 \pm 2T_p \sum_\nu \eta_\nu T_{s,\nu} , \qquad (7)$$

and yields the following expression for the spin asymmetry (2):

$$P = 2\sum_\nu \frac{T_{s,\nu}}{T_p}\eta_\nu = 2\sum_\nu \sqrt{\frac{\Gamma_{s,\nu}^{(n)}}{\Gamma_p^{(n)}}}\frac{\langle 1/2^+\nu|W|1/2^-\rangle}{i(E_- - E_\nu)} , \qquad (8)$$

where the neutron widths $\Gamma_{s,\nu}^{(n)} \propto T_{s,\nu}^2$ and $\Gamma_p^{(n)} \propto T_p^2$ must be evaluated at the energy of the p-resonance ($|1/2^-\rangle$ state).

Equation (8) clearly demonstrates the existence of the two enhancement factors mentioned above. The first of them is given by the ratio between the s- and p-wave capture amplitudes. In the neutron energy range of 1–100 eV it yields [note the kr factor before the p-wave component in (5)]:

$$\frac{T_s}{T_p} = \sqrt{\frac{\Gamma_s^{(n)}}{\Gamma_p^{(n)}}} \sim \frac{1}{kR} \sim 10^3\text{–}10^2 , \qquad (9)$$

where R is the radius of the nucleus. Equation (9) estimates the kinematical enhancement in neutron capture.

The second factor comes from the ratio η (4) of the weak interaction matrix element coupling the two compound states to the energy difference between them. Let us note that in the absence of a dense spectrum of compound states this mixing is given by the relative strength of the weak interaction in nuclei F (1). This value times the kinematical enhancement factor (9) estimates the role of the so called *valence mechanism* to the PNC effect in neutron capture (see sec. 3.1). This mechanism can provide a regular sign parity-violating contribution, however its magnitude is about $10^2 - 10^3$ times smaller than those measured in experiments.

On the other hand, owing to a very complicated structure of compound states their mixing is of almost random character, and the items of the sum (8) give uncorrelated contributions to it. Since the contributions of several nearest levels are important, the energy denominator in η is of the order of the mean level spacing D between the states of the same angular momentum and parity ($D \sim$ 1–100 eV).

The matrix element $\langle 1/2^+\nu|W|1/2^-\rangle$ contains the wave functions of compound states Ψ_c ($\Psi_c = |1/2^-\rangle$, or $|1/2^+\nu\rangle$). Each of them is a superposition of a very large number of simple basic states Φ_i, which can be chosen as products of particle-hole excitations above the ground state of the nucleus:

$$\Psi_c = \sum_i C_i \Phi_i \ , \tag{10}$$

with a normalization condition $\sum_i C_i^2 = 1$. The residual strong interaction mixes the basis states strongly within some characteristic energy interval $\Gamma_{\rm spr} \sim$ MeV, so that the number N of *principal* components, i.e., those giving the main contribution to the sum (10) and to the normalization condition, can be estimated as

$$N \sim \frac{\Gamma_{\rm spr}}{D} \sim 10^4 - 10^6 \ . \tag{11}$$

Since mixing of the basis states within $\Gamma_{\rm spr}$ range is almost complete, the contribution of a principal component to (10) is estimated as $C_i \sim 1/\sqrt{N}$. By the same token each of the principal components noticeably "participates" in about N compound states spread over the $\Gamma_{\rm spr}$ interval.

The matrix element between two compound states is

$$\langle \Psi_1|W|\Psi_2\rangle = \sum_{ij} C_i^{(1)} C_j^{(2)} \langle \Phi_i|W|\Phi_j\rangle \ . \tag{12}$$

Suppose W is a single-particle operator $W = \sum_{\alpha\beta}\langle\alpha|W|\beta\rangle a_\alpha^\dagger a_\beta$ where α, β are the single-particle states, and $a^\dagger, a$ are the creation-annihilation operators. For given α and β the matrix element $\langle \Phi_i|W|\Phi_j\rangle$ is not zero if Φ_i and Φ_j differ by the state of one particle only: $|\Phi_i\rangle = a_\alpha^\dagger a_\beta|\Phi_j\rangle$. Thus, if, say, i is fixed there is only a small number q ($q \sim$ 1–10) of different j contributing to the sum (12). Therefore the sum contains $\sim qN$ nonzero items. Their typical magnitude is

$$C_i C_j \langle \Phi_i|W|\Phi_j\rangle \sim \frac{1}{\sqrt{N}}\frac{1}{\sqrt{N}} W \ ,$$

where W is a typical single-particle matrix element. Since different items in (12) are incoherent, the total can be estimated as $\sqrt{qN}$ times each item:

$$W_{12} \equiv \langle \Psi_1|W|\Psi_2\rangle \sim \frac{1}{\sqrt{N}}\frac{1}{\sqrt{N}} W \sqrt{qN} = W\sqrt{\frac{q}{N}} \ . \tag{13}$$

Therefore, the matrix element between the compound states is suppressed by the $1/\sqrt{N}$ factor with respect to the single-particle matrix element. It is easy to see that estimate (13) is also true for a matrix element between a compound and a "regular" state, containing some small number of components Φ_i. In the general case one should use $N = \max\{N_1, N_2\}$ in (13), where $N_{1,2}$ are the numbers of principal components in the $\Psi_{1,2}$ states.

The mixing η of the two nearby compound states is given by

$$\eta_{12} \sim \frac{W_{12}}{E_1 - E_2} \sim W\sqrt{\frac{q}{N}}\,\frac{1}{D} \sim W\sqrt{\frac{q}{N}}\,\frac{N}{\Gamma_{\rm spr}} \sim \frac{W\sqrt{q}}{\Gamma_{\rm spr}}\sqrt{N} \ . \tag{14}$$

Thus, the dynamical enhancement factor produced by mixing of compound states is $\sqrt{N}$, and its magnitude can be about 10^2–10^3. The idea of this enhancement was first suggested by Haas *et al* (1959)

and discussed by Blin-Stoyle (1960), Shapiro (1969), Sushkov and Flambaum (1982), Kadmensky *et al* (1983), Flambaum and Sushkov (1984).

We must say that the real situation is more complicated, and (13) slightly overestimates the weak interaction matrix element between the compound states. The point is that the PNC interaction W induces transitions between single-particle states of equal angular momentum and opposite parity. These states usually belong to different nuclear shells and are separated by the energy interval $\Delta E = \omega_0 \sim$ 5–10 MeV $> \Gamma_{\rm spr}$. This means that the matrix element of W between the principal components Φ_i and Φ_j of the close-lying compound states is zero (Zaretsky and Sirotkin 1983, 1987, Kadmensky *et al* 1983) and we have to take into account the contribution of distant components to the compound states. The perturbation-theory estimate tells one that this contribution is suppressed by a factor of $\Gamma_{\rm spr}/\Delta E$, since $\Gamma_{\rm spr}$ characterises the strength of the residual strong interaction in the system. Thus, instead of (13) we obtain

$$W_{12} \sim W\sqrt{\frac{q}{N}}\,\frac{\Gamma_{\rm spr}}{\Delta E}\,,$$

and the mixing of the nearby compound states by the weak interaction is given by

$$\eta_{12} \sim \frac{W_{12}}{E_1 - E_2} \sim W\sqrt{\frac{q}{N}}\,\frac{N}{\Gamma_{\rm spr}}\,\frac{\Gamma_{\rm spr}}{\Delta E} \sim \frac{W\sqrt{q}}{\Delta E}\,\sqrt{N}. \tag{15}$$

In sec. 2.1 we present an accurate statistical calculation of the matrix element between compound states.

Combining (9) and (15) we obtain the following estimate for the spin asymmetry P of (8):

$$P \sim \frac{T_s}{T_p}\,\frac{\langle 1/2^+|W|1/2^-\rangle}{E_- - E_+} \sim \frac{1}{kR}\,\frac{W\sqrt{q}}{\Delta E}\,\sqrt{N} \sim F \times (10^4 - 10^6)\,, \tag{16}$$

where we put $W/\Delta E \sim F$ as a typical value of the PNC effect in the absence of any enhancement. Therefore, the mechanism of compound state mixing in the p-wave resonance fully accounts for large PNC asymmetries observed in experiments.

1.2 Criteria of Enhancement

Note that a strong residual interaction is necessary to have dynamical enhancement of weak interactions. For example, a dense spectrum of many-body states emerges in the ideal gas of noninteracting particles. However, the energy interval between the states Φ_i and Φ_j which can be mixed by the interaction W is the single-particle interval ΔE (since other particles are "spectators"). We must turn on the residual strong interaction V between the particles, which admixes the distant component Φ_j to the compound state closest to Φ_i, thus making the weak mixing (4) of nearby compound states possible. On the other hand, neither "chaos" nor "ergodicity" of the compound states is necessary to produce certain enhancement. We use these properties to develop a statistical theory and simplify our calculations. However, the enhancement can appear even in the case of a relatively small residual interaction V, or in a system with a sparse spectrum and no chaos. For example, using the perturbation theory in V we can estimate the weak mixing between the nearest compound states as:

$$\frac{\langle\Psi_1|W|\Psi_2\rangle}{E_1 - E_2} \sim \frac{\langle\Psi_1|W|\Phi_j\rangle\langle\Phi_j|V|\tilde{\Psi}_2\rangle}{(E_1 - E_2)(E_2 - E_j)}\,, \tag{17}$$

where $|\tilde{\Psi}_2\rangle$ contains only the principal components of $|\Psi_2\rangle$. If V is stronger than the minimal interval between the opposite parity levels $E_1 - E_2$ we can have some enhancement in comparison with the direct weak mixing of distant states $\langle\Psi_1|W|\Phi_j\rangle/(E_1 - E_j)$. It is known that there is no repulsion between levels of opposite parity. This means that for some fraction of levels one can always have $E_+ - E_- \ll D$, which makes the enhancement possible even for $V \leq D$, when there is no chaos. However, to have enhancement for each level we need $V \gg D$, and consequently a strong mixing of the components and, probably, chaos and ergodicity in the space of N principal components.

There are also more sophisticated conditions of enhancement. For example, to obtain estimate (15) we assumed the Breit-Wigner localisation of the components (the contribution of distant states decreases as $\Gamma_{\rm spr}/\Delta E$). However, in, say, the Band Random Matrix model the localization is exponential, i.e., the admixture of distant components is exponentially small (see Section 2.2). Thus, to ensure sizeable admixtures of distant components their direct mixing to the principal components of compound states by the residual strong interaction V is necessary. We discuss this question in detail in sec. 2.2. One more case with no dynamical enhancement for an arbitrary strong residual interaction is given by a model of Random Separable Interaction. Superlocalization (the number of principal components $N \sim 1$) which takes place in this model is due to strong destructive interference effects (Appendix B).

Besides the capture cross-section asymmetry one can study other PNC effects in neutron optics: the rotation of the polarization plane around the momentum vector of the beam ϕ, or the longitudinal polarization of the initially unpolarized neutron beam a. Analogously to (16) both effects can have very large magnitudes in the vicinity of a p resonance (Sushkov and Flambaum 1980a, 1981a, 1982): $\phi, a \sim (10^{-3}\text{–}10^{-2})l/l_0$, where l is the neutron path in the media, and l_0 is the attenuation length: $l_0 \sim$1–5 cm (of course, one can not have l much greater than l_0). Although, ϕ and a are usually several times smaller than P because of the neutron elastic scattering, which decreases the attenuation length.

1.3 Other Reactions: Radiative Capture, Fission. $\sqrt{N}$ Classification of Amplitudes

The method used in the previous section to estimate the contribution of compound state mixing to the parity-violating neutron capture amplitude can be applied to classify the amplitudes of other processes involving compound states (Flambaum and Sushkov 1984). The chief parameter of this classification is $\sqrt{N} \gg 1$. It allows one to find out dominant reaction mechanisms, and express the relative contributions of different reaction amplitudes in powers of $\sqrt{N}$.

Besides the matrix elements, the expressions for reaction amplitudes contain energy denominators $E - E_c + \frac{i}{2}\Gamma_c$, where E_c and Γ_c is the energy and width of a compound state. These denominators are N times smaller than the typical single-particle energy $\Delta E \sim \omega_0 \sim \Gamma_{\rm spr} \sim$ MeV:

$$\frac{1}{E - E_c + \frac{i}{2}\Gamma_c} = \frac{\Gamma_{\rm spr}}{D}\,\frac{D}{E - E_c + \frac{i}{2}\Gamma_c}\,\frac{1}{\Gamma_{\rm spr}} \sim N\frac{D}{E - E_c + \frac{i}{2}\Gamma_c}\,\frac{1}{\Gamma_{\rm spr}}\,. \tag{18}$$

Since the amplitudes are to be classified according to powers of the large parameter $\sqrt{N}$, we are not concerned with other parameters (e.g., $\Gamma_{\rm spr}/\omega_0$). The rules for estimating the amplitudes are:

(i) Each vertex (neutron capture, electromagnetic, weak, etc.) contains the factor $1/\sqrt{N}$, where $N = \max\{N_c, N_{c'}\}$, and N_c, $N_{c'}$ are the numbers of principal components of the nuclear states coupled in the vertex. In the ground state $N_c = 1$ and near the neutron threshold $N_c \sim \mathrm{MeV}/D$.
(ii) Every summation over the intermediate compound states $|c\rangle$ (the Green function) gives the N_c factor and the resonance energy dependence $D/(E - E_c + \frac{i}{2}\Gamma_c)$. The latter can provide an extra, resonance enhancement of up to D/Γ_c.

We should stress that the above rules produce a root-mean-squared estimate of the amplitude. Of course, fluctuations can change the relative magnitude of the amplitudes. Nevertheless, the $\sqrt{N}$ parameter is very large and the probability of a fluctuation which would violate the $\sqrt{N}$ hierarchy is very small.

To see how this classification works let us consider the process of neutron capture once more. By means of the optical theorem the total cross section can be expressed in terms of the forward-scattering amplitude as follows:

$$\sigma = \frac{4\pi}{k}\mathrm{Im}f(0)\,. \tag{19}$$

For slow neutron scattering ($kR \ll 1$) the scattering amplitude $f(0)$ can be presented as

$$f_0 - \frac{1}{2k}\left(\sum_s \frac{g\gamma_s^{(n)2}}{E - E_s + \frac{i}{2}\Gamma_s} + \sum_p \frac{g\gamma_p^{(n)2}}{E - E_p + \frac{i}{2}\Gamma_p}\right) \pm \frac{1}{2k}\sum_{sp} \frac{g(\gamma_s^{(n)}W_{sp}i\gamma_p^{(n)} - i\gamma_p^{(n)}W_{ps}\gamma_s^{(n)})}{(E - E_s + \frac{i}{2}\Gamma_s)(E - E_p + \frac{i}{2}\Gamma_p)}\,, \tag{20}$$

where f_0 is the s-wave potential scattering amplitude, $\gamma_s^{(n)}$ and $i\gamma_p^{(n)}$ are the amplitudes of neutron capture into the s and p compound states (proportional to the amplitudes T_s and T_p of sec. 1.1) normalized so that $\gamma_s^{(n)2} = \Gamma_s^{(n)}$, $\gamma_p^{(n)2} = \Gamma_p^{(n)}$, W_{sp} is the (imaginary) PNC matrix element coupling the s- and p-wave compound resonances, and g is the factor due to averaging over the spin projections of the target nucleus (the rules for calculating reaction amplitudes are given in Appendix A). The $\pm$ sign before the parity-violating term in (20) refers to neutrons with different helicities. Equations (19), (20) enable one to calculate the PNC cross section difference $\sigma_+ - \sigma_-$ and the neutron spin rotation, proportional to $\mathrm{Re}(f_+ - f_-)$ [see eq. (121)] at arbitrary (yet low) energy, including the thermal point (see experiments by Forte *et al* 1980, Vesna *et al* 1980). Amplitude (20) can be presented in the following diagrammatic form:

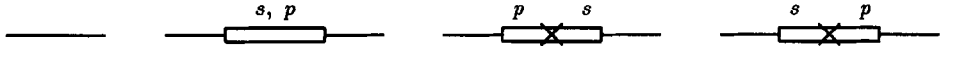

(21)

where the single line denotes the single-particle neutron states, the double line corresponds to the compound states, and the cross is the weak interaction vertex.

Let us first compare the potential and resonant s-wave scattering amplitudes. The resonant term [the second one in (20), or the second diagram in (21)] contains the neutron capture vertex $(1/\sqrt{N})$, the neutron emission vertex $(1/\sqrt{N})$, and the Green function of the compound state $(ND/(E - E_s + \frac{i}{2}\Gamma_s))$, which yields

$$f_{\mathrm{res}} \sim \frac{D}{E - E_s + \frac{i}{2}\Gamma_s}\,. \tag{22}$$

Therefore, the resonant scattering amplitude has zero order in powers of $\sqrt{N}$, just as the potential contribution. Indeed, it follows from the square-well model and experimental data (see, e.g., Bohr and

Mottelson 1969) that between the compound resonances at $|E - E_s| \sim D \gg \Gamma_s$ the ratio

$$\frac{f_{\rm res}}{f_0} \sim \frac{1}{ka}\,\frac{\Gamma_s^{(n)}}{D} \sim 0.05 - 0.5$$

($a = -f_0$ is the potential scattering length) is determined by the parameters other than $\sqrt{N}$.

The parity-violating contributions to (20), (21) contain three vertices ($1/N^{3/2}$) and two Green functions (N^2), and their estimate is

$$f_{\rm PV} \sim \sqrt{N}\,\frac{D}{E - E_s + \frac{i}{2}\Gamma_s}\,\frac{D}{E - E_p + \frac{i}{2}\Gamma_p}\,. \tag{23}$$

Therefore, this amplitude is $\sqrt{N}$ times enhanced with respect to the parity-conserving resonant amplitude (22). One can see that other PNC amplitudes, e.g.,

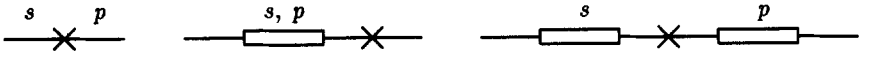

(24)

and the diagrams obtained from (24) by changing the order of vertices, or by swapping the s and p states do not have the $\sqrt{N}$ enhancement. These diagrams describe the PNC mixing of the single-particle neutron states, or the single-particle components of compound states (the so-called *valence mechanism*). It has been first considered by Zaretsky and Sirotkin (1983), and will be discussed in sec. 3.1.

The diagrams shown above form a convenient language of describing the interaction of a neutron with compound states. For example, the second and third diagrams in (24) account for the resonance increase of the neutron wave function due to virtual capture into the compound states. Note that all-order summation of the series of diagrams is equivalent to redefining the parameters of compound resonances (positions, widths, etc.), which are anyway taken from experiments. Using this approach Flambaum and Sushkov (1984) showed that resonance formulae for PNC effects are applicable at the neutron thermal point where the effects are 3 to 6 orders of magnitude smaller than those measured on-resonance. An alternative approach to the general description of PNC effects in neutron scattering based on Feshbach's projection formalism (Feshbach 1958, 1962) was suggested by Lewenkopf and Weidenmüller (1992). In this approach the operators P and Q project the total wave function onto open channels [single-particle s and p states, thin lines in (21), (24)], and closed channels (compound states shown with rectangles). In their notation $T_{QQ}^{\rm PV}$ corresponds to the PNC diagrams in (21), $T_{PP}^{\rm PV}$ corresponds to (24), and $T_{PQ}^{\rm PV}$, $T_{QP}^{\rm PV}$ describe neutron capture by the weak interaction (not shown here).

Let us now turn to the diagrams describing the (n,γ) reaction:

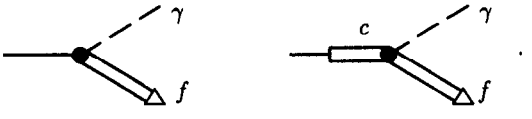

(25)

The first of them ($A_{\rm dir}$) corresponds to the direct radiative capture of the neutron into the final compound state f. It contains one vertex of the electromagnetic interaction, hence, it is proportional to $1/\sqrt{N_f}$. The second diagram ($A_{\rm res}$) describes the same process proceeding via the intermediate compound state c. It contains the neutron capture vertex ($1/\sqrt{N_c}$), the Green function of the compound

state $N_c D/(E - E_c + \frac{i}{2}\Gamma_c)$, and the photon emission vertex $(1/\sqrt{N_c})$, so $A_{\rm res} \propto N_c^0$. The ratio

$$\frac{A_{\rm res}}{A_{\rm dir}} \sim \sqrt{N_f}\frac{D}{E - E_c + \frac{i}{2}\Gamma_c} \tag{26}$$

shows that even in the off-resonance situation ($|E - E_c| \sim D$) the resonance mechanism in the (n,γ) reaction dominates for the transitions into the complex final states ($N_f \gg 1$). The direct and resonance contributions become comparable only for the transitions into the ground state and those close to it ($N_f \sim 1$).

The dominant contribution to the parity-violation effects in the (n,γ) reaction comes from the diagrams with the weak mixing of compound states:

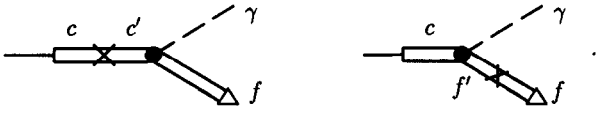

(27)

The first diagram contains the neutron capture vertex $(1/\sqrt{N_c})$, the weak interaction vertex $(1/\sqrt{N_c})$, the photon emission vertex $(1/\sqrt{N_c})$, and two compound state Green functions (N_c^2), which yields

$$A_{\rm PV} \sim \sqrt{N_c}\frac{D}{E - E_c + \frac{i}{2}\Gamma_c}\,\frac{D}{E - E_{c'} + \frac{i}{2}\Gamma_{c'}}\,. \tag{28}$$

Therefore, PNC effects in the (n,γ) reaction display the same factor of dynamical enhancement $\sqrt{N_c} \sim 10^2$–10^3 as in the neutron capture. The second diagram in (27) contains the weak mixing in the final state, and can be estimated as

$$\sim \sqrt{N_f}\frac{D}{E - E_c + \frac{i}{2}\Gamma_c}\,\frac{D_f}{E - \omega - E_{f'} + \frac{i}{2}\Gamma_{f'}}\,, \tag{29}$$

where D_f is the mean level spacing at $E \simeq E_f$ and ω is the photon energy. Since $N_f \ll N_c$ this contribution is much smaller then $A_{\rm PV}$ (28). Besides (27) there is a number of other parity-violating diagrams with the weak mixing of single-particle states, or with direct electromagnetic capture vertices, either not enhanced or even suppressed as $1/\sqrt{N_f}$.

It is instructive to consider a particular example of the ^{117}Sn (n,γ) reaction studied experimentally by Danilyan *et al* (1976), and Benkoula *et al* (1977). The transition into the final 0^+ state of the ^{118}Sn nucleus takes place from 1^+ and 1^- compound states by means of $M1$ or $E1$ γ emission. Taking into account the dominant parity-conserving and parity-violating contributions one obtains the following total reaction amplitude:

$$\frac{\langle 0^+|M1|1^+\rangle\langle 1^+|T_s|n\rangle}{E - E_+ + \frac{i}{2}\Gamma_+} + \frac{\langle 0^+|E1|1^-\rangle\langle 1^-|W|1^+\rangle\langle 1^+|T_s|n\rangle}{(E - E_- + \frac{i}{2}\Gamma_-)(E - E_+ + \frac{i}{2}\Gamma_+)}\,, \tag{30}$$

where $|n\rangle$ is the initial neutron state. We assumed in (30) that the neutron is captured into the s-wave resonance (this is true for low energy neutrons if their energy is not too close to a p-wave resonance). The circular polarization of the photon P_γ and the asymmetry parameter of the photon angular distribution $(W(\theta) = 1 + a\cos\theta)$ due to interference of the two terms in (30) are given by

$$P_\gamma = a = 2{\rm Re}\left(\frac{\langle 1^-|W|1^+\rangle}{E - E_-}\,\frac{\langle 0^+|E1|1^-\rangle}{\langle 0^+|M1|1^+\rangle}\right)\,. \tag{31}$$

It is worth noting that the energy denominator in this formula contains the difference $E - E_-$ rather than $E_+ - E_-$, as in (16). This gives a possibility of an additional resonant enhancement of the mixing, if $|E - E_-| \ll |E_+ - E_-|$, its magnitude being $|E_+ - E_-|/|E - E_-|$. In this estimate we assumed $|E - E_-| > \Gamma$, and neglected the p-wave neutron capture. The numerical estimate of the effect is (Sushkov and Flambaum 1982):

$$|a| \simeq 8 \times 10^{-4} \left|\frac{E1}{M1}\right| .$$

This value is in reasonable agreement with experimental data, if one assumes $|E1/M1| \sim 1$. Such value of this ratio is not too surprising for frequencies far from the maximum of the giant $E1$ resonance. It appears also that several compound resonances contribute to the parity-conserving $M1$ transition in the case of ^{118}Sn. However, in principle, there is a possibility of kinematical enhancement in (31), if $|E1/M1| > 1$.

The (n, γ) reaction was the first one where parity-violating nuclear forces were observed [see, e.g., review by Abov and Krupchitskii (1976)]. A detailed theoretical consideration of the problem can be found, e.g., in Flambaum and Sushkov 1985, where all possible correlations due to interference of the $E1$ and $M1$ γ-transitions for the s- and p-wave neutron capture are calculated (there are 8 P-odd and 9 P-even correlations). Their behaviour upon averaging over the final state is also examined, and according to it the correlations in the integral γ-spectrum are divided into three classes. Note that a formula which contained the enhancement of the circular polarization of γ-quanta near a p-wave compound resonance was presented by Lobov (1970), although the possibility of this enhancement was not stressed in that work, and a standard estimate, $P_\gamma \sim 10^{-4}$, was obtained, similarly to what one obtains at the thermal point or in an s resonance.

Another class of experiments where PNC effects have been observed is nuclear fission by polarized neutrons (Danilyan *et al* 1977, Vodennikov *et al* 1978, Andreev *et al* 1978, Petukhov *et al* 1979, Vesna *et al* 1980, see also references in Sushkov and Flambaum 1982). The quantity measured in these experiments is the asymmetry of emission of the light fragment with respect to the neutron spin ($W(\theta) = 1 + a \cos\theta$, for unpolarised nuclei). The most surprising feature of this phenomenon is that the correlation $\boldsymbol{\sigma} \cdot \mathbf{p}_f$ between the neutron spin and the momentum of the light fragment is a manifestation of parity-violating forces in the motion of a heavy particle: the nuclear fragment consisting of 10^2 nucleons. Another fact which needed explanation was the apparent survival of the effect in spite of a very large number of final states of the fragments. If the sign of the effect depended randomly on the final state of the system, as, say, in the (n, γ) reaction, the asymmetry measured for all final states at once would be strongly suppressed. A theory of this effect was considered in Flambaum and Sushkov (1980), Sushkov and Flambaum (1981a,b, 1982). The process of fission goes through a small number of intermediate collective states, fission channels. The P-odd correlations, as well as the usual P-even ones, are formed at this "cold" stage of the fission process due to mixing of opposite-parity rotational states by the dynamically enhanced weak interaction. Thus, the effect does not vanish after averaging over the final states of the fragments.

The main parity-conserving and parity-violating contributions to the reaction amplitude are given by

the diagrams

(32)

where the circle denotes the cold stage of fission. Similarly to the (n,γ) reaction, the first amplitude in (32) contains the neutron capture vertex $(1/\sqrt{N_c})$, the Green function of the compound nucleus (N_c), and the fission amplitude $(1/\sqrt{N_c})$[1], so that the result is independent of N_c:

$$f_a \sim \frac{D}{E - E_c + \frac{i}{2}\Gamma_c}\,. \tag{33}$$

The estimate for the second (parity-violating) amplitude in (32)

$$f_b \sim \sqrt{N_c}\frac{D}{E - E_c + \frac{i}{2}\Gamma_c}\,\frac{D}{E - E_{c'} + \frac{i}{2}\Gamma_{c'}} \tag{34}$$

contains the $\sqrt{N_c}$ dynamical enhancement factor. Thus, one obtains the following rough estimate for the asymmetry parameter a:

$$a \sim \sqrt{N_c}F\frac{D}{E - E_{c'} + \frac{i}{2}\Gamma_{c'}} \sim 10^{-4} - 10^{-3}.$$

This value is indeed close to those obtained experimentally for the ^{233}U, ^{235}U and ^{239}Pu nuclei. Note that there is a resonant energy dependence near the opposite parity (p-wave) compound resonance $E_{c'}$ (fission is dominated by the s-wave resonances E_c).

A common feature of all PNC effects considered above is the existence dynamical enhancement, proportional to $\sqrt{N}$, when the parity-violating amplitude contains the weak mixing of compound states. Of course, such enhancement should not be confined to nuclear processes only, but must be a generic property of all many-body systems of interacting particles with dense spectra of states (compound nuclei, rare-earth and actinide atoms, molecules, clusters, spin systems, quantum dots in solids, etc.) For example, the existence of dynamical enhancement has been recently demonstrated in numerical calculations for the rare-earth atom of Ce, and ^{8}B, ^{9}Be nuclei (see sec. 2.2). This enhancement originates from a high spectral density of the excited states, or, equivalently, from extremely small energy spacings D between them. Indeed, the distance between the levels decreases exponentially with the number of excited particles n ($D \propto e^{-\alpha n}$), since the total number of possible states (number of combinations) increases exponentially. In such a system the mixing of compound states by some weak perturbation is proportional to $\sqrt{N} \propto 1/\sqrt{D}$, i.e., is exponentially enhanced. This is possibly a quantum-mechanical analogue of the exponential divergence of trajectories in classical chaotic systems.

In a macroscopic system the density of states is infinitely large, although no enhancement has been observed so far (if we neglect the famous puzzle of biological asymmetry of the world). There are

[1]The factor $1/\sqrt{N_c}$ in the fission amplitude describes the admixture of the wave function of the cold deformed nucleus in the wave function of the compound state c. This factor gives a reasonable estimate of the fission widths of above-barrier resonances: $\Gamma_f \sim (1/N)(1/\tau) \sim 0.1$–$1$ eV, where $1/\tau \sim v/R \sim 100$ keV, v is the velocity of the fragments at the fission barrier, R is the barrier size, and τ is the lifetime of the cold state.

several reasons for suppression of the enhancement, e.g., finite state widths, effects of temperature, finite energy resolution. Interestingly, the examination of the latter produced an unexpected result: averaging of random-sign PNC effects does not necessarily lead to their suppression, and a certain "violation" of the Central Limit Theorem takes place due to unusual statistical properties of the compound-state mixing (see sec. 4).

1.4 Hamiltonian of the Nuclear PNC Weak Interaction

The nucleon-nucleon PNC interaction can be represented by the following effective Hamiltonian:

$$W_{ab} = \frac{G}{\sqrt{2}}\frac{1}{2m}[(g_{ab}\boldsymbol{\sigma}_a - g_{ba}\boldsymbol{\sigma}_b)\{\mathbf{p}_a - \mathbf{p}_b, \delta(\mathbf{r}_a - \mathbf{r}_b)\} + g'_{ab}(\boldsymbol{\sigma}_a \times \boldsymbol{\sigma}_b)\nabla_a\delta(\mathbf{r}_a - \mathbf{r}_b)] \ , \tag{35}$$

where $\boldsymbol{\sigma}_{a,b}$, $\mathbf{r}_{a,b}$ and $\mathbf{p}_{a,b}$ are the (doubled) spins, the coordinates and the momentum operators of the nucleons a and b [protons (p), or neutrons (n)], m is the nucleon mass, $\{\ ,\ \}$ is the anticommutator, and g_{ab}, g'_{ab} are dimensionless constants. They take into account the renormalization of the Fermi weak interaction by the strong interaction ($ab = pp, pn, np, nn$). The form of the contact interaction (35) written in the lowest, first order in $\mathbf{p}/m$ follows from the P-odd transformation properties of the potential. This interaction dates back to the work by Feynman and Gell-Mann (1958). The constants g_{ab} can be, in principle, considered as phenomenological parameters, similar to those of the Landau-Migdal parametrization of the strong interaction. On the other hand, the Hamiltonian (35) can be derived as a contact limit of the one-boson-exchange interaction (see, e.g., Desplanques *et al* 1980, Dubovik and Zenkin 1986), which takes into account π-, ρ- and ω-meson exchange. In this case g_{ab} are expressed in terms of the weak (f_π, h^T_ρ, h^T_ω) and strong meson-nucleon interaction constants and meson masses, with an account of the long-range and exchange nature of the interaction and the nucleon-nucleon repulsion at small distances by means of the parameters W_π and W_ρ (McKellar 1968, Lobov 1980, Flambaum *et al* 1984a,b, Adelberger and Haxton 1985). The values of these constants were considered in a number of works (see papers cited above and references therein). It is necessary to note that by using Fierz transformation exchange matrix elements of the contact interaction (35) can always be reduced to the direct ones, and thus included in the definition of the g_{ab} constants. Then the Hamiltonian W_{ab} will have only direct matrix elements. This convention is used throughout the paper.

If one considers the interaction of an unpaired valence nucleon with the core of paired nucleons, the interaction (35) produces the following single-particle parity-violating weak potential:

$$w_a = \sum_b \langle b|W_{ab}|b\rangle = \frac{G}{\sqrt{2}}\frac{g_a}{2m}\{\boldsymbol{\sigma}\cdot\mathbf{p}, \rho(r)\} \ , \tag{36}$$

where the sum is carried over all core nucleons b, and $\rho(r)$ is the nuclear density normalized as $\int \rho(r)d^3r = A$ ($A \gg 1$). The constants g_a of the potential (36) are given by $g_p = \frac{Z}{A}g_{pp} + \frac{N}{A}g_{pn}$, $g_n = \frac{Z}{A}g_{np} + \frac{N}{A}g_{nn}$, and can be expressed in terms of the weak meson-nucleon coupling (see references above; below we present the result of Flambaum *et al* 1984a,b):

$$\begin{aligned} g_p &= 2.0\times10^5 W_\rho\left[\,176\tfrac{W_\pi}{W_\rho}f_\pi - 19.5h^0_\rho - 4.7h^1_\rho + 1.3h^2_\rho - 11.3(h^0_\omega + h^1_\omega) - 1.7h^{1\prime}_\rho\right] \ , \\ g_n &= 2.0\times10^5 W_\rho\left[-118\tfrac{W_\pi}{W_\rho}f_\pi - 18.9h^0_\rho + 8.4h^1_\rho - 1.3h^2_\rho - 12.8(h^0_\omega - h^1_\omega) + 1.1h^{1\prime}_\rho\right] \ . \end{aligned} \tag{37}$$

Using the "best" values of f_π, h^T_ρ and h^T_ω from (Desplanques *et al* 1980) together with $W_\rho = 0.4$ and $W_\pi = 0.16$ [these values are based on the calculation of PNC nucleon scattering by ^{4}He (Dmitriev *et al*

1983, Flambaum *et al* 1985), and agree with those obtained by McKellar 1968 and Lobov 1980] yields: $g_p \simeq 4.6$, $g_n \simeq 0.2$. The smallness of g_n is caused by the mutual cancellation of the π- and ρ-meson contributions. It should not be taken too seriously because of the large uncertainties in the values of constants used to calculate g_a. Sometimes a different form of the weak potential (36) is used:

$$w = \frac{1}{2}\varepsilon\{\boldsymbol{\sigma}\mathbf{p}, f(r)\}\ , \quad \text{where } f(r) \approx \rho(r)/\rho_0\ , \quad \varepsilon = \frac{G}{\sqrt{2}m}\rho_0 g = 1.0 \times 10^{-8} g\ , \tag{38}$$

and ρ_0 is the average nuclear density. In this case $\varepsilon_p \simeq 4 \times 10^{-8}$ and $\varepsilon_n \lesssim 1 \times 10^{-8}$.

The potential (36) is believed to play a leading role in various nuclear PNC effects [see, e.g., calculations of the nuclear anapole moment (Flambaum and Khriplovich 1980, Flambaum *et al* 1984b, Haxton *et al* 1989, Bouchiat and Piketty 1991)]. Indeed, w contains a coherent contribution of A nucleons. However, it was noticed (Zaretsky and Sirotkin 1983, 1987, Kadmensky *et al* 1983) that the matrix element of (36) between the principal components of compound states close to the neutron threshold is zero. The point is that for a pseudo-scalar operator (36) $\langle\alpha|w|\beta\rangle \neq 0$ only for the single-particle states α, β of different parity and identical angular momentum (e.g., $s_{1/2}$ and $p_{1/2}$). It is known (see, e.g., Bohr and Mottelson 1969) that such orbitals belong to different nuclear shells. They are separated by the energy $\omega_0 \sim$ 5–10 MeV, which is greater than the spreading width of the principal components $\Gamma_{\rm spr} \simeq 2$ MeV. Therefore, the matrix elements of w between the compound states must involve distant, small components, which can be described as a perturbation-theory admixture to the principal components due to the strong residual nucleon-nucleon interaction. This mechanism can be described as the induced parity-nonconserving interaction (IPNCI) (see sec. 2.3). Its magnitude is proportional to the strength of the original PNC potential (36), and it directly couples the principal components of the compound states. It will be shown in sec. 2.3 that this two-body interaction is an order of magnitude ($\sim A^{1/3}$) stronger than the direct two-nucleon PNC interaction (35), and that the IPNCI has a different spin and isotopic structure.

There is another effect which influences the strength of the nuclear PNC potential. Even if the constants g_{ab} of the PNC nucleon-nucleon interaction (35) were known precisely, the PNC potential of the nucleus w would be different from that of (36) with constants given by (37). This happens due to *renormalization* of w by the residual strong interaction. Similar effect changes the magnitude of the parity and time-invariance violating (P,T-odd) nuclear potential. These questions are considered in Appendix D. The P,T-odd potential is renormalized by the momentum-independent part of the strong interaction. The renormalization of the PNC potential is produced by the momentum-dependent spin-flip component of the strong interaction. The latter increases the $g_{p,n}$ constants with respect to their initial values (37). The size of the renormalization depends on the constants of π- and ρ-meson exchange underlying the strong interaction. It turns out that the π-meson exchange contribution alone is large enough to generate instability (a pole) in the nuclear response to the weak potential. Thus, the question of magnitude of the nuclear PNC potential seems to be related to the question of stability of the nucleus against π-meson tensor forces, and in particular, to the problem of π condensation in nuclei.

2 Matrix Elements Between Compound States

It has been shown in the Introduction that there are several enhancement factors (kinematical, dynamical, resonance) which increase the observable PNC effects in nuclei by up to 6 orders of magnitude with respect to the basic strength of the weak interaction (1). The most universal of them is dynamical enhancement (see sec. 1.3). This factor emerges when the weak interaction mixes nearby compound states, and is estimated as $\sqrt{N} \sim 10^2$–10^3, where N is the number of principal components of the compound states. However, facilitating the experimental observation of PNC effects, the same "mechanism" greatly complicates the calculation of the effect. Moreover, it makes any calculation of the effect for a particular resonance in a given nuclei simply impossible. Of course, the energies and widths of the compound resonances which appear explicitly in the formulae describing the effect [e.g., (8)] can be found experimentally. The main problem then lies with the matrix elements $(c|W|c')$ between the compound states.

According to the statistical theory of compound resonances this matrix element is a Gaussian random variable, and its values are uncorrelated for different c, c'. Thus, the aim of the theoretical work is to calculate the r.m.s. value of this matrix element. The latter can be directly compared with experimental results of Bowman *et al* (1990) and Frankle *et al* (1991). In contradistinction with previous experiments, the measurements of the parity-violating asymmetry P in these works were performed for series of 17 p resonances in $n+^{238}$U and 23 p resonances in $n+^{232}$Th (about one-third of them are expected to be $p_{1/2}$ resonances, which produce high P values), and provided the r.m.s. PNC matrix elements: $\sqrt{\overline{W^2}} = 0.58^{+0.50}_{-0.25}$ meV in ^{239}U, and $\sqrt{\overline{W^2}} = 1.39^{+0.55}_{-0.38}$ meV in ^{233}Th. These values are in agreement with a crude estimate: $\sqrt{\overline{W^2}} \sim (W_{\rm sp}/\sqrt{N})(\Gamma_{\rm spr}/\Delta E) \sim 1$ meV for $N \sim \Gamma_{\rm spr}/D \sim 10^5$. Here $W_{\rm sp} \sim (1\ {\rm eV}) \times g_p \sim 4$ eV is a typical single-particle PNC matrix element (see, e.g., Flambaum 1993, Flambaum and Vorov 1993). However, one could get much more precise information about the nuclear PNC weak interaction from an accurate theoretical calculation of $\sqrt{\overline{W^2}}$. We should mention that besides the above quoted number Frankle *et al* (1991) produced an unexpected result: the values of P turned out to be positive for all 7 p resonances, where the effects were greater than 2σ. This might mean the existence of a large regular contribution to the PNC asymmetry, produced e.g., by a certain degree of coherence in the compound resonances. We postpone the discussion of this question until sec. 3.

Several approaches have been suggested to calculate matrix elements between compound states. Urin and Vyazankin (1991) expressed the mean square matrix element in terms of the strength function of a cold nucleus, and calculated the latter semiempirically in the framework of "temperature mechanism". Johnson *et al* (1991) based their calculation on the the work by French *et al* (1988) and employed the assumption that the mean square matrix element of the PNC interaction is proportional to that of the residual shell-model strong interaction (see sec. 2.5). In the next section we consider the statistical theoretical method described in (Flambaum 1993, Flambaum and Vorov 1993, Flambaum 1994a, Flambaum *et al* 1994). It can be applied to calculation of mean square matrix elements between compound states (chaotic eigenstates) in various many-body systems.

2.1 Statistical Theory

The wave function of a compound state may be expressed as the sum over simple components $|\Phi_i\rangle$ which are many-particle excitations over the shell-model ground state $|0\rangle$:

$$|\Psi\rangle = \sum_i C_i|\Phi_i\rangle, \qquad |\Phi_i\rangle = a^\dagger_\alpha a_\beta a^\dagger_\gamma a_\delta \ldots |0\rangle \ . \tag{39}$$

Consider a single-particle operator (e.g., the weak potential):

$$\hat{M} = \sum_{\alpha\beta} M_{\alpha\beta} a^\dagger_\alpha a_\beta = \sum_{\alpha\beta} M_{\alpha\beta}\hat{\rho}_{\alpha\beta} \ , \tag{40}$$

where $\hat{\rho}_{\alpha\beta} = a^\dagger_\alpha a_\beta$ is the density matrix operator, and $M_{\alpha\beta} = \langle\alpha|\hat{M}|\beta\rangle$. The matrix element of the operator $\hat{M}$ between the compound states Ψ_1 and Ψ_2 is given by

$$M_{12} \equiv \langle\Psi_1|\hat{M}|\Psi_2\rangle = \sum_{ij} C^{(1)*}_i C^{(2)}_j \langle\Phi_i|\hat{M}|\Phi_j\rangle \ , \tag{41}$$

or

$$M_{12} = \sum_{\alpha\beta} M_{\alpha\beta}\langle\Psi_1|\hat{\rho}_{\alpha\beta}|\Psi_2\rangle \equiv \sum_{\alpha\beta} M_{\alpha\beta}\rho^{(12)}_{\alpha\beta} \ . \tag{42}$$

The magnitude of $\rho^{(12)}_{\alpha\beta}$ determines the "weight" of the single-particle transition $\alpha \to \beta$ $M_{\alpha\beta}$ in M_{12}. We suppose that in a "chaotic" compound state the mean values of the matrix elements (averaged over many compound states Ψ_1 and Ψ_2) are zero:

$$\overline{M_{12}} \equiv \overline{\langle\Psi_1|\hat{M}|\Psi_2\rangle} = 0 \ , \qquad \overline{\rho^{(12)}_{\alpha\beta}} \equiv \overline{\langle\Psi_1|\hat{\rho}_{\alpha\beta}|\Psi_2\rangle} = 0 \ , \tag{43}$$

which is equivalent to the assumption of random and uncorrelated distributions of C's:

$$\overline{C^{(1)}_i} = \overline{C^{(2)}_j} = \overline{C^{(1)*}_i C^{(2)}_j} = 0 \ .$$

Thus, the matrix element (41) is the sum of a large number of uncorrelated random items. According to the Central Limit Theorem, this makes the statistics of the matrix elements Gaussian (we indeed checked this, see sec. 2.2). Note that statistical independence of $C^{(1)}_i$ and $C^{(2)}_j$ is ensured by the fact that Ψ_1 and Ψ_2 are the states of different symmetry, e.g., having opposite parity.

Our aim is to calculate the mean square matrix element or the correlator between matrix elements of different operators with the same selection rules (e.g., P-odd and P,T-odd interactions):

$$\overline{|M_{12}|^2} = \sum_{\alpha\beta\alpha'\beta'} M_{\alpha\beta} M_{\beta'\alpha'} \overline{\rho^{(12)}_{\alpha\beta}\rho^{(21)}_{\beta'\alpha'}} = \sum_{\alpha\beta} |M_{\alpha\beta}|^2 \overline{|\rho^{(12)}_{\alpha\beta}|^2} \ , \tag{44}$$

$$\overline{M_{12}W_{21}} = \sum_{\alpha\beta} M_{\alpha\beta} W_{\beta\alpha} \overline{|\rho^{(12)}_{\alpha\beta}|^2} \ . \tag{45}$$

In (44), (45) we used the fact that transitions between different pairs of single-particle states are uncorrelated: $\overline{\rho^{(12)}_{\alpha\beta}\rho^{(21)}_{\beta'\alpha'}} = \delta_{\alpha\alpha'}\delta_{\beta\beta'}\overline{|\rho^{(12)}_{\alpha\beta}|^2}$, which follows from the statistical properties of the expansion coefficient in (39) for compound states (we check these properties in sec. 2.2):

$$\overline{C_i C^*_j} = \delta_{ij}\overline{C^2_i} \ , \tag{46}$$

(C's are chosen to be real). The mean square component $\overline{C_i^2}$ is connected with the strength function introduced by Wigner (1955),

$$\rho_w(E,i) = \sum_\lambda C_i^{(\lambda)2}\delta(E-E_\lambda)\ , \tag{47}$$

where i and λ enumerate the basis states and the eigenstates, respectively. Averaging (47) one obtains

$$D\overline{\rho_w(E,i)} = \overline{C_i^{(\lambda)2}} \equiv w(E_i;E,\Gamma,N)\ . \tag{48}$$

Here D is the locally averaged level spacing between the states of given spin and parity: $D^{-1} = \overline{\rho(E)} = \overline{\sum_\lambda \delta(E-E_\lambda)}$, and the function $w(E_i;E,\Gamma,N) \equiv \overline{C_i^{(\lambda)2}}$ ($E_\lambda \approx E$) has been introduced to describe the spreading of the component i over the eigenstates λ. This function depends on the number of principal components N in the sum (39), the spreading width Γ and the energy E_i of the component, and on the energy of the compound state E (in fact, on their difference $E-E_i$)[2]. In the simplest model description (Bohr and Mottelson 1969) $w(E_i;E,\Gamma,N)$ has a Breit-Wigner (or Lorentzian) shape:

$$w(E_i;E,\Gamma,N) = \frac{1}{N}\,\frac{\Gamma^2/4}{(E-E_i)^2+\Gamma^2/4}\ , \qquad N = \frac{\pi\Gamma}{2D}\ . \tag{49}$$

The spreading width Γ is connected to the mean-square off-diagonal Hamiltonian matrix element V^2 by $\Gamma = 2\pi V^2/D$, and the last relation in (49) follows from $\sum_i C_i^{(\lambda)2} = 1$, or, equivalently, $\int w(E_i;E,\Gamma,N)dE_i/D = 1$. The strength function (49) also appears as the solution of Wigner's Band Random Matrix (BRM) model (Wigner 1955) for $1 \ll \frac{V^2}{D^2} \ll b$, valid at $|E_i - E| < Db$, where b is the bandwidth of the matrix.

Using equations (41), (46) and (48) we obtain:

$$\begin{aligned}\overline{|\rho_{\alpha\beta}^{(12)}|^2} &\equiv \overline{\langle\Psi_1|\hat\rho_{\alpha\beta}|\Psi_2\rangle\langle\Psi_2|\hat\rho_{\beta\alpha}|\Psi_1\rangle} = \sum_{ij}\overline{C_i^{(1)2}}\ \overline{C_j^{(2)2}}\langle\Phi_i|\hat\rho_{\alpha\beta}|\Phi_j\rangle\langle\Phi_j|\hat\rho_{\beta\alpha}|\Phi_i\rangle \\ &= \sum_{ij} w_1(E_i)w_2(E_j)\langle\Phi_i|\hat\rho_{\alpha\beta}|\Phi_j\rangle\langle\Phi_j|\hat\rho_{\beta\alpha}|\Phi_i\rangle\ ,\end{aligned} \tag{50}$$

where $w_1(E_i) \equiv w(E_i;E_1,\Gamma_1,N_1)$ and $w_2(E_j) \equiv w(E_j;E_2,\Gamma_2,N_2)$. Below we assume $N_2 \geq N_1$ ($\Gamma_2/D_2 \geq \Gamma_1/D_1$), i.e., the number of principal components among $|\Phi_j\rangle$ is greater than or equal to the number of principal components among $|\Phi_i\rangle$. The operator $\hat\rho_{\beta\alpha} = a_\beta^\dagger a_\alpha$ transfers a nucleon from the orbital α to the orbital β. The matrix element $\langle\Phi_j|\hat\rho_{\beta\alpha}|\Phi_i\rangle$ is not zero for $|\Phi_j\rangle = a_\beta^\dagger a_\alpha|\Phi_j\rangle$ only. Therefore, $E_j - E_i \simeq \epsilon_\beta - \epsilon_\alpha \equiv \omega_{\beta\alpha}$ (ϵ_α and ϵ_β are the single-particle energies) and the summation over j at fixed i includes only one state. We can use closure and simplify (50):

$$\sum_j\langle\Phi_i|\hat\rho_{\alpha\beta}|\Phi_j\rangle\langle\Phi_j|\hat\rho_{\beta\alpha}|\Psi_i\rangle = \langle\Phi_i|\hat\rho_{\alpha\beta}\hat\rho_{\beta\alpha}|\Phi_i\rangle = \langle\Phi_i|\hat n_\alpha(1-\hat n_\beta)|\Phi_i\rangle\ ,$$

since $\hat\rho_{\alpha\beta}\hat\rho_{\beta\alpha} = a_\alpha^\dagger a_\beta a_\beta^\dagger a_\alpha = a_\alpha^\dagger a_\alpha(1-a_\beta^\dagger a_\beta) = \hat n_\alpha(1-\hat n_\beta)$, where $\hat n_\alpha$ is the occupation number operator. Thus, we obtain

$$\overline{|\rho_{\alpha\beta}^{(12)}|^2} = \sum_i w_1(E_i)w_2(E_i+\omega_{\beta\alpha})\langle\Phi_i|\hat n_\alpha(1-\hat n_\beta)|\Phi_i\rangle\ . \tag{51}$$

[2]We neglect the dependence of Γ on i in the expression (48) for $\overline{C_i^{(\lambda)2}}$. This is justified when the number of "decay channels" (off-diagonal matrix elements $H_{ij} \neq 0$) of the basic component Φ_i is large, which makes the fluctuations of Γ small, similarly to the fluctuations of the radiative widths of compound states. However, there is a weak regular dependence of Γ on energy which can be easily taken into account. A numerical experiment for the atom of Ce (sec. 2.2) confirms this picture.

The matrix element $\langle\Phi_i|\hat{n}_\alpha(1-\hat{n}_\beta)|\Phi_i\rangle$ is equal to 1 if in the component Φ_i the orbital α is occupied and β is vacant (this condition makes the transition $\alpha \to \beta$ possible). In other cases it is zero. Since w_1 and w_2 in (51) are smooth functions of energy (they vary on a typical energy scale $\sim \Gamma$), the matrix element of the $\hat{n}_\alpha(1-\hat{n}_\beta)$ operator can be replaced by its average value:

$$\langle n_\alpha(1-n_\beta)\rangle_1 \simeq \langle\Psi_1|\hat{n}_\alpha(1-\hat{n}_\beta)|\Psi_1\rangle \ . \tag{52}$$

The $\simeq$ sign is a reminder that the left-hand side is the local average value over Ψ_1 states. Practically, when the number of components is very large, the fluctuations of $\langle\Psi_1|\hat{n}_\alpha(1-\hat{n}_\beta)|\Psi_1\rangle$ are small.

Substituting this average into (51) and replacing the sum over i by the integral over dE_i/D_1 we obtain:

$$\overline{|\rho^{(12)}_{\alpha\beta}|^2} = \langle n_\alpha(1-n_\beta)\rangle_1 \sum_i w_1(E_i)w_2(E_i+\omega_{\beta\alpha}) = \langle n_\alpha(1-n_\beta)\rangle_1 \int w_1(E_i)w_2(E_i+\omega_{\beta\alpha})\frac{dE_i}{D_1} \ . \tag{53}$$

This result can be written in the following form:

$$\overline{|\rho^{(12)}_{\alpha\beta}|^2} = \langle n_\alpha(1-n_\beta)\rangle_1 D_2\tilde{\delta}(\Gamma_1,\Gamma_2,\Delta) \ , \tag{54}$$

where we defined

$$\tilde{\delta}(\Gamma_1,\Gamma_2,\Delta) \equiv \frac{1}{D_2}\int w(E_i;E_1,\Gamma_1,N_1)w(E_j+\omega_{\beta\alpha};E_2,\Gamma_2,N_2)\frac{dE_i}{D_1} \ , \qquad (\Delta \equiv E_2-E_1-\omega_{\beta\alpha}) \ . \tag{55}$$

The above definition is consistent if $w(E_i;E,\Gamma,N)$ depends on the difference E_i-E. One can easily check the following property of the function $\tilde{\delta}$:

$$\int \tilde{\delta}(\Gamma_1,\Gamma_2,\Delta)d\Delta = 1 \ , \tag{56}$$

and obtain for the Breit-Wigner model strength functions (49) that

$$\tilde{\delta}(\Gamma_1,\Gamma_2,\Delta) = \frac{1}{\pi}\frac{\Gamma/2}{\Delta^2+\Gamma^2/4} \ , \qquad (\Gamma=\Gamma_1+\Gamma_2), \tag{57}$$

also has a Breit-Wigner form. Due to (56) one may call $\tilde{\delta}$ a "spread" δ-function [if $\Gamma_{1,2} \to 0$, then $\tilde{\delta}(\Gamma_1,\Gamma_2,\Delta) \to \delta(\Delta)$].

Using (44), (54) we can now calculate the mean square matrix element between compound states:

$$\overline{|M_{12}|^2} = \sum_{\alpha\beta}|M_{\alpha\beta}|^2\langle n_\alpha(1-n_\beta)\rangle_1 D_2 \ \tilde{\delta}(\Gamma_1,\Gamma_2,E_2-E_1-\omega_{\beta\alpha}) \ , \tag{58}$$

where the summation is carried out over the single-particle orbitals α and β. If the number of excited particles is large we can use Fermi-gas formulae for the occupation numbers:

$$\langle n_\alpha(1-n_\beta)\rangle \simeq n(\epsilon_\alpha)(1-n(\epsilon_\beta)), \qquad n(\epsilon) = \frac{1}{1+e^{(\epsilon-\mu)/T}} \ . \tag{59}$$

The temperature T and the chemical potentials (Fermi energies) μ_p, μ_n for protons and neutrons can be found from the standard conditions:

$$\sum_\alpha \epsilon_\alpha n_\alpha = E, \qquad \sum_p n_p = Z, \qquad \sum_n n_n = N, \tag{60}$$

where E is the compound state energy, Z and N are the proton and neutron numbers. Equations (58)–(60) allow one to do computer calculations of the mean square matrix elements between compound states. Note that in the case of interacting particles the ideal-gas equation (59) could be refined. The simplest way to do this is to introduce spreading widths of the single-particle states, which smooth the Fermi step even at $T = 0$. One can also use a more consistent approach in the spirit of the Landau theory of Fermi liquids and take into account the dependence of the interaction energy of quasi-particles on temperature. The energy of the system with respect to its ground-state energy $E - E_0$ and the renormalized quasi-particle energies $\tilde{\epsilon}_\alpha$ [to be used in (59)] are then given by:

$$E - E_0 = \sum_\alpha \epsilon_\alpha \delta n_\alpha + \frac{1}{2} \sum_{\alpha\beta} V_{\alpha\beta} \delta n_\alpha \delta n_\beta \ , \tag{61}$$

$$\tilde{\epsilon}_\alpha = \epsilon_\alpha + \sum_\beta V_{\alpha\beta} \delta n_\beta \ , \tag{62}$$

where $\delta n_\alpha = n_\alpha(T) - n_\alpha(0)$, and $V_{\alpha\beta}$ is the matrix element of the effective two-body interaction (e.g., the Landau-Migdal strong interaction).

For the two-body operator

$$\hat{V} = \frac{1}{2} \sum_{\alpha\beta\gamma\delta} a^\dagger_\alpha a^\dagger_\beta \langle \alpha, \beta | \hat{V} | \gamma, \delta \rangle a_\gamma a_\delta \equiv \frac{1}{2} \sum_{\alpha\beta\gamma\delta} a^\dagger_\alpha a^\dagger_\beta V_{\alpha\beta\gamma\delta} a_\gamma a_\delta \ , \tag{63}$$

the mean square matrix element can be obtained in a similar way:

$$\overline{|M_{12}|^2} \equiv \overline{|\langle \Psi_1 | \hat{V} | \Psi_2 \rangle|^2} = \frac{1}{4} \sum_{\alpha\beta\gamma\delta} |V_{\alpha\beta\gamma\delta} - V_{\alpha\beta\delta\gamma}|^2 \langle n_\alpha n_\beta (1 - n_\gamma)(1 - n_\delta) \rangle_1 D_2 \ \tilde{\delta}(\Gamma_1, \Gamma_2, \omega - \omega_{\gamma\delta,\alpha\beta}) \ , \tag{64}$$

where $\omega \equiv E_2 - E_1$, and $\omega_{\gamma\delta,\alpha\beta} = \epsilon_\gamma + \epsilon_\delta - \epsilon_\alpha - \epsilon_\beta$ is the energy of the two-particle transition: $\alpha, \beta \to \gamma, \delta$.

We can also calculate the correlator C_{MW} between matrix elements of two operators M and W with identical selection rules:

$$C_{MW} \equiv \frac{\overline{M_{12} W_{21}}}{\left(\overline{|M_{12}|^2} \ \overline{|W_{12}|^2} \right)^{1/2}} = \frac{\sum_{\alpha\beta} M_{\alpha\beta} W_{\beta\alpha} \overline{|\rho^{(12)}_{\alpha\beta}|^2}}{\left(\sum_{\alpha\beta} |M_{\alpha\beta}|^2 \overline{|\rho^{(12)}_{\alpha\beta}|^2} \right)^{1/2} \left(\sum_{\alpha\beta} |W_{\alpha\beta}|^2 \overline{|\rho^{(12)}_{\alpha\beta}|^2} \right)^{1/2}} \tag{65}$$

One can easily see that $|C_{MW}| = 1$ if the matrix elements $W_{\alpha\beta}$ and $M_{\alpha\beta}$ are proportional to each other ($M_{\alpha\beta} = \text{const} \times W_{\alpha\beta}$), or if there is only one dominating single-particle transition, say, $s \to p$ ($M_{sp} \gg M_{\alpha\beta}$ and $W_{sp} \gg W_{\alpha\beta}$ for all $\alpha \neq s$, $\beta \neq p$). Usually there are several important single-particle transitions near the Fermi surface ($q \sim 10$). If there are no special reasons for the coherence or cancellations one could expect $|C_{MW}| \sim 1/\sqrt{q} \sim 0.3$. However, in the most interesting case of a P-odd and a P,T-odd interactions there are pairs of opposite sign contributions. Indeed, the matrix elements of the weak (PNC) interaction are imaginary: $W_{\beta\alpha} = W^*_{\alpha\beta} = -W_{\alpha\beta}$. The matrix elements of the P,T-odd interaction are real: $M_{\beta\alpha} = M_{\alpha\beta}$. Therefore, we have pairs of opposite sign terms:

$$W_{\alpha\beta} M_{\beta\alpha} |\rho^{(12)}_{\alpha\beta}|^2 + W_{\beta\alpha} M_{\alpha\beta} |\rho^{(12)}_{\beta\alpha}|^2 = W_{\alpha\beta} M_{\beta\alpha} \left(|\rho^{(12)}_{\alpha\beta}|^2 - |\rho^{(12)}_{\beta\alpha}|^2 \right) \propto n_\alpha (1 - n_\beta) - n_\beta (1 - n_\alpha) \ . \tag{66}$$

This partial cancellation makes the correlator small ($|C_{MW}| \leq 0.3$), which means that in practice the matrix elements of the P,T-odd and the P-odd weak interactions are statistically independent (see sec. 2.4 and Appendix C).

Note that equations (58), (59) for the matrix element M_{12} have simple interpretation. The transition $\alpha \to \beta$ takes place if the orbital α is occupied and β is vacant. Thus, the factor $n_\alpha(1-n_\beta)$ selects the transitions near the Fermi surface. In the limit $\Gamma_1+\Gamma_2 \to 0$ $\tilde{\delta}$ transforms into a conventional δ-function. Therefore, it reflects the "energy conservation" for the quasistationary states with finite widths Γ_1, Γ_2. The $\hat{M}$ operator "favours" the transitions between the compound states with the energy difference $E_2 - E_1 \equiv \omega$ close to $\omega_{\beta\alpha}$, where $\omega_{\beta\alpha} \equiv \epsilon_\beta - \epsilon_\alpha$ is the energy difference between the single-particle orbitals coupled by $\hat{M}$. In the case of $\omega = \omega_{\beta\alpha}$,

$$\sqrt{\overline{|M_{12}|^2}} \sim |M_{\alpha\beta}|\sqrt{\frac{2D_2}{\pi\Gamma}} \sim \frac{|M_{\alpha\beta}|}{\sqrt{N_2}} , \tag{67}$$

where $M_{\alpha\beta}$ is the single-particle matrix element (we used (57) to make this estimate). Recall that $N_2 \geq N_1$. Therefore we see that the result of the statistical calculation (58) agrees with the rough estimate (13) made in the Introduction. Far from the "resonance", at $|\omega - \omega_{\beta\alpha}| > \Gamma$ there is an extra suppression factor $\Gamma/|\omega-\omega_{\beta\alpha}|$ (in the Breit-Wigner model). This suppression is especially important for calculations of the weak matrix elements between nearby compound states, where $\omega = 0$, $\omega_{\beta\alpha} \sim$ 5–10 MeV $\geq \Gamma \approx 2$ MeV (see also discussions in Zaretsky and Sirotkin 1983, 1987, Kadmensky *et al* 1983).

Starting from eq. (50) and using closure to sum over j (we assumed $N_1 \leq N_2$) we arrived at eq. (54) for the mean square matrix element of the density matrix operator. However, starting from

$$\overline{|\rho^{(12)}_{\alpha\beta}|^2} = \overline{\langle\Psi_2|\hat{\rho}_{\beta\alpha}|\Psi_1\rangle\langle\Psi_1|\hat{\rho}_{\alpha\beta}|\Psi_2\rangle} ,$$

and summing over i first (for $N_1 \approx N_2$, or $N_1 \geq N_2$) one would come to a different answer:

$$\overline{|\rho^{(12)}_{\alpha\beta}|^2} = \langle n_\beta(1-n_\alpha)\rangle_2 D_1 \tilde{\delta}(\Gamma_1,\Gamma_2,\omega-\omega_{\beta\alpha}) . \tag{68}$$

Equations (54) and (68) are identical if the following relation is valid:

$$\langle n_\alpha(1-n_\beta)\rangle_1 D_2 = \langle n_\beta(1-n_\alpha)\rangle_2 D_1 . \tag{69}$$

This can be checked, e.g., in a model where a number of particles are statistically distributed over a larger number of orbitals. However, the approximate Fermi-gas formulae for the occupation numbers (59) violate the identity (69). This violation is not important for the calculation of $\overline{|M_{12}|^2}$ from (58), because of the summation over α,β and since $D_1 \approx D_2$ for $N_1 \approx N_2$ (this happens for the weak interaction matrix elements where $E_1 \approx E_2$, $\Gamma_1 \approx \Gamma_2$). Also, for $N_1 \sim N_2$ one can use a symmetric form of the result [half the sum of (54) and (68)]:

$$\overline{|\rho^{(12)}_{\alpha\beta}|^2} = \frac{\langle n_\alpha(1-n_\beta)\rangle_1 D_2\Gamma_2 + \langle n_\beta(1-n_\alpha)\rangle_2 D_1\Gamma_1}{2\pi[(\omega-\omega_{\beta\alpha})^2 + (\Gamma_1+\Gamma_2)^2/4]} . \tag{70}$$

In the case of $\omega_{\beta\alpha} \gg \Gamma$, $\omega \approx 0$ eq. (70) coincides with the perturbation theory result [equations (30)-(33) and (27) of Flambaum (1993)]:

$$\overline{|\rho^{(12)}_{\alpha\beta}|^2} = \frac{\overline{|V_2|^2}}{\omega^2_{\alpha\beta}}\langle n_\alpha(1-n_\beta)\rangle_1 + \frac{\overline{|V_1|^2}}{\omega^2_{\beta\alpha}}\langle n_\beta(1-n_\alpha)\rangle_2 ,$$

if one recalls that $\Gamma = 2\pi\overline{|V|^2}/D$, and the admixture of the distant component $|\Phi_j\rangle = a^\dagger_\beta a_\alpha|\Phi_i\rangle$ (Φ_i is one of the principal components of Ψ_1) to Ψ_2 is $V/\omega_{\alpha\beta}$.

For the sake of completeness we also present formulae for the mean diagonal matrix elements:

$$\overline{\langle\Psi_1|\hat{\rho}_{\alpha\beta}|\Psi_1\rangle} = \sum_i \overline{C_i^{(1)2}}\langle\Phi_i|a_\alpha^\dagger a_\beta|\Phi_i\rangle = \delta_{\alpha\beta}\langle n_\alpha\rangle_1 \ , \tag{71}$$

$$\overline{\langle\Psi_1|\hat{M}|\Psi_1\rangle} = \sum_{\alpha\beta} M_{\alpha\beta}\overline{C_i^{(1)2}}\langle\Phi_i|a_\alpha^\dagger a_\beta|\Phi_i\rangle = \sum_\alpha M_{\alpha\alpha}\langle n_\alpha\rangle_1 \ , \tag{72}$$

$$\overline{\langle\Psi_1|\hat{V}|\Psi_1\rangle} = \frac{1}{2}\sum_{\alpha\beta\gamma\delta} V_{\alpha\beta\gamma\delta}\overline{C_i^{(1)2}}\langle\Phi_i|a_\alpha^\dagger a_\beta^\dagger a_\gamma a_\delta|\Phi_i\rangle = \frac{1}{2}\sum_{\alpha\beta}(V_{\alpha\beta\beta\alpha} - V_{\alpha\beta\alpha\beta})\langle n_\alpha n_\beta\rangle_1 \ . \tag{73}$$

Let us summarize the results of this section. Using the statistical approach formulae (58), (64) for the mean square matrix elements between compound states have been obtained. The answer is expressed in terms of the parameters of the compound states (N, Γ), the single-particle energies ($\omega_{\alpha\beta}$), and the orbital occupancies [$n_\alpha(1-n_\beta)$, these can be calculated using the Fermi distribution]. In order to apply eqs. (58), (64) one also needs to know the function $\tilde{\delta}$, which depends on the strength functions of the compound states components and has a model Breit-Wigner representation (57). Although, this model may suit to the description of the principal components, its validity for the distant, small components is questionable. This point is extremely important for correct calculation of the PNC matrix elements, since the weak PNC interaction mixes the principal components of one compound states with the small components of the other, and *vice versa* [see secs. 1.1, 1.4, and the discussion after equation (67)]. It will be shown in sec. 2.3 that by taking into account the residual strong interaction an effective induced parity-nonconserving interaction, which mixes the principal components of the compound states can be introduced.

The statistical approach presented above relies heavily on the properties of compound states, such as those given by eqs. (46), (49). These properties are expected to be common for various many-body systems, if the two-body interaction is strong enough to produce "chaos" in the dense spectrum of excited states. In the next section we discuss the results of numerical calculations of chaotic eigenstates of the Ce atom (Flambaum *et al* 1994), as well as those of nuclear shell-model calculations by Horoi *et al* (1994) for 12 nucleons in the (*sd*) shell, and by Auerbach and Brown (1994) for ^{9}Be and ^{9}B. This allows us to check the assumptions usually made in statistical theories of compound states, to study the behaviour of the strength function beyond (49), to check the validity of the mean square matrix element calculation, and to demonstrate the existence of enhancement of small perturbations.

2.2 Numerical Experiment: Compound States in Atoms and Nuclei

It is a well known fact that rare-earth atoms have very complicated spectra (Martin *et al* 1978), and exhibit Wigner-Dyson statistics of energy levels at excitation energies above 2 eV (Camarda and Georgopulos 1983). These atoms have several electrons in open shells and the structure of corresponding eigenstates is expected to be similar to that of compound states in nuclei. On the other hand the number of basis configurations in atoms is much smaller than that in nuclei near the neutron threshold. This makes atomic calculations much more feasible and realistic, and allows one to control the results against the experimental spectra measured at all energies from the ground state well into the compound states region.

The Ce atom ($Z = 58$) contains 4 particles in open shells. There are 7 orbitals involved: $4f_{5/2}$, $4f_{7/2}$,

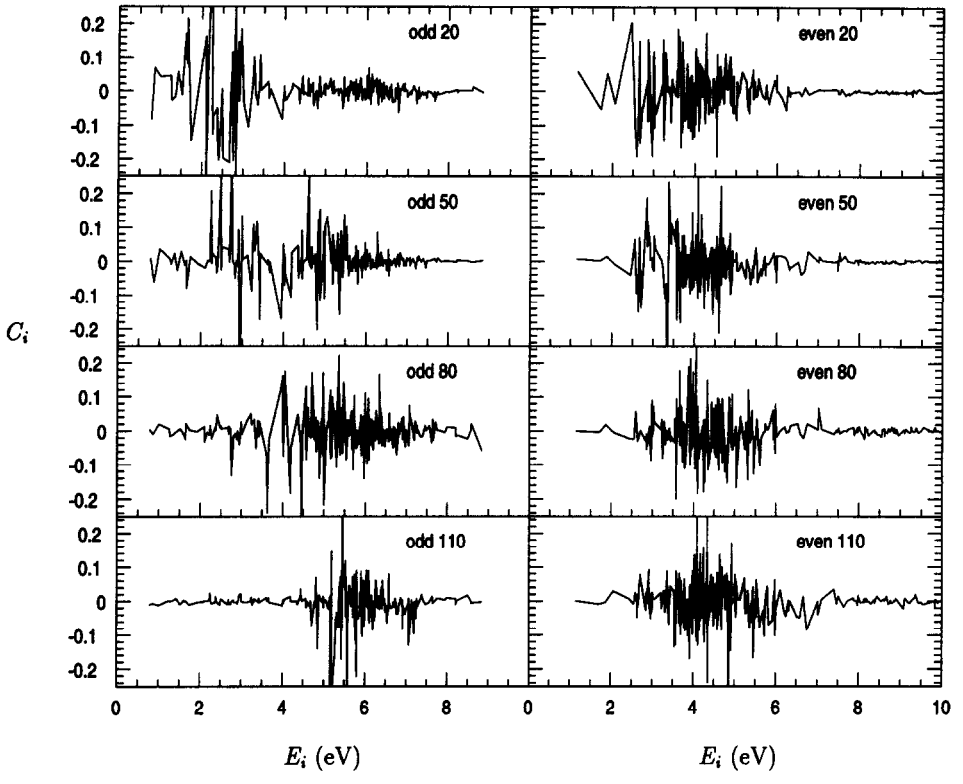

Figure 1: Odd and even $J = 4$ eigenstates of Ce. Shown are the eigenstates' components C_i in the basis of Φ_{Ji} states vs the energies of the basis states $E_i \equiv H_{ii}$.

$6s_{1/2}$, $5d_{3/2}$, $5d_{5/2}$, $6p_{1/2}$, $6p_{3/2}$. We studied $J^\pi = 4^-$, 4^+ manifolds, which contained 260 and 276 states respectively. The Hamiltonian matrices $H_{ik} = \langle \Phi_{Ji}|\hat{H}|\Phi_{Jk}\rangle$ were calculated using the basis of Φ_{Ji} states constructed of the Hartree-Fock orbitals. Statistical analysis of the matrices showed that the dependence of the off-diagonal matrix elements H_{ik} upon i and k is almost random. Since there are 4 particles coupled by the two-body interaction about 40% of the matrix elements are zeros. The distribution of the nonzero matrix elements can be approximated by $P(H_{ik}) \propto |H_{ik}|^{-1/2} e^{-|H_{ik}|/V}$, where $V = 0.12$ eV is the characteristic value of the off-diagonal matrix element. We observed that larger matrix elements are mainly concentrated along the main diagonal thus imposing a band-like structure on the matrix with a bandwidth $b \simeq 80$ (see Flambaum *et al* 1994, Gribakina *et al* 1995 for details). Therefore we can compare our results with predictions of the band random matrix model (Wigner 1955). The average spacing between the basis state energies $E_i \equiv H_{ii}$ is $D \simeq 0.03$ eV, which is much smaller than V. This means that basis states are strongly mixed by the residual interaction V. Indeed, the eigenstates $|\Psi_\lambda\rangle = \sum_i C_i^{(\lambda)} |\Phi_{Ji}\rangle$ are "chaotic" superpositions of large numbers ($N \sim 100$) of basis states with $\overline{C_i} = 0$ (see Fig. 1).

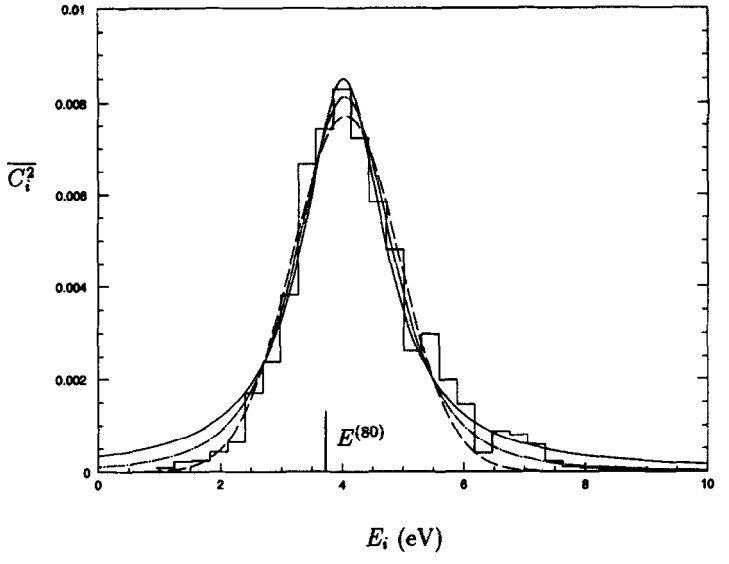

Figure 2: Fitting $\overline{C_i^2}$ with $w(E_i; E, \Gamma, N)$ for the 80th even eigenstate. The least-square Breit-Wigner (solid curve), squared Breit-Wigner (dash-dot line), and interpolation exponential (dashed curve) fits are shown.

To apply the statistical approach of sec. 2.1 we need to know the strength function (48), or the distribution of the mean-square components $w(E_i; E, \Gamma, N)$. This also gives the number of principal components N and the spreading width Γ. In order to find them we performed local averaging of C_i^2 over 19 neighbouring eigenstates. A typical result of this procedure is shown in Fig. 2. Since each of the bins used to calculate $\overline{C_i^2}$ contains about 10^2 components from 19 eigenstates, fluctuations of about 10% are to be expected. The observed rate of fluctuations agrees with the existence of a smooth curve $w(E_i)$ behind the histogram shown. In Fig. 2 we show the least-square fit of the $\overline{C_i^2}$ histogram with a model Breit-Wigner function $w(E_i; E + \Delta E, \Gamma, N)$ of (49) [3]. This fit yields $N = 118$ and $\Gamma = 1.64$ eV. The latter value of the spreading width is in good agreement with the model estimate: $\Gamma = 2\pi V^2/D \simeq 2$ eV. By fitting $\overline{C_i^2}$ for other eigenstates in the spectrum we found the energy dependence of N and Γ (see Flambaum *et al* 1994 for details).

Despite an overall reasonable agreement of the Breit-Wigner fit with $\overline{C_i^2}$ one may notice that the latter shows faster decrease at the wings of the central maximum. Note that at $|E - E_i| > \Gamma$ the approximation (49) reproduces the first order perturbation theory result $\overline{C_i^2} \simeq \frac{V^2}{(E-E_i)^2}$ (it also requires $|E - E_i| \ll Db$ in the Wigner's BRM). If the Hamiltonian matrix has a band-like structure the coupling of states outside the band happens in higher orders of the perturbation theory, which, of course, display a faster decrease

[3] ΔE is introduced to account for a regular low energy displacement of the eigenvalue with respect to the maximum of $\overline{C_i^2}$, which is a manifestation of uncompensated level repulsion near the lower edge of the spectrum. It corresponds to the second order perturbation theory energy shift $\Delta E = \sum_i \frac{V_i^2}{E - E_i}$.

with energy. For example, the BRM model (Wigner 1955) predicts a modified exponential drop[4]:

$$w(E_i;E,\Gamma,N) \propto \exp\left\{-2\xi \ln\left(\xi e^{-1}\sqrt{2q^{-1}\ln[\xi/\sqrt{q}]}\right)\right\}, \quad \text{where} \quad \xi = \frac{|E-E_i|}{Db}\,, \quad q = \frac{V^2}{D^2 b}\,. \tag{74}$$

To check this and to estimate the quality of the fit two other approximations have been tried. Introducing the shape function $f(\varepsilon)$: $w(E_i;E+\Delta E,\Gamma,N) = \frac{1}{N} f(\varepsilon)$, where $\varepsilon \equiv \frac{E_i-E-\Delta E}{\Gamma}$, they are characterized by $f(\varepsilon) = (1+4\varepsilon^2)^{-2}$ (squared Breit-Wigner fit), and $f(\varepsilon) = \exp\left(1-\sqrt{1+4\varepsilon^2}\right)$ (interpolation exponential fit), while $f(\varepsilon) = (1+4\varepsilon^2)^{-1}$ corresponds to the Breit-Wigner fit (49). The squared Breit-Wigner shape takes into account the fact that outside the bandwidth the coupling of states happens by means of the next, second, order of perturbation theory. A detailed statistical analysis shows that the quality of the fits is almost the same around the maximum. However, at the tails the drop of the Breit-Wigner curve is too slow, whereas that of the exponential one is too fast.

To make this feature more obvious $\overline{C_i^2}$ is plotted in Fig. 3 using semilogarithmic scale. It is clear that the decrease of $\overline{C_i^2}$ at $|E_i - E| > \Gamma$ is much steeper than that predicted by the Breit-Wigner model. However, good agreement with the asymptotic formula (74) is observed in a certain energy range. The exception is a prominent high-energy shoulder for the numerical $\overline{C_i^2}$ values due to the perturbative mixing of some distant configurations. Therefore, we see that whereas the Breit-Wigner model for $w(E_i;E,\Gamma,N)$ correctly describes the principal components of the eigenstates, the mixing of distant states (small components) is more complicated. It depends on the structure of the Hamiltonian matrix (the existence of an effective band b), and should rather be handled by means of the perturbation theory.

These results are in agreement with the (sd)-shell model nuclear calculations (Horoi *et al* 1994, Zelevinsky 1994). They showed that $\overline{C_i^2}$ decreases faster than the Breit-Wigner curve and much slower than a Gaussian one. We would like also to quote from another nuclear study (French *et al* 1988) which stressed that 'spreadings due to interactions between configurations which are very far apart in energy must not be treated by statistical methods, these being appropriate only for strongly interacting subspaces. The proper procedure is to ignore such interactions or treat them in the lowest-order perturbation theory (which itself supplies a criterion to distinguish strongly from weakly interacting configurations)'.

One of the main goals of the numerical experiment on Ce was to check the statistical approach to calculation of the mean square matrix element [formula (54)]. Having in mind to calculate the matrix elements of a parity-violating pseudoscalar operator like that of (36), let us consider the simplest zero-rank reduced density matrix operator $\hat{\rho}^0_{nlj,n'l'j} = \sum_m \hat{\rho}_{nljm,n'l'jm} = \sum_m a^\dagger_{nljm} a_{n'l'jm}$. Then one obtains instead of (54), (68):

$$\overline{\left(\rho^{(12)0}_{nlj,n'l'j}\right)^2} = \begin{cases} \langle n_{nlj}(1-\frac{n_{n'l'j}}{2j+1})\rangle_1 D_2\ \tilde{\delta}(\Gamma_1,\Gamma_2,\Delta)\,, & \text{(a)} \\ \langle n_{n'l'j}(1-\frac{n_{nlj}}{2j+1})\rangle_2 D_1\ \tilde{\delta}(\Gamma_1,\Gamma_2,\Delta)\,, & \text{(b)} \end{cases} \tag{75}$$

where $\Delta = E_2 - E_1 - \omega_{n'l'j,nlj}$, and n_{nlj} is the occupancy of the nlj orbital, given by the expectation value of the operator $\hat{n}_{nlj} = \sum_m a^\dagger_{nljm} a_{nljm}$.

In Figs. 4 and 5 the statistical-theoretical r.m.s. matrix elements obtained from eq. (75) are compared

[4]This formula is different from the asymptotic solution (35a) in (Wigner 1955), since the latter is incorrect. The derivation of the correct expression (74) is given in (Flambaum *et al* 1994).

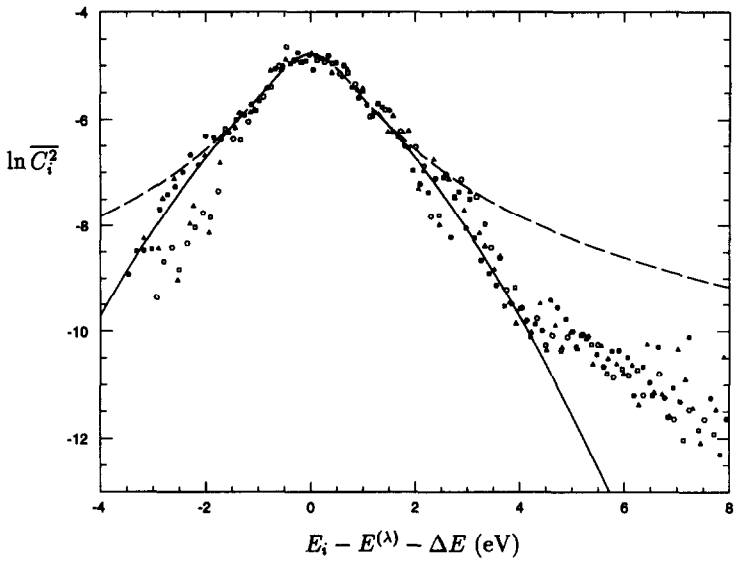

Figure 3: Semilogarithmic plot of the window-averaged $\overline{C_i^2}$ for the $J^\pi = 4^+$ levels: 60th (open triangles), 70th (open squares), 80th (open hexagons), 90th (solid triangles), 100th (solid squares), and 110th (solid hexagons). The asymptotic behaviour (74) with $V = 0.114$ eV, $D = 0.032$ eV, and $b = 80$ ($q = 0.16$) is shown by solid curve. Dashed line is the Breit-Wigner approximation (49) ($N = 120$, $\Gamma = 1.8$ eV).

with those obtained by locally averaging the true matrix elements between the eigenstates. The comparison made for a number of single-particle transitions $nlj - n'l'j'$ generally confirms the validity of the statistical approach of sec. 2.1 to calculation of the matrix elements. One may notice that in a number of cases the matrix elements obtained via the statistical approach reproduce quite subtle features of the curves from the direct numerical calculations. There is also a reasonable overall agreement between the two answers: (75a), and (75b). Some of the data indicate that a linear combination of the two formulae (75), or (54) and (68), might often yield a better result.

We should add that we also examined the statistics of the eigenstate components, normalized within each bin of Fig. 2 as $C_i/\sqrt{\overline{C_i^2}}$, and that of the matrix elements $\rho^{(\lambda\mu)0}_{nlj,n'l'j}$ between the compound states. We observed that with the excitation energy increasing the eigenstates become "more chaotic" (larger N's), and the above mentioned statistics tend towards Gaussian limit.

Let us now consider the admixture of the state Ψ_λ to the state Ψ_μ due to the effect of a perturbation $\hat{M}$. The magnitude of the admixture is given by:

$$\eta = \left| \frac{\langle \Psi_\lambda | \hat{M} | \Psi_\mu \rangle}{E^{(\lambda)} - E^{(\mu)}} \right| . \tag{76}$$

According to the estimates made in sec. 1.1, this quantity must be dynamically enhanced. The dynamical enhancement factor for the Ce levels at 2–3 eV is estimated at $\sqrt{N} \sim 10$. The numerical model

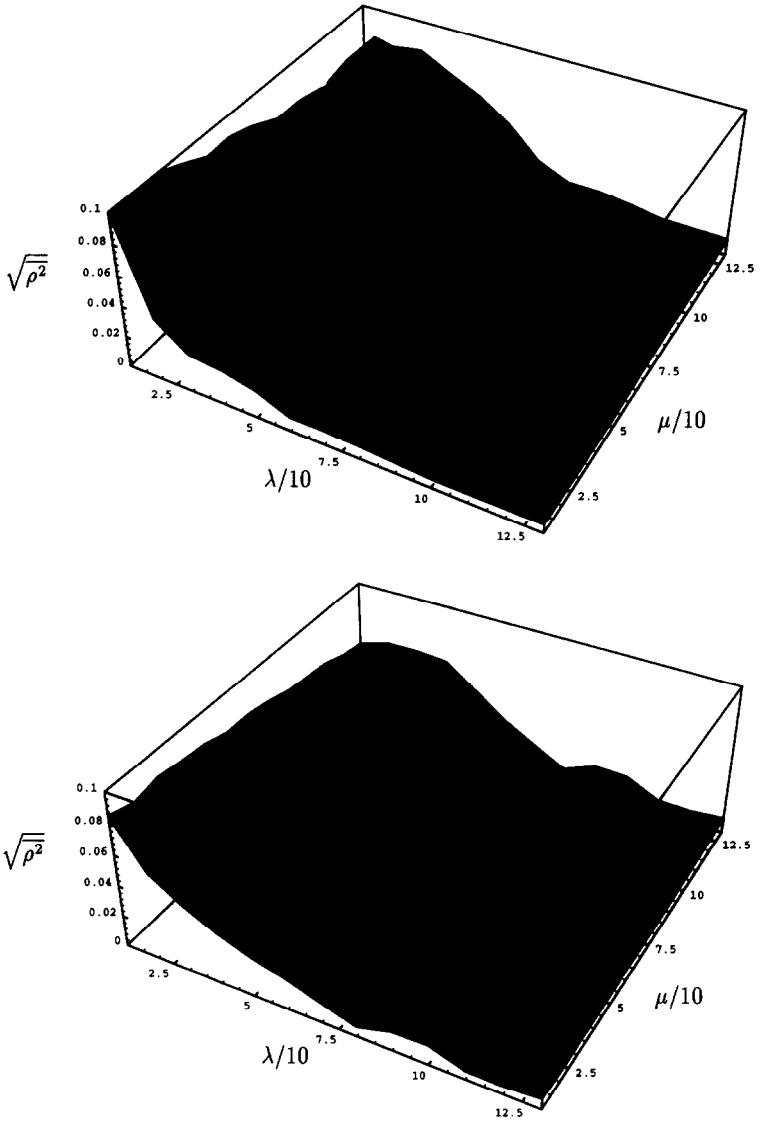

Figure 4: Comparison of the numerical calculation of the matrix elements $\left[\overline{(\rho^{(\lambda\mu)0}_{6s_{1/2},6p_{1/2}})^2}\right]^{1/2}$ ($j = 1/2$, $J = 4$) between chaotic states with the results of the statistical theoretical approach. Upper graph: window-averaged matrix element from the numerical calculations. Lower graph: obtained from eq. (75a) using the Breit-Wigner approximation for $w(E_i; E, N, \Gamma)$.

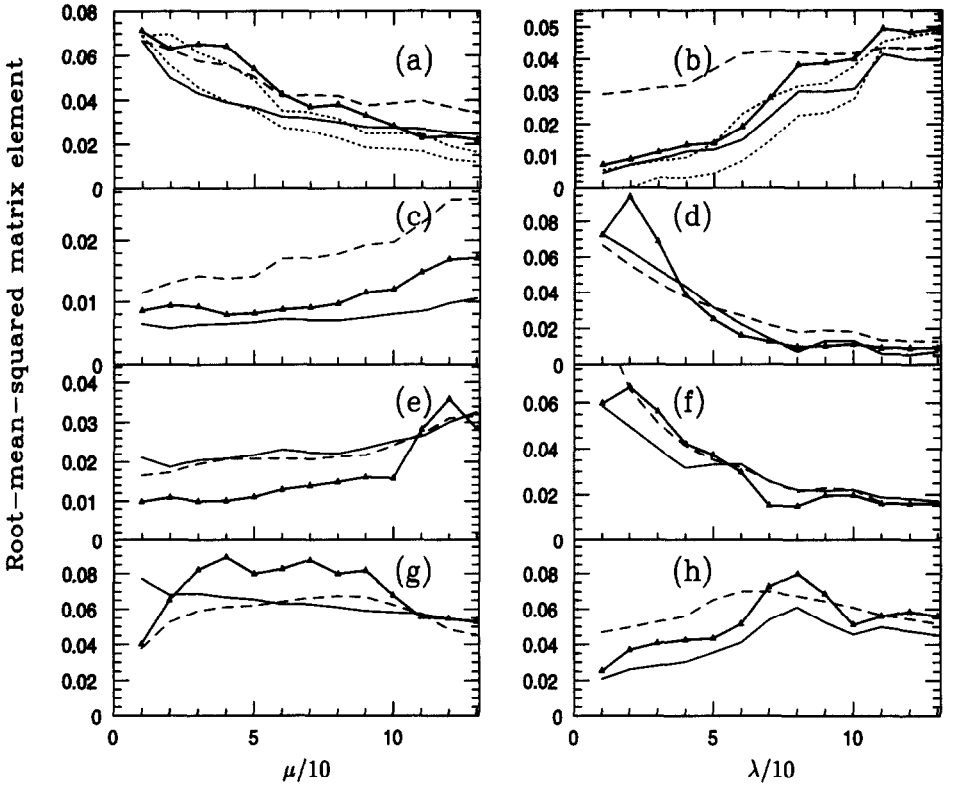

Figure 5: Comparison between the direct calculation (solid triangles) of the r.m.s. matrix elements of the reduced density matrix operator $\left[\left(\rho^{(\lambda\mu)0}_{nlj,n'l'j}\right)^2\right]^{1/2}$ and the results obtained from formulae (75a) (solid curve) and (75b) (dashed curve) using the Breit-Wigner approximation for $w(E_i; E, N, \Gamma)$. Left column: odd state $\lambda = 80$; right column: even state $\mu = 80$. The figures correspond to the following transitions $nlj - n'l'j$: a,b - $6p_{1/2} - 6s_{1/2}$; c,d - $6s_{1/2} - 6p_{1/2}$; e,f - $5d_{5/2} - 4f_{5/2}$; g,h - $4f_{5/2} - 5d_{5/2}$. Dotted curves in figures a and b show the results for the squared Breit-Wigner $w(E_i; E, N, \Gamma)$.

considered in this section enables us to verify the existence of dynamical enhancement. As an example, we calculated the mixing coefficients between the 21–70 odd levels and the 1–140 even levels using the mixing operator $\hat{M} = \hat{\rho}^0_{6s_{1/2}6p_{1/2}}$. For each of the 50 odd levels the 140 mixing coefficients η (76) were calculated, and we chose the maximal of them. Usually it corresponded to the mixing of the odd level with the closest even one. The distribution of the resulting 50 values of η is presented in Fig. 6.

A simple analytical approximation can be derived to describe the distribution of η. If one considers the mixing of states of different J^π manifolds, it is a reasonable assumption that the spacing between the nearest levels $|E^{(\lambda)} - E^{(\mu)}|$ obeys Poissonian statistics (no level repulsion). Assuming further that the

numerator in (76) has a typical magnitude of M_0, one obtains the following probability density:

$$f(\eta) = \frac{\eta_0}{\eta^2} e^{-\eta_0/\eta} , \tag{77}$$

where $\eta_0 = M_0/D$ gives the typical magnitude of mixing, and D is the average spacing between nearest levels from the different manifolds. It is worth noting that the distribution (77) has an infinite mean $\overline{\eta} = \infty$, since the corresponding integral diverges as $\int d\eta/\eta$. This means that the number of large values of η is large. The probability to observe $\eta \geq \eta_1$ is $P(\eta > \eta_1) \simeq \eta_0/\eta_1$ (provided $\eta_1 \gg \eta_0$). The model distribution (77) is used in Fig. 6 to fit the histogram, producing $\eta_0 = 1.15$ eV^{-1}.

To demonstrate the existence of enhancement, let us find out the magnitude of the single-particle mixing $\eta_{\rm sp}$, which one might expect in a sparse, "regular" spectrum of a system with one valence particle. In this case the matrix element of $\hat{\rho}^0_{6s_{1/2}6p_{1/2}}$ is equal to 1, and the mixing coefficient is $\eta_{\rm sp} = 1/\omega_{6p_{1/2}6s_{1/2}} \simeq 0.5$ eV^{-1}. Thus, we see that the characteristic mixing $\eta_0 = 1.15$ eV^{-1} is greater than $\eta_{\rm sp}$ by a factor of 2.3 (dynamical enhancement). The dynamical enhancement factor in our example turned out to be smaller than the potential value of $\sqrt{N} \simeq 10$. This can be understood from (75), since both $\tilde{\delta}$ and the occupancy factor in it are smaller than their maximal values. A very important feature of Fig. 6 is that some particular values of η exceed $\eta_{\rm sp}$ by one or even two orders of magnitude. These large values are due to fluctuations in the energy denominator of η (76). This gives a possibility of very small denominators, and hence, very large mixing (*statistical enhancement*, see sec. 4). The average value of enhancement corresponding to the set of data in Fig. 6 is $\overline{\eta}/\eta_{\rm sp} \simeq 13$, mostly due to statistical enhancement.

There was a special nuclear shell-model calculation of the light nuclei ^{9}B and ^{9}Be devoted to a search for dynamical enhancement of the weak interaction (Auerbach and Brown 1994). Using $0s$, $0p$, $1s0d$, and $1p0f$ oscillator orbitals and the WBT interaction of Warburton and Brown (1992) they obtained 647 and 3266 $J^\pi = 1/2^-,\ 1/2^+$ levels respectively. Then, the admixtures of 500 even levels to 20–40 odd levels produced by the weak potential $w = \epsilon_T \boldsymbol{\sigma}\mathbf{p}$ were evaluated. As expected, the single particle mixing in this system is very small: $\eta_{\rm sp} \simeq 2 \times 10^{-7}$. The typical mixing of compound states $\eta_0 = $ r.m.s.$(w)/D$ was found to be 13 times larger, which confirms the existence of dynamical enhancement in this system. The authors say that there is a qualitative agreement for the dynamical enhancement factor with the estimate $\sqrt{N} \sim 10$. We should note that the data in Table 1 of (Auerbach and Brown 1994) demonstrates also the effect of statistical enhancement, particular values of admixture exceeding $\eta_{\rm sp}$ 100 times (the median enhancement of about 30). Unfortunately, no comparison with statistical theory for matrix elements between compound states is presented.

Finally, we would like to mention other important results obtained by Horoi *et al* (1994). They demonstrated the similarity between the information entropy of individual eigenfunctions $S^\lambda = -\sum_i (C_i^\lambda)^2 \ln[(C_i^\lambda)^2]$ and the thermodynamic entropy found from the level density[5]. They also showed that despite the strong nucleon interaction the occupancies of the single-particle orbitals agree with the Fermi-Dirac distribution and there is a strong correspondence between chaos and thermalization, including a consistent way of defining temperature for the chaotic many-body system. In fact this may

[5]We should mention that Flambaum *et al* (1994) showed that in Ce the entropy localization length $L_H^\lambda \simeq 2.075 \exp(S^\lambda)$ (Casati *et al* 1990) of compound states is related to the number of principal components by $L_H^\lambda \simeq 1.4 N_\lambda$.

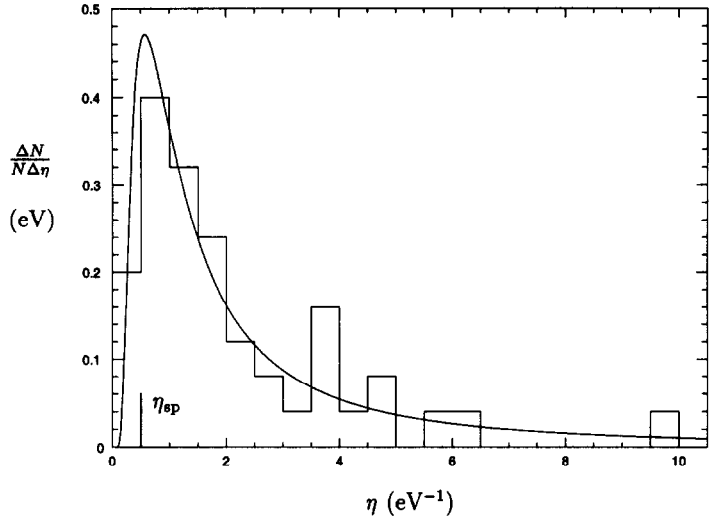

Figure 6: Distribution of the maximal mixing $\eta = \max_\mu \left\{ \left| \rho^{(\lambda\mu)0}_{6s_{1/2}6p_{1/2}} / (E^{(\mu)} - E^{(\lambda)}) \right| \right\}$, $(\mu = 0 - 140)$, for the 50 odd levels $\lambda = 20 - 70$. The histogram is fitted by $f(\eta) = \eta_0 \eta^{-2} \exp(-\eta_0/\eta)$ with $\eta_0 = 1.15$ eV^{-1}. The results of the χ^2-square test for the first 4 and 10 bins are: $\chi^2(3) = 0.45$, $\chi^2(9) = 6.21$. Also shown is the magnitude of the single-particle mixing $\eta_{sp} = 0.5$ eV^{-1}. Five η values of 50 fall beyond $\eta = 10$: $\eta = 12.5,\ 20.4,\ 37.7,\ 41.8,\ 98.0$.

be viewed as a justification of our numerical approach to the calculation of matrix elements between compound states in nuclei [see eqs. (58)–(64) and sec. 2.4].

2.3 Induced Parity-Nonconserving Interaction

This section is based mostly on the results of Flambaum and Vorov (1993,1995a), and Flambaum (1994a). Similar results were later obtained by Johnson and Bowman 1995 within the framework of a doorway state approach (see sec. 2.5). The magnitude of PNC effects depend on the weak interaction matrix elements between compound states. There are two sources of the PNC effects: the single-particle weak potential w (36), which describes the interaction of a nucleon with the weak mean field of the nucleus and the residual two-particle weak interaction W (35). In principle, the matrix elements of w and W should be calculated with respect to the true eigenstates of the strong interaction Hamiltonian. However, in practice some truncated set of basis states is used to describe physical states at excitation energies smaller than the gap between single-particle shells. For example, describing nuclear compound states and the parity-violating mixing of them it is natural (Johnson *et al* 1991, Flambaum and Vorov 1993) to take only the principal components into account. The number of these components is already 10^5 in compound nuclei. The principal components have energies close to the energy of the compound state, dominate the normalization sum and are built of the valence-shell (open) orbitals. As is known, the latter do not contain opposite parity orbitals with the same angular momentum, which can be coupled by the single-particle weak potential w. Thus, the matrix element of w between the compound states is zero in the principal-component approximation (Zaretsky and Sirotkin 1983, 1987, Kadmensky

et al 1983).

To calculate the matrix element of w correctly one has to take "small" components into account, i.e., consider the transitions between the single-particle orbitals α, β of opposite parity and identical angular momentum, belonging to different shells. Therefore, for the P-odd (or a P,T-odd) interaction $|\omega_{\beta\alpha}| = |\epsilon_\beta - \epsilon_\alpha| \sim 5$–$10$ MeV $\gg \Gamma$. We have seen in sec. 2.2 that the Breit-Wigner approximation (49) for $C_i^{(\lambda)2}$ is practically not applicable at the tails, where $|E_\lambda - E_i| \sim |\omega_{\beta\alpha}| \gg \Gamma$. However, one can easily find the necessary admixture of the small components Φ_i using the first order perturbation theory in the residual strong interaction V:

$$|\Psi_\lambda\rangle = |\tilde{\Psi}_\lambda\rangle + \sum_i |\Phi_i\rangle \frac{\langle\Phi_i|V|\tilde{\Psi}_\lambda\rangle}{E_\lambda - E_i} , \tag{78}$$

where $\tilde{\Psi}_\lambda$ is the principal-component part of the compound state, and the sum runs over the distant components not included in $\tilde{\Psi}_\lambda$ ($\langle\Phi_i|\tilde{\Psi}_\lambda\rangle = 0$). Now we can calculate the matrix element of w between the close opposite parity compound states Ψ_λ and Ψ_μ:

$$\langle\Psi_\lambda|w|\Psi_\mu\rangle = \sum_k \frac{\langle\tilde{\Psi}_\lambda|w|\Phi_k\rangle\langle\Phi_k|V|\tilde{\Psi}_\mu\rangle}{E - E_k} + \sum_i \frac{\langle\tilde{\Psi}_\lambda|V|\Phi_i\rangle\langle\Phi_i|V|\tilde{\Psi}_\mu\rangle}{E - E_i} , \tag{79}$$

where $E_\lambda \approx E_\mu \equiv E$.

The single-particle weak potential (36) can be simplified, if we use the approximation of constant density $\rho(r) \simeq \rho_0$ inside the nucleus:

$$w = \frac{Gg}{2\sqrt{2}m}\{(\boldsymbol{\sigma}\mathbf{p})\rho(r) + \rho(r)(\boldsymbol{\sigma}\mathbf{p})\} \simeq \frac{\xi}{m}\boldsymbol{\sigma}\mathbf{p} , \tag{80}$$

$$\text{where} \qquad \xi = \frac{Gg}{2\sqrt{2}}\rho_0, \qquad \rho_0 = \frac{2p_F^3}{3\pi^2} , \tag{81}$$

and $g = g_p, g_n$ and $\xi = \xi_p, \xi_n$, depending on the nucleon considered. Further simplifications are possible if we use the relation

$$\mathbf{p} = im[H_0, \mathbf{r}] , \tag{82}$$

where $[\ldots]$ is the commutator, and $H_0 = \mathbf{p}^2/2m + U(r)$ is the single-particle Hamiltonian of the nucleus [writing the commutator we neglected the spin-dependent part of the strong nuclear potential $U(r)$]. Then the first term in the right hand side of (79) can be transformed as follows:

$$\sum_{ki} \frac{C_i^{(\lambda)}\langle\tilde{\Phi}_i|[H_0, \mathbf{r}]|\Phi_k\rangle\langle\Phi_k|V|\tilde{\Psi}_\mu\rangle}{E - E_k} = \sum_{ki} \frac{C_i^{(\lambda)}(E_i - E_k)\langle\tilde{\Phi}_i|\mathbf{r}|\Phi_k\rangle\langle\Phi_k|V|\tilde{\Psi}_\mu\rangle}{E - E_k} \simeq \langle\tilde{\Psi}_\lambda|\mathbf{r}V|\tilde{\Psi}_\mu\rangle ,$$

where we used the expansion of $\tilde{\Psi}_\lambda$ in terms of its principal components $\tilde{\Phi}_i$: $|\tilde{\Psi}_\lambda\rangle = \sum_i C_i^{(\lambda)}|\tilde{\Phi}_i\rangle$, replaced $E_i - E_k$ with $E - E_k$ in the numerator, since $|E_i - E| \sim \Gamma \ll |E - E_k|$ for the principal components i, and used closure to sum over k. Proceeding similarly with the second term of (79) we can express the matrix element of w between the compound states via the matrix element between their principal-component parts:

$$\langle\Psi_\lambda|w|\Psi_\mu\rangle = \langle\tilde{\Psi}_\lambda|\sum_a [i\xi_a\boldsymbol{\sigma}_a\mathbf{r}_a, V]|\tilde{\Psi}_\mu\rangle , \tag{83}$$

where the sum runs over the nucleons (in fact only the nucleons near the Fermi surface contribute to this sum, see below). Now we can define the induced parity-nonconserving interaction (IPNCI)

$$V^{\mathrm{IPNCI}} = i\sum_a [\xi_a \boldsymbol{\sigma}_a \mathbf{r}_a, V] \tag{84}$$

which describes the effective coupling of the principal components of compound states due to the weak potential w.

We should note that in deriving formula (83) for the IPNCI some approximations were used (the constant nuclear density, and spin-independent Hamiltonian H_0). When doing numerical calculations these approximations are not necessary. Instead, one can consider the weak potential w as a perturbation. It can be taken into account in the single-particle orbitals: $|\bar{\alpha}\rangle = |\alpha\rangle + \sum_{\alpha'} |\alpha'\rangle\langle\alpha'|w|\alpha\rangle/(\epsilon_\alpha - \epsilon_{\alpha'})$. Thus, we can express the result in terms of the residual two-particle strong interaction V renormalized by the weak interaction ($V^{\mathrm{IPNCI}}_{\alpha\beta\gamma\delta} \equiv \langle\alpha\beta|V^{\mathrm{INPCI}}|\gamma\delta\rangle = \langle\bar{\alpha}\bar{\beta}|V|\bar{\gamma}\bar{\delta}\rangle$):

$$V^{\mathrm{IPNCI}}_{\alpha\beta\gamma\delta} = \sum_{\alpha'} \frac{w_{\alpha\alpha'}V_{\alpha'\beta\gamma\delta}}{\epsilon_\alpha - \epsilon_{\alpha'}} + \sum_{\beta'} \frac{w_{\beta\beta'}V_{\alpha\beta'\gamma\delta}}{\epsilon_\beta - \epsilon_{\beta'}} + \sum_{\gamma'} \frac{V_{\alpha\beta\gamma'\delta}w_{\gamma'\gamma}}{\epsilon_\gamma - \epsilon_{\gamma'}} + \sum_{\delta'} \frac{V_{\alpha\beta\gamma\delta'}w_{\delta'\delta}}{\epsilon_\delta - \epsilon_{\delta'}}\,, \tag{85}$$

where $w_{\alpha\alpha'} \equiv \langle\alpha|w|\alpha'\rangle$, etc. The effective P-odd two-body interaction V^{IPNCI} enables one to express the parity-violating matrix element between the compound states [see eq. (64)] in terms of the matrix elements (85) between valence-shell single-particle orbitals. Using (80), (82) one can show that in the constant density approximation (85) is the matrix element of the V^{IPNCI} operator (84).

The approximate analytical expression (84) is convenient to study the coordinate, spin, and isospin structure and the strength of the IPNCI. It will be shown that the IPNCI is an order of magnitude stronger than the residual two-particle weak interaction W. To find the explicit form of the IPNCI, the Landau-Migdal parametrization of the strong interaction can be used:

$$V(1,2) = C\delta(\mathbf{r}_1 - \mathbf{r}_2)[f + f'\boldsymbol{\tau}_1\boldsymbol{\tau}_2 + h\boldsymbol{\sigma}_1\boldsymbol{\sigma}_2 + h'(\boldsymbol{\tau}_1\boldsymbol{\tau}_2)(\boldsymbol{\sigma}_1\boldsymbol{\sigma}_2)]\,, \tag{86}$$

where $C = \pi^2/p_F m = 300\ \mathrm{MeV}\times\mathrm{fm}^3$ is the universal Migdal constant (Migdal 1967) and the parameters f, f', h, h' are in fact functions of r via density dependence, e.g., $f = f_{\mathrm{in}} - (f_{\mathrm{ex}} - f_{\mathrm{in}})[\rho(r) - \rho(0)]/\rho(0)$. Values of f_{in} and f_{ex} characterize the strength of the interaction inside the nucleus and on its surface, respectively). The interaction (86) dates back to the Fermi liquid theory by Landau (Landau 1958). The numerical values of the parameters widely used for heavy nuclei are (see Migdal 1967, Brown 1971, Khodel and Saperstein 1982): $f_{\mathrm{in}} = -0.075$, $f_{\mathrm{ex}} = -1.95$, $f'_{\mathrm{in}} = 0.675$, $f'_{\mathrm{ex}} = 0.05$, $h_{\mathrm{in}} = h_{\mathrm{ex}} = 0.575$, and $h'_{\mathrm{in}} = h'_{\mathrm{ex}} = 0.725$.

Calculating the commutator in (84) one obtains:

$$\begin{aligned} i\sum_{a=1,2} [\xi_a \boldsymbol{\sigma}_a \mathbf{r}_a, V] = 2\ C\xi_\tau \delta(\mathbf{r}_1 - \mathbf{r}_2)[(h' - h)(\tau_{1z} - \tau_{2z})\ \mathbf{r}_1 \cdot (\boldsymbol{\sigma}_2 \times \boldsymbol{\sigma}_1) \\ +\ (h' - f')(\boldsymbol{\tau}_2 \times \boldsymbol{\tau}_1)_z \mathbf{r}_1 \cdot (\boldsymbol{\sigma}_1 - \boldsymbol{\sigma}_2)]\,, \end{aligned} \tag{87}$$

where ξ_τ is defined by $\xi = \xi_0 + \xi_\tau\tau_z$, and $\tau_z = -1(+1)$ is the isospin projection for protons (neutrons), so that $\xi_\tau = (\xi_n - \xi_p)/2$. The first term in (87) induces $pn \to pn$ transitions, while the second one, $pn(np) \to np(pn)$. For contact interactions, the second term (which is in fact the exchange term to the

first one) can be reduced to the first term by means of the Fierz transformation (see, e.g., Okun 1982), yielding

$$V^{\rm IPNCI}(1,2) = \frac{Q}{2}\,\delta(\mathbf{r}_1-\mathbf{r}_2)(\tau_{1z}-\tau_{2z})\,\mathbf{r}_1\cdot(\boldsymbol{\sigma}_2\times\boldsymbol{\sigma}_1) \;\longrightarrow\; Q\mathbf{r}_p(\boldsymbol{\sigma}_p\times\boldsymbol{\sigma}_n)\delta(\mathbf{r}_p-\mathbf{r}_n)\;, \qquad (88)$$

$$\text{where}\quad Q = 2C(\xi_n-\xi_p)(f'-h) = \frac{4}{3}\,\frac{p_F^2}{m}\,\frac{G}{\sqrt{2}}(g_p-g_n)(h-f')\;.$$

We stress that this expression is valid within the nucleus only (recall that $Q\propto\xi\propto\rho$). When using this expression one has to assume that the exchange term $pn\to np$ is excluded. However, the conventional choice of the parameters of the Landau-Migdal interaction assumes the same. This means that the second term in expression (87) for the IPNCI should simply be omitted (to avoid double counting) and the final expression for the IPNCI includes the $pn-pn$ interaction only. Therefore, the constant in the IPNCI (88) should be given by

$$Q = 2(\xi_n-\xi_p)(h'-h)C = \frac{4}{3}\,\frac{p_F^2}{m}\,\frac{G}{\sqrt{2}}\,(g_p-g_n)h_{pn}\;, \qquad (89)$$

where $h_{pn}=h-h'$ is the constant of the residual strong proton-neutron spin-flip interaction. The problem with the definition of the IPNCI constant arises from the fact that the Landau-Migdal interaction is a phenomenological effective interaction, rather than the true *ab initio* strong interaction. For example, it contains some fictitious spin dependence coming from the Fierz transformation of the exchange term for the spin-independent interaction $C\delta(\mathbf{r}_1-\mathbf{r}_2)$. However, this fictitious spin dependence does not contribute to the IPNCI, since in the case of an initial spin-independent interaction the Fierz transformation gives $h'-h=f'-h=0$. Therefore, only the "real" spin dependence of the strong interaction (e.g., due to π-meson exchange) contributes to the IPNCI.

It is possible now to compare the IPNCI (88), (89) with the initial two-nucleon weak interaction W (35). These interactions have different isotopic and coordinate structure ($V^{\rm IPNCI}$ contains the radius-vector $\mathbf{r}$ instead of the momentum $\mathbf{p}$, or the derivative ∇). Using the nuclear radius $R=r_0A^{1/3}$, where $r_0=1.15$ fm $\sim p_F^{-1}$ is the internucleon distance, we estimate $r\sim R$, $p_Fr\sim p_FR\sim A^{1/3}$, and

$$\frac{V^{\rm IPNCI}}{W}\sim\frac{Qr}{\frac{G}{m}p_F}\sim p_Fr\sim A^{1/3}\;. \qquad (90)$$

For heavy nuclei where neutron-nucleus PNC effects have been measured the nucleon number is $A\simeq 114$–240. Thus, the IPNCI (88) is an order of magnitude stronger than the initial two-body weak interaction W acting within the valence shell. The numerical results for matrix elements of $V^{\rm IPNCI}$ between valence-shell states in the Th-U region and those of the initial interaction W are presented in Appendix C, Table 2. Their comparison on the whole confirms the estimate (90). It is worth mentioning once more that selection rules (change of parity and conservation of the angular momentum) forbid matrix elements of the single-particle weak potential between the valence orbitals presented in Table 2. Therefore, the IPNCI and the residual two-body interaction W are the only sources of parity nonconservation in the compound states within the "principal component" approach. The equations expressing the root mean square matrix element between compound states in terms of the matrix elements of $V^{\rm IPNCI}$ and W from Table 2 were presented in sec. 2.1.

Of course, the explicit form (88) of the IPNCI based on the approximation (83) is semiquantitative. In particular, due to the smallness of $h-h'$ in Q, corrections to (88) may be relatively large for particular

matrix elements. Especially large corrections may come from the interference term (proportional to $g_p g_n$), when calculating the mean square value (64) of the weak matrix element (85) between compound states. This quantity is a sum of products of the matrix elements between nucleon orbitals:

$$\overline{|\langle\Psi_1|V^{\rm IPNCI}|\Psi_2\rangle|^2} \propto \sum V^{\rm IPNCI}_{\alpha\beta\gamma\delta} V^{\rm IPNCI}_{\delta\gamma\beta\alpha} \propto \sum V_{\alpha'\beta\gamma\delta} V_{\delta\gamma\beta'\alpha} w_{\alpha\alpha'} w_{\beta'\beta} + \dots \ .$$

The coefficients before g_p^2 and g_n^2 in this sum are positive, and the result is stable. On the other hand, the coefficients before the interference term proportional to $g_p g_n$ are not necessarily of the same sign and the result tends to decrease after the summation (in comparison with the terms proportional to g_p^2 and g_n^2). Therefore, the result for the mean square matrix element is proportional to $g_p^2 + g_n^2$ with a somewhat smaller coefficient before $g_p g_n$, rather than to $(g_p - g_n)^2$ [as it would appear from the strength constant Q (89) of the approximate IPNCI (88)].

Numerical calculations of the r.m.s. matrix elements between compound states show that the contribution of the IPNCI (88), (89) is about 7–12 times greater than direct contribution of the initial two-body weak interaction W (35), thus confirming the estimate (90).

It should be emphasized that formulae (84) and (88) for the IPNCI have been obtained using perturbation theory considerations [see eq. (78), (79)]. Indeed, the IPNCI (84) is of the first order in residual strong interaction V. The results of the all-order treatment are presented in Appendix C. However, the "self-consistency" (RPA) iterations $w \to V^{\rm IPNCI} \to w + \delta w \to V^{\rm IPNCI} + \delta V^{\rm IPNCI} \to \dots$ etc. of the $V^{\rm IPNCI}$ obtained from the momentum-independent strong interaction (86) would not change the result, since $V^{\rm IPNCI}$ (88) does not contribute to the single-particle weak potential of the core ($\delta w = \langle V^{\rm IPNCI}\rangle_{\rm core} = 0$). The situation changes if one takes into account the momentum-dependent corrections to the Landau-Migdal interaction. In this case, the summation of the series produces an additional enhancement factor ~ 1.5 (see Appendix C). This enhancement in fact corresponds to the renormalization of the single-particle weak potential w by the momentum-dependent nuclear forces (Flambaum and Vorov 1994). This renormalization is even stronger if one uses the "ab initio" strong interaction in the form of $(\pi + \rho)$-exchange (Appendix D).

Similarly to the IPNCI, one can consider the induced P,T-odd interaction. However, it turns out that the latter has the same structure and strength as the initial two-body P,T-odd interaction (Appendix C), and does not display the $A^{1/3}$ enhancement (90). The single-particle P,T-odd potential is renormalized by the main velocity-independent component of the strong interaction, which reduces the corresponding strength constants η_p and η_n by a factor of ~ 1.5–1.8 (Appendix D).

2.4 Application of Statistical Theory to Calculation of Parity and Time-Invariance Violating Effects in Nuclei, and Comparison with Experiment

The statistical approach to calculating mean square matrix elements (sec. 2.1) and the notion of the IPNCI were applied by Flambaum and Vorov (1993) to evaluate the PNC weak mean square matrix element for ^{233}Th. The numerical calculations were performed using a single-particle basis of states

obtained in the Woods-Saxon potential with the spin-orbit interaction:

$$U(r) = -U_0 f(r) + U_{ls}(\boldsymbol{\sigma}\cdot\mathbf{l})\frac{\hbar^2}{m_\pi^2 c^2}\frac{1}{r}\frac{df}{dr} + U_C(r)\ , \tag{91}$$

where $f(r) = \left(1+\exp\frac{r-R}{a}\right)^{-1}$, l is the orbital angular moment, $U_C(r)$ is the Coulomb correction for protons: $U_C(r) = \frac{3Ze^2}{2R}\left(1-\frac{r^2}{3R^2}\right)$, $r \le R$, and $U_C(r) = \frac{Ze^2}{r}$, $r > R$, R and a being the nuclear radius and the diffusity parameter. The numerical values of the parameters were taken according to Bohr and Mottelson (1969) for ^{233}Th: they are close to those established for heavy nuclei like lead to reproduce their single-particle properties.

The mean square PNC matrix element $\overline{W^2}$ was calculated by means of formula (64), using the Breit-Wigner approximation (57) for $\tilde{\delta}$, and the parity-violating two-body interaction $V^{\rm IPNCI}$ (85). In the latter the residual strong interaction V was chosen in the Landau-Migdal form (86), with the constants depending on radius via $\rho(r) = \rho(0)f(r)$. Note that the exchange matrix elements in (64) should be omitted if we use the Landau-Migdal interaction, since exchange is already taken into account in this contact interaction by the appropriate choice of f, f', g, and g'. The single-particle weak nuclear potential w (36) was used. The single-particle occupancies were calculated from (59) at $T = 0.6$ MeV. This value of temperature was obtained to satisfy conditions (60) for the excitation energy E equal to the neutron separation energy. It is convenient to present the r.m.s. matrix element $\sqrt{\overline{W^2}}$ in the following form:

$$\sqrt{\overline{W^2}} = \sqrt{\frac{2D}{\pi\Gamma_{\rm spr}}}\sqrt{\Sigma_{pp}g_p^2 + \Sigma_{nn}g_n^2 + \Sigma_{pn}g_p g_n}\ , \tag{92}$$

where Σ_{pp}, Σ_{nn}, and Σ_{pn} are the contributions to the sum (64) from the squared proton, squared neutron and interference terms, respectively, and the factor $\sqrt{\frac{2D}{\pi\Gamma_{\rm spr}}} = 1/\sqrt{N}$ reminds one about the suppression of the matrix element between compound states. For $g_p = 4$ and $g_n = 1$ equation (92) yielded $\sqrt{\overline{W^2}} = 2.08$ meV, in good agreement with the experimental value $1.39^{+0.55}_{-0.38}$ meV for ^{233}Th (Frankle *et al* 1991). On the other hand, we can use the experimental $\sqrt{\overline{W^2}}$ and the calculated value of Σ_{pp} to determine the value of g_p (assuming that $g_p^2 \gg g_n^2$). The result is: $g_p = 2.67^{+1.05}_{-0.73}$. Having in mind that there is some error in the statistical calculation of $\sqrt{\overline{W^2}}$, we can say that this value is in agreement with the theoretical value $g_p = 4$. The only essential assumption made in the above calculation of $\sqrt{\overline{W^2}}$ was that concerning the distribution of the components (49). As far as the uncertainty in the value of $\sqrt{N}$ is concerned, the two estimates: $\sqrt{N} = \sqrt{\frac{\pi\Gamma_{\rm spr}}{2D}}$ (for $D = 17$ eV in ^{233}Th and $\Gamma_{\rm spr} \approx 2$ MeV), and $\sqrt{N} \simeq \sqrt{\Gamma_0^{(n)}/\Gamma_c^{(n)}}$, give approximately the same answer $\sqrt{N} \simeq 4.3\times10^2$ [$\Gamma_0^{(n)}$ and $\Gamma_c^{(n)}$ above are the width of the single-particle s or p resonance (Bohr and Mottelson 1969) and the neutron width of the compound s or p resonance respectively].

The valence mechanism takes into account the weak mixing of the single-particle components (in ^{233}Th, $4s$ and $4p$ neutron states). Its contribution can be estimated as

$$w_{\rm val} \sim \frac{1}{N} i\langle 4s|w|4p\rangle \simeq \frac{1}{N} g_n 0.8\ {\rm eV} \simeq 2\times10^{-3}\ {\rm meV}\ . \tag{93}$$

Thus the statistical, compound-resonance contribution is 10^3 greater than (93) due to the extra $\sqrt{N}$.

Similarly to the calculation of the PNC matrix element $\sqrt{\overline{W^2}}$ Flambaum and Vorov (1995b) calculated the r.m.s. matrix element of the P,T-odd interaction [Appendix C, eq. (C22)] and the correlator

$C(W, W^{\rm PT})$ (65) between the P-odd and P,T-odd matrix elements for ^{233}Th. They obtained:

$$\sqrt{\overline{(W^{\rm PT})^2}} = 0.20\ \eta\ \text{meV}\ , \tag{94}$$

where η is the characteristic constant of the P,T-odd interaction (C15). The ratio of the PNC and P,T-odd matrix elements is $\sqrt{\overline{(W^{\rm PT})^2}}/\sqrt{\overline{W^2}} \sim 0.1\eta/g$. This is explained by the fact that $W^{\rm PT}$ does not have the $A^{1/3}$ enhancement, whereas the W does (see Appendix C and sec. 2.3). This result can have important consequences for the experimental search for P,T-odd forces: the naive estimate of the magnitude of a P,T-odd effect as that of a PNC effect times η/g must be reduced by an order of magnitude. The correlator

$$|C(W, W^{\rm PT})| \simeq 0.1 \tag{95}$$

turned out to be small, in agreement with earlier estimates [see eq. (66)].

2.5 Other Approaches to Calculation of Matrix Elements Between Compound States

2.5.1 The doorway state approach and the IPNCI.

The doorway state (or collective 0^- resonance) approach becomes more and more popular in calculations of PNC effects. It was first used by Kadmensky *et al* (1983) to estimate the matrix elements of the weak interaction between compound states [ten years later this idea was re-examined by Flambaum 1993]. Auerbach (1992) and Auerbach and Bowman (1992) used it to estimate regular valence-type contributions. Recently Johnson and Bowman (1995) adopted this approach to derive equations for the IPNCI ($\delta V^{\rm PV(2)}_{\rm Doorway}$ in their notation).

The main assumption of the doorway state approach is that the spin-dipole 0^- state $|D_\mu\rangle \propto \sum_a \boldsymbol{\sigma}_a \cdot \mathbf{r}_a |\mu\rangle$ (actually, two states with isospins $T = 0$ and $T = 1$) built on the compound state μ dominates the PNC matrix element between the two compound states λ and μ:

$$\langle\lambda|w|\mu\rangle = \langle\lambda|D_\mu\rangle\langle D_\mu|w|\mu\rangle\ . \tag{96}$$

Of course, one can always construct a state $|D_\mu\rangle \propto w|\mu\rangle$ to make (96) valid. However, this state is not a stationary, and even not a quasistationary state, i.e., it can not be treated using the stationary perturbation theory. One can interpret the "energy" of this state as an "average" energy in the perturbation theory sum:

$$|\delta\mu\rangle = \sum_\nu \frac{|\nu\rangle\langle\nu|w|\mu\rangle}{E_\mu - E_\nu} \longrightarrow -\frac{|D_\mu\rangle}{\omega_\mu}\langle D_\mu|w|\mu\rangle\ , \tag{97}$$

where $w_\mu = E_{D_\mu} - E_\mu$. Starting from this point two ways of calculations are possible. To obtain the results of sec. 2.3 one need to use the commutator relation $\mathbf{p} = im[H, \mathbf{r}]$, and then

$$\langle D_\mu|\mathbf{p}|\mu\rangle = \langle D_\mu|im[H, \mathbf{r}]|\mu\rangle = (E_{D_\mu} - E_\mu)im\langle D_\mu|\mathbf{r}|\mu\rangle\ .$$

Applying the doorway state assumption: $|D_\mu\rangle\langle D_\mu|\boldsymbol{\sigma}\mathbf{r}|\mu\rangle = \boldsymbol{\sigma}\mathbf{r}|\mu\rangle$ and eq. (79) we come back to eq. (84). Johnson and Bowman (1995) used an oscillator relation $\mathbf{p} = im\omega\mathbf{r}$, where ω is the oscillator frequency. Therefore, $\delta V^{\rm PV(2)}_{\rm Doorway}$ differs from $V_{\rm IPNCI}$ of eq. (84) essentially by the factor ω/ω_μ. Basing on experimental data Johnson and Bowman (1995) take $\omega_\mu = 1.25\omega$ in the isoscalar channel, and

$\omega_\mu = 3\omega$ in the isovector channel, and explained this shift as produced by a renormalization of the weak potential by the strong interaction. There is an apparent disagreement between the damping of the PNC interaction obtained by Johnson and Bowman (1995) and its enhancement due to renormalization by the (momentum-dependent) residual strong interaction (Flambaum and Vorov 1994). It results from the two facts. First, we believe that similarly to our eq. (D4) there should be another term in eq. (A.2) of (Johnson and Bowman 1995), which cancels the first term if the contact-type residual strong interaction is momentum independent. Thus, no renormalization takes place in this approximation (see discussion at the end of sec. 2.3, and Appendix D). Second, the weak potential is indeed renormalized by a momentum-dependent part of the residual strong interaction which was taken into account in (Flambaum and Vorov 1994) and was omitted by Johnson and Bowman (1995). However, a complete agreement between the two approaches can be achieved. Indeed, using the doorway language one can calculate the renormalization of the weak potential of the nucleus in the following way. Due to the weak interaction w the ground state of the target nucleus $|0^+\rangle$ gets an admixture of $|0^-\rangle \equiv |D_0\rangle$:

$$|\tilde{0}\rangle = |0^+\rangle + \beta|0^-\rangle = |0^+\rangle + \sum_t \frac{|D_{t0}\rangle\langle D_{t0}|w|0^+\rangle}{\omega_{t0}} , \tag{98}$$

where $t = 0, 1$ distinguishes the isoscalar and isovector doorways. The mean strong field in the state $|\tilde{0}\rangle$ differs from that in $|0^+\rangle$. This difference is a correction to the weak potential w:

$$\delta w(1) = \sum_t \omega_{t0}^{-1} \left(\langle 0^+|V(1,2)|D_{t0}\rangle\langle D_{t0}|w|0^+\rangle + \langle 0^+|w|D_{t0}\rangle\langle D_{t0}|V(1,2)|0^+\rangle \right) , \tag{99}$$

where the matrix elements of $V(1,2)$ are taken over the target nucleons (variable 2). Then, using the commutator or oscillator relation between $\mathbf{p}$ and $\mathbf{r}$ one obtains the analytical expression ($\delta w \propto \langle [V, \sum_a \boldsymbol{\sigma}_a \cdot \mathbf{r}_a] \rangle_{\rm core}$) for the correction to the potential. The latter can be introduced into an equation like (D13) (Appendix D) to obtain the renormalized potential self-consistently ("all-orders" treatment). Another possibility is to introduce corrected values of the frequencies ω_{t0} into eq. (99) based on experimental data for the 0^- excitation strength function.

It is worth stressing once more that the method of Johnson and Bowman (1995) is a different technical approach to calculate the action of the single-particle weak potential w within valence shell configurations by means of the induced two-body interaction, and there is much similarity between their analytic results for $\delta V^{\rm PV(2)}_{\rm Doorway}$ and that for $V_{\rm IPNCI}$ (sec.2.3). Comparing these approaches, we do not see why the use of the commutator relation between $\mathbf{p}$ and $\mathbf{r}$ is less accurate than the oscillator relation (which is, in fact, a particular case of the former).

2.5.2 Model space and statistical spectroscopy approach.

An alternative approach to calculation of the r.m.s. parity-violating matrix elements between compound states was suggested by Johnson *et al* (1991) (see also Johnson and Bowman 1995) based on the statistical spectroscopy methods of French *et al* (1988). The main assumption is that the mean square PNC matrix element M^2 can be taken to be proportional to that of a schematic interaction U_2:

$$M^2 = \alpha_P^2 \overline{(U_2)^2} . \tag{100}$$

The constant α_P^2 is calculated as

$$\alpha_P^2 = \frac{{\rm Tr}(V^{\rm PV})^2}{{\rm Tr}(U_2)^2} , \tag{101}$$

where the traces in the numerator and denominator are evaluated in a given model space. It is supposed that α_P^2 should be insensitive of the specific choice of states over which the traces are taken, so that, e.g., plane waves [Johnson *et al* 1991, Johnson and Bowman (1995)] can be used. The value of $\overline{U_2^2} = 2.6$ keV^2 for ^{239}U is taken from (French *et al* 1988). Within the latter the mean square matrix elements are evaluated using ensemble averaging techniques and scaling properties ($\overline{U_2^2} \propto D$). We should note that there is some similarity between this approach and that of sec. 2.1. For example, in the non-interacting particles limit eq. (51) of sec. 2.1 ($w_{1,2}$ are proportional to delta functions if the matrix element is calculated between single-configuration states) is equivalent to eq. (12) of French *et al* (1988). The interaction of particles is taken into account by French *et al* 1988 by calculating a convolution of non-interacting particles strength densities with a bivariate Gaussian describing the spreading of configurations. The operator U_2 in (French *et al* 1988) is a residual shell model interaction in the form of a surface delta function. Johnson *et al* (1991) replaced it by an ordinary delta function $U_2 = g\delta(\mathbf{r}_1 - \mathbf{r}_2)$ with $g = 26$ MeV fm^3 when calculating the trace in (101). Using the one-body weak interaction $w = (C_\rho + C_\pi \tau_z)\boldsymbol{\sigma}\mathbf{p}$ based on the meson-nucleon weak constants from Desplanques *et al* (1980) they obtained $M = 3.07$ meV for ^{239}U. A slightly larger value of $M = 3.24$ meV is obtained when the two-body piece were added to $V^{\rm PV}$[6]. The experimental value of M for ^{239}U is $0.58^{+0.50}_{-0.25}$ meV (Bowman *et al* 1990).

The drawback of the procedure outlined in eqs. (100), (101) is that different operators have different selection rules. For example, U_2 has nonzero matrix elements between principal components of the compound states, whereas the one-body PNC potential w does not. This makes α_P^2 dependent on the choice of the model space, i.e., if one restricts it to the principal components only, $\alpha_P^2 = 0$ for $V^{\rm PV} = w$. Moreover, even if a large model space is used to calculate the traces in (101), the result will be different to the average over nearby compound states (the latter is measured in experiments). Indeed, eqs. (58), (64) are sensitive to the position of the maximum of the distribution of the corresponding matrix elements (via ω-dependence of the spread delta function $\tilde{\delta}$). This means that α_P^2 in (100) (local averaging) can be strongly different from α_P^2 in (101) (average over all model space). Consequently, the M values of Johnson *et al* (1991) ignore a factor like $\Gamma_{\rm spr}/\omega_0 \sim 1/5$. However, the accuracy can be substantially improved by using the IPNCI which acts in the subspace of principal components. In this case the factor $\Gamma_{\rm spr}/\omega_0 \sim 1/5$ does not appear which justifies the application of eq. (101) to $\delta V^{\rm PV(2)}_{\rm Doorway}$. This was done in the recent work of Johnson and Bowman (1995).

3 Regular Contributions to PNC Effects

Statistical nature of dynamical enhancement of weak interactions in compound nuclei considered in sec. 1.1 and employed in the calculation of the mean square matrix element (sec. 2.1) implies randomness of matrix elements of weak interaction between complicated states of opposite parity. Therefore one would expect the random sign of the corresponding PNC effects, e.g., the asymmetry (2). Recent Los Alamos experiments (Frankle *et al* 1991) show, contrary to this expectation, that neutron capture into p-wave compound resonances in ^{233}Th leads to the asymmetry of the same sign for all 7 resonances where the effect is greater then two standard deviations (other resonances are probably $p_{3/2}$-resonances

[6]Note that these numbers (Johnson and Bowman 1995) are about three times greater than those quoted in Johnson *et al* 1991 due to numerical errors in the latter.

where the effect must be zero). Its magnitude can be characterised by the average of $P\sqrt{E}$ over these 7 resonances

$$B \equiv \left\langle P\sqrt{E/1\ \mathrm{eV}} \right\rangle = 0.3(\pm 10\%). \tag{102}$$

Note that this value is much larger than $B = 0.08 \pm 0.06$ of Bowman *et al* 1992 obtained by means of statistical analysis for all p resonances which accounted for both random and regular contributions. Despite the fact that the experimental data obtained for other nuclei does not show strong deviations from randomness, the results for ^{233}Th initiated a lot of theoretical activity (Flambaum 1992, Bowman *et al* 1992, Auerbach 1992, Lewenkopf and Weidenmüller 1992, Gudkov 1993, Auerbach 1994, Auerbach *et al* 1994, Hussein *et al* 1994, Flambaum and Zelevinsky 1994). None of these works gives a reliable explanation of the regular effect comparable in magnitude with the random effect. Nevertheless, the review would be incomplete if we simply ignore them.

3.1 Valence Mechanism

Near the neutron threshold there is only one component in the compound state which has an exit into the continuous spectrum. This component (valence component) corresponds to the unexcited target nucleus wave function times the neutron wave function. The valence component gives a regular sign contribution to the parity-violating effects since the coefficient C_0 before this component in the compound state (10) or (39) appears in the expression for the PNC amplitude twice: the first time in the capture amplitude $T_{s,p} \propto C_0^{(s,p)}$, and the second time in the weak interaction matrix element, i.e., $f_{\mathrm{PV}} \propto C_0^2$.

There have been many calculations of the valence contribution (see Zaretsky and Sirotkin 1983, 1987, Olkhovsky and Zaichenko 1983, Desplanques and Noguera 1984, Noguera and Desplanques 1986, Flambaum 1992, Bowman *et al* 1992, Koonin *et al* 1992, Lewenkopf and Weidenmüller 1992). Below we present a simple analytical derivation of the valence contribution as per Flambaum (1992) and discuss briefly the recent results of other authors.

The parity-violating part of the scattering amplitude is

$$f_{\mathrm{PV}} = -\frac{m}{2\pi\hbar^2}\langle\Psi_f|w|\Psi_i\rangle\ , \tag{103}$$

where Ψ_f and Ψ_i are the wave functions of the system, corresponding to the scattering waves at large neutron-nucleus distances. Outside the nucleus the wave function Ψ of the system is a product of the target nucleus wave function and the neutron wave function ψ. The behaviour of the continuous spectrum wave function ψ in the region with zero potential is determined by the scattering phase shifts. For $kr \ll 1$, but $r > R$ (k is the momentum of the neutron), it is more convenient to express this wave function in terms of the scattering amplitudes. Close to a $p_{1/2}$-wave compound resonance the neutron wave function is

$$\psi = e^{i\mathbf{kr}}\chi_\pm + \psi_{\mathrm{scat}} \quad \longrightarrow \quad \left[1 + \frac{f_s}{r} + i\frac{f_{p_{1/2}}}{kr^2}(\boldsymbol{\sigma}\cdot\mathbf{n})(\boldsymbol{\sigma}\cdot\mathbf{n}_k)\right]\chi_\pm\ , \tag{104}$$

where $\chi_\pm$ is the spinor corresponding to the right or left helicity of the neutron: $\boldsymbol{\sigma}\cdot\mathbf{n}_k\chi_\pm = \pm\chi_\pm$, $\mathbf{n}_k = \mathbf{k}/k$, and $\mathbf{n} = \mathbf{r}/r$. The s-wave and $p_{1/2}$-wave scattering amplitudes are given by

$$f_s = -a - \frac{1}{2k}\sum_s \frac{\Gamma_s^{(n)}}{E - E_s + \frac{i}{2}\Gamma_s}\ , \qquad f_{p_{1/2}} = -\frac{1}{2k}\sum_p \frac{\Gamma_p^{(n)}}{E - E_p + \frac{i}{2}\Gamma_p}\ , \tag{105}$$

where a is the potential part of the scattering length [compare with the parity-conserving part of (20)], and the extra i factor for the p-wave amplitude is written out explicitly in this section [see eq. (104)]. Note that the wave function (104), (105) contains the contributions from all compound resonances including the distant ones.

To calculate the valence contribution to PNC effects one has to know the neutron wave function inside the nucleus, where it is strongly distorted by the interaction with excited nucleons. There are two ways to overcome this problem:

1. Using commutator relations we can transform the weak interaction Hamiltonian into the surface form and use the wave function (104) which is "exact" outside the nucleus.
2. We can match the wave function (104) with a solution for the neutron in the average nucleus potential. This solution can be approximated by the nearest to $E = 0$ single-particle discrete state or resonance wave function ($4s_{1/2}$ and $4p_{1/2}$ in ^{233}Th).

Let us start with the commutator method. Using $\mathbf{p} = im[H, \mathbf{r}]$ and neglecting spin-dependent terms (e.g., the spin-orbit interaction) in the Hamiltonian H of a nucleon in the nucleus, we can decompose the weak potential w (36) into the following sum

$$w = w_0 + \tilde{w}, \qquad w_0 = i\frac{Gg}{\sqrt{2}}[H, \rho\boldsigma\cdot\mathbf{r}] ,$$
$$\tilde{w} = -\frac{Gg}{4\sqrt{2}m}[\mathbf{n}\cdot\mathbf{p}\rho'\boldsigma\cdot\mathbf{r} + \rho'(\mathbf{n}\cdot\mathbf{p})(\boldsigma\cdot\mathbf{r}) + (\boldsigma\cdot\mathbf{r})(\mathbf{n}\cdot\mathbf{p})\rho' + \boldsigma\cdot\mathbf{r}\rho'\mathbf{n}\cdot\mathbf{p}] , \tag{106}$$

where $\tilde{w}$ is proportional to $\rho' = d\rho/dr$ (it comes from the commutator $[H, \rho]$) and peaks at the surface of the nucleus, and g is the nucleon weak interaction constant (g_n in our case). For the sake of simplicity a spinless spherical target is considered. The interaction w_0 does not contribute to $f_{\rm PV}$ (103). Indeed, the wave functions Ψ_i and Ψ_f correspond to the same energy. Therefore, the matrix element of the commutator with the Hamiltonian ($w_0 \propto [H, \rho\boldsigma\cdot\mathbf{r}]$) is zero[7]. In the simplest model of the constant nuclear density $\rho = \rho_0\theta(R - r)$, and $\rho' = -\rho_0\delta(r - R)$. Introducing $w = \tilde{w}$ into eq. (103) and using the wave function (104) one obtains the valence contribution to the PNC forward scattering amplitude (103) and the resonance asymmetry of the capture cross section:

$$f_{\rm PV}(0) = \pm f_{p_{1/2}}\frac{4}{k}\frac{Gg_n}{\sqrt{2}}\rho_0\left(1 + \frac{f_s}{2R}\right) , \tag{107}$$

$$\sigma = \frac{4\pi}{k}{\rm Im}f(0) = \frac{4\pi}{k}{\rm Im}(f_{p_{1/2}} + f_{\rm PV}) , \tag{108}$$

$$P_{\rm val} = \frac{\sigma_p^+ - \sigma_p^-}{\sigma_p^+ + \sigma_p^-} = \frac{4}{k}\frac{Gg_n}{\sqrt{2}}\rho_0\left(1 + \frac{{\rm Re}f_s}{2R}\right) = 0.9\times10^{-3}g_n\left(1 + \frac{{\rm Re}f_s}{2R}\right)\sqrt{\frac{1\ {\rm eV}}{E}} . \tag{109}$$

Note that if we use an experimental amplitude f_s, the valence contributions from all compound resonances are taken into account, since all of them contribute to f_s (105). Typically, $f_s \simeq -R$, e.g., for ^{232}Th between s resonances $1 + {\rm Re}f_s/2R = 0.42$ (Mughabhab *et al* 1981). Comparing (109) with B (102) one can see that $P_{\rm val}$ is almost 10^3 times smaller than that derived by averaging over 7 resonances.

Bowman *et al* (1992) derived the average asymmetry $\langle P\rangle$ (see eq. (117) below) by separating single-particle components in the sum over compound resonances in eq. (8) (*distant-state interpretation*).

[7]Of course, this matrix element is not zero when mixing of distant single-particle states is considered, as in sec. 2.3.

Let us show how to obtain their result from eqs. (103) and (104). Following their work we assume that inside the nucleus the single-neutron component is dominated by a single-particle resonance or a bound state close to the neutron threshold. The wave function of the state with $E \approx 0$ has the simple asymptotic behaviour r^{-l}, where l is the orbital angular momentum of the neutron. Therefore, this wave function can be easily matched with the corresponding component of the wave function (104), and the neutron wave function inside the nucleus is given by

$$\psi(r) = \frac{f}{f^{\rm sp}} \psi^{\rm sp}(r) \,, \tag{110}$$

where $\psi^{\rm sp}(r)$ is the single-particle resonance wave function, $f = f_s$, or $f = f_{p_{1/2}}$ for the s- or $p_{1/2}$-waves respectively [see eq. (105)], and $f^{\rm sp}$ is the single-particle resonance scattering amplitude

$$f_s^{\rm sp} = -\frac{1}{2k} \frac{\Gamma_s}{E - \epsilon_s + \frac{i}{2}\Gamma_r} \,, \qquad f_{p_{1/2}}^{\rm sp} = -\frac{1}{2k} \frac{\Gamma_p}{E - \epsilon_p + \frac{i}{2}\Gamma_r} \,. \tag{111}$$

In the above ϵ_s and ϵ_p are energies of the single-particle resonances, and Γ_s, Γ_p are their neutron widths: $\Gamma_s \equiv \gamma_s^2 = 2k/Rm$, and $\Gamma_p \equiv \gamma_p^2 = 2k^3R/3m$ in the square-well model (Bohr and Mottelson 1969). The parity-violating amplitude for the scattering from the single-particle resonances ns and $n'p$ over the target 0^+ ground state is (compare with the last term in eq. (20):

$$f_{\rm PV}^{\rm sp} = \frac{i}{k} \frac{\gamma_s \langle 0^+ ns|W|0^+ n'p\rangle \gamma_p}{(E - \epsilon_{ns} + \frac{i}{2}\Gamma_{ns})(E - \epsilon_{n'p} + \frac{i}{2}\Gamma_{n'p})} = \frac{4ikf_s^{\rm sp}\langle 0^+ ns|W|0^+ n'p\rangle f_{p_{1/2}}^{\rm sp}}{\gamma_s \gamma_p} \,, \tag{112}$$

where we used (111) to express the result in terms of $f^{\rm sp}$. Now we can use (103), (108), (110) and (112) to find the resonance part of the valence contribution to the PNC forward scattering amplitude:

$$f_{\rm PV}(0) = \frac{4ikf_s f_{p_{1/2}} \langle 0^+ ns|W|0^+ n'p\rangle}{\gamma_s \gamma_p} \,, \tag{113}$$

$$P_{\rm res} = \frac{4k{\rm Re}(f_s) i\langle 0^+ ns|W|0^+ n'p\rangle}{\gamma_s \gamma_p} \tag{114}$$

$$= \frac{2\sqrt{3}m{\rm Re}(f_s) i\langle 0^+ ns|W|0^+ n'p\rangle}{k} \,, \tag{115}$$

where in the last expression we used square-well model $\gamma_{s,p}$. The wave functions of the single-particle states ns and np are normalized to unity over the nuclear volume. In the case of $n+^{232}$Th, $4s_{1/2}$ and $4p_{1/2}$ are best candidates for these states.

Suppose that the s-wave amplitude f_s is saturated by one single-particle resonance ns:

$$f_s = -\frac{1}{2k} \frac{\Gamma_s}{E - \epsilon_{ns} + \frac{i}{2}\Gamma_r} \,. \tag{116}$$

Then in the case $|E - \epsilon_s| \gg \Gamma_r$ the asymmetry (114) turns into

$$P_{\rm res} = 2\frac{\gamma_s}{\gamma_p} \frac{\langle ns|w|n'p\rangle}{i(E - \epsilon_{ns})} \,. \tag{117}$$

This result in fact coincides with that in the absence of compound states. Indeed, it can be obtained from (8) by simply replacing the compound states with the single-particle resonances: $1/2^- \to n'p$ and $1/2^+\nu \to ns$, and assuming that there is only one single-particle s-resonance nearby. We should note

that inclusion of more than one ns-resonance into (117) using one amplitude γ_s (as done by Bowman *et al* (1992)) would be incorrect, since distant single-particle resonances have different amplitudes γ_s.

The calculations in the square-well model and the more refined ones (Flambaum and Vorov 1993) using the Woods-Saxon potential with the spin-orbit correction give close values of the weak matrix element for ^{232}Th:

$$\langle 4s_{1/2}|w|4p_{1/2}\rangle \simeq -ig_n 0.9 \text{ eV} . \tag{118}$$

If one takes $E - \epsilon_{4s} = -1.7$ MeV, as in (Bowman *et al* 1992), the value of the PNC effect (117) is

$$P_{\rm res} = 1.2 \times 10^{-3} g_n \sqrt{\frac{1 \text{ eV}}{E}} . \tag{119}$$

This value is in reasonable agreement with (109). A similar result obtained by Bowman *et al* (1992): $B = 2.9 \times 10^{-3} g_n$ is larger since the weak interaction matrix element has been overestimated by extending the nuclear density ρ in the weak Hamiltonian (36) beyond the nuclear boundary (they put $\rho = \text{const}$) and using large-size oscillator wave functions. Note that formulae (107), (109) and (113)–(115) include contributions from all compound s-wave resonances, whereas (117) includes only those from distant states.

Lewenkopf and Weidenmüller (1992) considered the valence mechanism within the Feshbach projection formalism. They take into account the weak mixing of the s and p neutron valence components and explicitly include the interaction of the p-wave component with compound resonances [second diagram in (24)]. The authors believe that this interaction gives rise to a specific *barrier penetration* enhancement. However, their numerical result, $B = (0.25\text{–}0.75) \times 10^{-3} g_n$, is in agreement with (109). This is not surprising because the "experimental" amplitudes (105) include the above interaction exactly. Therefore, there seems to be no grounds for any special barrier enhancement except for the usual kinematical one.

Koonin *et al* (1992) performed numerical calculations of the PNC asymmetry in the p-wave neutron capture. They used an *optical potential method* to calculate the neutron wave function, and to determine the corresponding value of P (2). The optical potential method corresponds to averaging of the true neutron wave function over compound resonances. Therefore, the result of Koonin *et al* is in fact $\langle \sigma_p^+ - \sigma_p^- \rangle / \langle \sigma_p^+ + \sigma_p^- \rangle$ rather than $\langle P \rangle$. This method can be quite accurate for the valence PNC amplitude in the range of overlapping resonances or between the resonances. However, it is not so good for the calculation of the effect at the resonance, since the neutron wave function does not satisfy the correct boundary condition given by the asymptotic form (104), (105). Thus, the result of Koonin *et al* can be viewed only as an order of magnitude estimate of the valence contribution at the resonance. Surprisingly, their numerical value $B = 0.3 \times 10^{-3} g_n$ is very close to that of eq. (109).

In some of the works discussed above the authors claim that they can explain the observed average value of the effect. However, this would require $g_n \sim 300$, [$\varepsilon \sim 3 \times 10^{-6}$]. First of all this value of g_n, which is in fact the coefficient of renormalization of the Fermi weak interaction by the strong interaction, looks unreasonably large (see, e.g., eq. (37), or estimates by Koonin *et al* (1992), which yield $|g_n| \lesssim 1$). This value of g_n is also excluded by the experimental data. Firstly, the statistical contribution to P is compatible with $g_n \sim 1$. Secondly, there are measurements of PNC effects in nuclei with sparse

compound resonance spectra, such as ^{124}Sn (Forte *et al* 1980), ^{208}Pb (Abov *et al* 1989), and others. In these nuclei the dynamical enhancement factor is small and one can extract some limits on the valence contribution directly. For example, Forte *et al* (1980) measured the angle of spin rotation for thermal neutrons in ^{124}Sn:

$$\phi(^{124}\mathrm{Sn}) = (0.48 \pm 1.49) \times 10^{-6} \text{ rad cm}^{-1} . \tag{120}$$

The angle of the neutron spin rotation is given by (see, e.g., Stodolsky 1974)

$$\phi = \frac{4\pi N_0 l}{k} \mathrm{Re} f_{\mathrm{PV}} , \tag{121}$$

where N_0 is the density of atoms, and l is the neutron path. Using f_{PV} from eq. (107) or (113) one can obtain a limit on the strength of the neutron weak potential:

$$|g_n| \lesssim 1, \quad \text{or} \quad |\varepsilon| \lesssim 1 \times 10^{-8} . \tag{122}$$

Thus, the contribution of the valence mechanism can account for less 1% of the observed average PNC effect in ^{232}Th.

3.2 Correlations among Compound State Components and the Quasi-elastic Mechanism

Valence mechanism takes into account the contribution of the compound state component where the target nucleus is not excited. We can call this an "elastic" contribution. Different compound resonances give a coherent contribution to the PNC amplitude in this "elastic" process. However, the coherence can not be lost completely after the first neutron-nucleon collision inside the nucleus. Moreover, there is a process in which the s-wave capture and the p-wave capture continue to work coherently. If after the first collision the s-wave neutron is transformed into the p-wave, its strong field acting on the target nucleons is given by the matrix element $\langle p|V|s\rangle$. The transition of a p-wave neutron into the s-wave produces the same strong field $\langle s|V|p\rangle$. Therefore, similar target nucleus states can be excited in the p-wave and s-wave compound resonances. This possibility of creating a certain degree of coherence among the compound state components was considered in (Flambaum 1992, 1993). The estimates showed that the above described "quasielastic" contribution can hardly exceed the valence one.

However, the question of correlations between "chaotic" compound states should be considered more carefully. To derive the expression for the dynamical enhancement factor and matrix elements between the compound states (secs. 1.1 and 2.1) it was assumed that:

1. When the residual interaction is strong (much greater than the level spacing) the number of principal components N is large. This produces the enhancement factor of $\sqrt{N}$.
2. The components $C_i^{(\lambda)}$ [eq. (39)] of compound states are statistically independent: $\overline{C_i^{(\lambda)} C_j^{(\mu)}} \propto \delta_{ij}\delta_{\lambda\mu}$.

At first sight these assumptions seem very natural. However, they are not necessarily true. There is some correlation in the components imposed by the orthogonality condition. More importantly, the number of "independent variables" (different two-body matrix elements of the strong interaction) is proportional to N_s^4, where N_s is the number of single-particle orbitals, whereas the number of expansion

coefficients $C_i^{(\lambda)}$ is N^2, and increases exponentially with the number of orbitals. Thus, strictly speaking, they cannot be statistically independent. If the correlations are of the order of $1/N$ they can of course be neglected. In Appendix B we consider the example of a system (random separable residual interaction) where the result is quite opposite, and the above assumptions are maximally violated:

1. $N \sim 1$ at arbitrary strong residual interaction, and consequently, there is no dynamical enhancement of perturbations.
2. $\overline{C_i^{(\lambda)} C_j^{(\lambda)}} \propto \delta_{ij}$, i.e., the components of a given eigenstate are uncorrelated, whereas $\overline{C_i^{(\lambda)} C_i^{(\mu)}} \sim \overline{C_i^{(\lambda)2}}$ ($\lambda \neq \mu$ are nearby eigenstates), which means very strong correlations between close eigenstates.

These strange properties result from very strong interference effects taking place in this model. If we imagine that a real compound nucleus were described by a similar model, it would be very easy to explain the sign correlations of PNC effects for different resonances observed in Th (Frankle *et al* 1991).

3.3 Doorway States and Giant Resonances

Auerbach (1992), and Auerbach and Bowman (1992) suggested to use doorway state approach to calculate the regular contribution to the PNC asymmetries. They assumed that the spin-dipole 0^- state $|D_\mu\rangle$ built on a compound state $|\mu\rangle$ dominates the PNC matrix element between the two compound states λ and μ [see eq. (96)]. This assumption combined with the extraction of the regular valence-type contribution from the equation for the PNC asymmetry (8) gave the following result:

$$P_D = -\frac{2\gamma_s}{\gamma_p} \frac{\langle 0^+ n s_{1/2} | w | 0^+ n' p_{1/2} \rangle}{i\omega_D} , \tag{123}$$

where ω_D is the excitation energy of the 0^- spin-dipole doorway $|D_\mu\rangle$ ($\sim$ 7 MeV). This result looks similar to the valence contribution (117) and cannot explain the size of the average effect observed in ^{232}Th.

3.4 Two-particle One-hole Doorway States

Recently Hussein *et al* (1994) suggested that the sign correlation effect in the PNC asymmetry in Th can be explained by a contribution of a non-collective $2p-1h$ doorway [regular contribution of such states was also mentioned by Flambaum (1992)]. They assumed that parity violation occurs through the coupling of a p-wave doorway to a nearby s-wave doorway, and obtained the average value of P:

$$\langle P \rangle = \frac{M}{\Delta E} \frac{\gamma_{D_s}}{\gamma_{D_p}} , \tag{124}$$

where M is a characteristic "weak" matrix element between p and s doorways, ΔE is a characteristic energy distance between these doorways, and γ_{D_p}, γ_{D_s} are neutron decay amplitudes of the doorways (kinematically $\gamma_{D_p}/\gamma_{D_s} \sim 1/kR$). Hussein *et al* claim that this mechanism can reproduce $\langle P \rangle = 0.08$. However, we believe that they strongly overestimate the $2p-1h$ contribution. The only source of enhancement for this mechanism in comparison with the valence mechanism is a higher density of the $2p-1h$ states with respect to $1p$ states. However, Hussein *et al* do not take into account that this also reduces the weak interaction matrix element. More importantly, the spreading width of the $2p-1h$ state is not smaller than that of the $1p$ state ($\Gamma_{spr} \sim 1$ MeV) since the number of possible final states for the

decay of the former is not smaller. Thus, a relatively small spacing between $2p-1h$ states ($D \sim 30$ keV) does not give any enhancement at all, since the corresponding denominator is $\Delta E \sim |D + \frac{i}{2}\Gamma_{\rm spr}| \sim 1$ MeV. Even after using $M = 1.0$ eV and $\Delta E = 50$ keV the result of Hussein *et al* is not large enough, and a statistical fluctuation has to be assumed to further increase the ratio $\gamma_{D_s}/\gamma_{D_p}$ by a factor of about 4. The probability of such fluctuation is quite small. Indeed, it cannot be achieved by small γ_{D_p} (in this case other doorways will give larger contributions to the p-wave capture amplitudes), and the probability of large γ_{D_s} is exponentially small for a Gaussian distribution. It seems easier to believe that all 7 PNC asymmetries in Th have the same sign due to a fluctuation. Our conservative estimate of the $2p-1h$ contribution (124) does not exceed that of the valence mechanism, mostly because of a large spreading width in the denominator ΔE.

3.5 Rotational Doublets

The experimental pattern of the target of ^{232}Th gives a hint that this nucleus, and consequently the compound nucleus ^{233}Th, might be a special case due to some peculiarities of its structure as compared to "normal" deformed heavy nuclei like ^{238}U, which apparently exhibits random PNC asymmetry. Indeed, Th isotopes display strong octupole correlations (Bohr and Mottelson 1974, Leander 1982, Otsuka 1986, Nazarewicz 1990, Jolos and von Brentano 1994). Octupole deformations lead to the existence of nearby rotational parity doublets. Such doublets are known to play crucial role in PNC effects in nuclear fission by polarized neutrons (Flambaum and Sushkov 1980). It was suggested by Auerbach (1994), Auerbach *et al* (1994), Flambaum and Zelevinsky (1994) that these doublets can produce regular PNC asymmetry in Th. Below we use the approach of the latter work.

Let us assume that static octupole deformation is already present in the first (ground state) potential well of Th. However, this assumption is not critical. At excitation energies near the neutron threshold, the nuclear wave function in the space of the deformation parameters certainly has a significant portion of large octupole deformation, $\beta_3 \simeq 0.35$ (Pashkevich 1984, Bengtsson *et al* 1987, Ćwiok *et al* 1994). For sufficiently strong deformations, the use of adiabatic approximation is justified. This allows one to write down the nuclear wave functions as products of the orientational D-functions and the wave functions of internal motion $|\chi\rangle$ (Bohr and Mottelson 1974). In the case of axial symmetry the projection $K = \mathbf{In}$ of the total angular momentum $\mathbf{I}$ onto the axis of symmetry $\mathbf{n}$ is conserved and can be used to label the wave functions $|\chi\rangle = |a, K\rangle$. In the neutron capture by a spinless target we are interested in the states with $|K| = 1/2$. For a given intrinsic state with $K \neq 0$ the presence of octupole deformation, or of any other deformation which is axially symmetric but has no symmetry with respect to reflection in the equatorial plane, leads to the rotational doublets with definite parity $\Pi = \pm 1$,

$$|aKI^{\Pi}M\rangle = \left(\frac{2I+1}{8\pi}\right)^{1/2}\left[D^I_{MK}(\varphi,\vartheta,0)|a,K\rangle + \Pi(-1)^{I+K}D^I_{M-K}(\varphi,\vartheta,0)|a,-K\rangle\right]. \qquad (125)$$

The energy splitting of the doublet states implies that there is a physical interaction which couples the "right" and "left" configurations $|a,\pm K\rangle$. One can imagine various particular mechanisms of this coupling, e.g., tunneling of an excess cluster. In the case of $K = 1/2$ the Coriolis force acting in the first order can be sufficient to generate this coupling, similar to the decoupling parameter in normal spectra of odd-A deformed nuclei (Bohr and Mottelson 1974).

Since the likely energy splitting within the doublet is of the order of several keV one can expect that mixing of the opposite parity doublet states by the weak interaction is much stronger than mixing of the single-particle orbitals separated by MeV energies. However, a direct mixing of the states (125) with the same intrinsic structure and opposite Π is possible only if the weak perturbation W violates time-reversal symmetry as well as the parity (Sushkov and Flambaum 1980b). Indeed, the mixing matrix element can be expressed in terms of the intrinsic expectation values of the weak interaction,

$$\langle aKI^{-\Pi}M|W|aKI^{\Pi}M\rangle = \frac{1}{2}\Big(\langle a,K|W|a,K\rangle - \langle a,-K|W|a,-K\rangle\Big)\ . \tag{126}$$

Since W is a pseudoscalar, the matrix element $\langle a,K|W|a,K\rangle$ should be proportional to the intrinsic pseudoscalar K. On the other hand, it means that this quantity, together with K, changes its sign under time-reversal which would contradict to the T-invariance of W. One can see from (126) that only a T-odd interaction leading to the opposite sign of the two matrix elements in brackets can mix the doublet states directly[8]. Thus, mixing of the doublet should be mediated by another ("normal", P,T-even) interaction H' leading to non-adiabatic admixtures of different configurations $|b,K'\rangle$. For instance, this could be the interaction already mentioned as a source of the energy splitting within the doublet. The interaction H' influences PNC in the first order via the matrix elements $\langle a,-K|H'|b,K\rangle$ which appears in the P-conserving mixing matrix element

$$\langle aKI^{\Pi}M|H'|bKI^{\Pi}M\rangle = \Pi A_{IK}\langle a,-K|H'|b,K\rangle \tag{127}$$

with the amplitude A_{IK} depending on the nature of the interaction H'. When both H' and W are taken into account the total rotational function (125) acquires an admixture of opposite parity,

$$|aKI^{\Pi}M\rangle \ \rightarrow\ |\overline{aKI^{\Pi}M}\rangle = |aKI^{\Pi}M\rangle + \eta|aKI^{-\Pi}M\rangle, \tag{128}$$

where η is the mixing amplitude:

$$\eta = -2\frac{\Pi A_{IK}}{E-E_{-\Pi}}\sum_b \frac{\langle a,-K|H'|b,K\rangle\langle b;K|W|a;K\rangle}{E-E_b}, \tag{129}$$

E is the neutron energy, and the rotational energy splitting of the doublet b in the denominator of (129) has been neglected. The mixing η is directly related to the observed PNC asymmetry (8),

$$P = 2\sqrt{\frac{\Gamma_s^{(n)}}{\Gamma_p^{(n)}}}\,\eta\ . \tag{130}$$

If the splitting of the doublet states $|aKI^{\Pi}M\rangle$ is caused by the same interaction H' it also can be expressed in terms of the amplitude A_{IK},

$$E_{\Pi} - E_{-\Pi} = 2\Pi A_{IK}\langle a,-K|H'|a,K\rangle\ . \tag{131}$$

In this case the resulting PNC admixture (129) at the resonance energy $E \approx E_{\Pi}$ does not depend on A_{IK}.

Note that in the sum (129) the numerator contains two matrix elements and both of them are suppressed as $\sim 1/\sqrt{N}$ for the generic compound wave functions a and b. Therefore, the contribution of the closest

[8]Note that for a P,T-odd interaction a direct mixing within the doublet is not forbidden which can be of some interest for the problem of search for parity and time-invariance violating nuclear forces.

states with the energy difference about D in the compound nucleus is not dynamically enhanced. However, one can consider the contribution of distant states b. If the product of the matrix elements peaks for the states b at the distance of $E_b - E \simeq \omega$ from the resonance, one can apply closure to obtain

$$\eta = 2\Pi \frac{A_{IK}\langle a, -K|H'W|a, K\rangle}{\omega(E - E_{-\Pi})} , \tag{132}$$

and, in the case (131), at $E \approx E_\Pi$ we come to the remarkably simple result

$$\eta = \frac{\langle a, -K|H'W|a, K\rangle}{\omega\langle a, -K|H'|a, K\rangle} . \tag{133}$$

Thus, in this scheme one can expect the admixture amplitude of the order $\eta \simeq W^{\rm sp}/\omega$, where $W^{\rm sp}$ is a typical single-particle matrix element of the weak interaction, $W^{\rm sp} \sim 5$ eV. For the Coriolis interaction as H', the transition energy ω between the deformed single-particle orbitals with $\Delta m = \pm 1$ is of the order of 100 keV, which yields an optimistic $\eta \sim 5 \times 10^{-5}$. It can be compared with the mixing between the compound states of opposite parity $\eta_{\rm comp} \sim \sqrt{\overline{W^2}}/D \sim 10^{-4}$, which means that the regular contribution of parity doublets should be considered quite seriously.

The mechanism presented above is based on the assumption that the pear shape of the nucleus and the related doublet structure persist at required excitation energies. If this is the case, the complicated intrinsic states are superpositions

$$|a, \pm K\rangle = \sum_i C_i^{(a)} |\Phi_i, \pm K\rangle \tag{134}$$

of simple quasiparticle configurations $|\Phi_i, \pm K\rangle$ with amplitudes $C_i^{(a)}$ independent of the sign of K. Then the matrix element in (133) contains a regular contribution

$$\langle a, -K|H'W|a, K\rangle \simeq \sum_i C_i^{(a)2} \langle \Phi_i, -K|H'W|\Phi_i, K\rangle . \tag{135}$$

As shown in (Flambaum and Zelevinsky 1994) the ratio (133) between the PNC matrix element (135) and a similar expression for the doublet splitting (131) can be calculated explicitly using the statistical approach of sec. 2.1.

4 Statistical Enhancement and Behaviour of PNC Effects upon Averaging

Considering PNC effects we so far assumed that the energy of the system E is a well defined quantity. It meant, e.g., that studying the spin-asymmetry in neutron capture one could tune the neutron energy to the p-resonance and obtain the corresponding kinematical enhancement, together with the dynamical one. Consequently, the energy resolution was supposed to be better than the level spacing D and the resonance width Γ. The mixing of opposite parity levels by the weak perturbation is inversely proportional to the energy distance $|E_+ - E_-|$ between them (and the overall magnitude of the dynamical enhancement is proportional to $1/\sqrt{D}$). As is known the level spacings decrease exponentially with energy, which, in principle, gives rise to a possibility of observing very large dynamical enhancement factors. However, it is likely that when the level spacing becomes very small, it would no longer be possible to resolve individual resonances, and the measured quantity would be an average of the effect over

many resonances. This situation is quite possible not only for neutrons or other particles (photons, protons, etc.) of higher energies, but also in other reactions (e.g., chemical reactions). Considering it is also important for answering the question: what happens to the dynamical enhancement of perturbations when the size of the system grows towards macroscopic limit?

The compound-state (dynamical) mechanism of enhancement implies that the effects for different resonances are random variables with zero mean (or a very small mean value produced, e.g, by the valence contribution; the rotational doublet mechanism discussed in sec. 3.5 for Th seems to be a rather special case). Thus, one faces an interesting and vital question: Can the statistical in nature dynamical enhancement of perturbation survive averaging over a large set of compound states? At first sight it seems impossible, since the effect has random signs for different resonances, and its magnitude should therefore decrease as $n^{-1/2}$, where n is the number of resonances. This is a well-known consequence of the Central Limit Theorem (CLT) of the probability theory. However, the larger the set of compound states involved in averaging, the more probable it is to find a pair of opposite parity levels with a very small energy separation (there is no level repulsion between the levels of opposite parity). Hence a very large value of the effect can be achieved for a particular pair of levels, thus making the average effect large!

Consider the average value of the effect X given by the following sum over individual resonances involved:

$$X = \frac{\sum_{i=1}^{n} x_i}{n}, \tag{136}$$

where x_i is the contribution of the ith resonance. Its characteristic magnitude is $x_c \propto D^{-1}$, where D is the mean level spacing between levels of opposite parity. In the sequence of n levels there is a large probability to find a spacing of $|E_+ - E_-| \sim D/n$, which makes some $x_i \sim nx_c$, and therefore produces a typical value of $X \sim x_c$, not decreasing with n. These arguments give one an indication that dynamical enhancement can survive after averaging. This fact indeed contradicts the standard CLT, and is connected with a peculiar statistics of the PNC effects (the corresponding probability density behaves as $f(x) \simeq a/x^2$ at $x \gg x_c$, if the states' widths are neglected, and thus has an infinite variance). In some sense this means that there is an additional *statistical* enhancement, manifesting itself in measurements done with poor energy resolution. Below we present an accurate derivation of this statement and consider its applications to different reactions and possible experiments [details can be found in (Flambaum and Gribakin 1994)]. The closest analogue of this effect is, probably, Ericson fluctuations in the differential cross sections of nuclear reactions (Erikson and Mayer-Kuckuk 1966). Random variables with similar peculiar statistics also emerge in the problem of anomalous diffusion in disordered media (Bouchad and Georges 1990).

4.1 Probability Distribution of a Single-Resonance PNC Effect

Any parity-nonconserving effect results from (and is proportional to) the mixing of states of opposite parity. The mixing coefficient is

$$\eta_{ik} = \frac{w_{ik}}{E_i - E_k}, \tag{137}$$

where E_i, E_k are the energies of the resonant states, and w_{ik} is the weak interaction matrix element between them (compare with eq. (4): i can be included in the matrix element to make it real). The

formula for the PNC effect also includes capture or emission amplitudes, and a sum over the resonances. The result can be presented in the following general form [see, e.g., eq. (8)]:

$$x_i = \frac{A_i}{E_i - E_0} + \sum_k{}' B_{ik} \,, \tag{138}$$

where E_0 is the opposite parity level nearest to the ith state, and the primed sum represents similar contributions from the mixing with other states. Repulsion between opposite-parity levels emerges only in the second order of the weak interaction and hence can be neglected. Thus, the probability to find E_0 in the ΔE vicinity of E_i is simply proportional to ΔE (for small ΔE) that makes the probability to find large values of x_i relatively large. Random matrix theories show (see, e.g., Brody *et al* 1981) that the probability density for the interacting energy levels E_k is

$$P(E_0, E_1, \ldots, E_k, \ldots) \propto \prod_{k<j} |E_k - E_j| \,. \tag{139}$$

It means that the probability to find the second level in the same interval ΔE around E_i is very small: $P \propto \Delta E^3$. Therefore, the possibility to obtain large values of x_i is determined exclusively by the first term in eq. (138).

Let us introduce a new variable y_i,

$$y_i = x_i - \sum_k{}' B_{ik} = \frac{A_i}{E_i - E_0} \tag{140}$$

which gives the contribution of the nearest level mixing. The probability density for $y \equiv y_i$ is

$$f_0(y) = \int f_D(\varepsilon) g(A) \delta(y - A/\varepsilon)\, d\varepsilon dA \,, \tag{141}$$

where $\varepsilon \equiv E_i - E_0$, f_D is the probability density for the interval ε, which depends on the mean level spacing D in the $\{E_k\}$ manifold, $g(A)$ is the probability density of $A \equiv A_i$. It is quite easy to obtain the behaviour of $f_0(y)$ at both small and large y values:

$$f_0(y)|_{y\to 0} = g(0)\overline{|\varepsilon|} \,, \quad \text{where} \quad \overline{|\varepsilon|} = \int |\varepsilon| f_D(\varepsilon) d\varepsilon \,, \tag{142}$$

$$f_0(y)|_{y\to\infty} = \frac{a}{y^2} \,, \quad \text{where} \quad a = f_D(0)\overline{|A|} = f_D(0) \int g(A)|A| dA \,. \tag{143}$$

At large y the contribution of the admixtures of the distant states in (140) can be neglected, so one can put $x = y$. It means that the probability to find large values of the effect is given by

$$f(x)|_{x\to\infty} = \frac{a}{x^2} \,. \tag{144}$$

Although the distribution $f(x)$ is properly normalized [$\int f(x)dx = 1$], its mean $\int x f(x) dx$ can only be calculated as the principle value, and its higher moments including the variance $\int x^2 f(x) dx$ are infinite.

All we need from $f(x)$ is its asymptotic behaviour at large x. However, we can use some model considerations to find out more about its actual shape. It is easy to check that the distribution of the spacing between nearest opposite-parity levels is given by

$$f_D(\varepsilon) = D^{-1} \int_{2|\varepsilon|}^{\infty} P_D(S) dS \,, \tag{145}$$

where $P_D(S)$ is the level spacing distribution in one manifold. Note that the probability to find large values of x does not depend upon a particular shape of $P_D(S)$. Indeed, due to the normalization condition for $P_D(S)$, $f_D(0) = D^{-1}$, and the constant $a = \overline{|A|}/D$ in (144) represents some characteristic value of the effect x. As is known, $P_D(S)$ can be described by the famous Wigner formula

$$P_D(S) = \frac{\pi S}{2D} e^{-\pi S^2/4D} . \tag{146}$$

It follows then from eq. (145) that the distribution of ε is Gaussian:

$$f_D(\varepsilon) = D^{-1} e^{-\pi\varepsilon^2/D^2} , \quad \text{where} \quad \varepsilon_0^2 \equiv \overline{\varepsilon^2} = D^2/2\pi . \tag{147}$$

The $g(A)$ distribution depends on a particular effect considered. For the mixing coefficient η (137) A is the matrix element of the weak interaction ($A_i = w_{i0} \equiv w$) between compound states, and should have Gaussian probability density

$$g(w) = \frac{e^{-w^2/2w_0^2}}{\sqrt{2\pi} w_0} . \tag{148}$$

The calculation of the integral (141) with the functions from (147) and (148) yields the so-called Cauchy distribution for the nearest-level mixing coefficient η

$$f_0(\eta) = \frac{1}{\pi} \frac{\eta_c}{\eta^2 + \eta_c^2} , \quad \text{where} \quad \eta_c = \frac{\sqrt{2\pi} w_0}{D} = \frac{w_0}{\varepsilon_0} , \tag{149}$$

where η_c is the characteristic magnitude of mixing. At $\eta \gg \eta_c$ the function $f_0(\eta)$ turns into (144) with $a \equiv \eta_c/\pi$.

Using η as a model variable we can examine the contribution of other levels, given by the primed sum in (138). For example, if we assume that the effect is produced by mixing of level i with the *two* opposite-parity neighbouring levels E_1 and E_2 [$\eta = w_1/(E_i - E_1) + w_2/(E_i - E_2)$], the probability density can be written as follows:

$$\begin{aligned} f(\eta) &= \int \frac{e^{-w_1^2/2w_0^2}}{\sqrt{2\pi} w_0} \frac{e^{-w_2^2/2w_0^2}}{\sqrt{2\pi} w_0} \frac{P_D(\varepsilon_1 + \varepsilon_2)}{D} \delta\left(\eta - \frac{w_1}{\varepsilon_1} - \frac{w_2}{\varepsilon_2}\right) dw_1 dw_2 d\varepsilon_1 d\varepsilon_2 \\ &= \frac{\sqrt{\pi}}{\eta_0 \sqrt{2}} \int_0^{\pi/2} \frac{(\cos\varphi + \sin\varphi)\cos\varphi \sin\varphi d\varphi}{\left[\frac{\pi}{2}(\cos\varphi + \sin\varphi)^2 + \frac{\eta^2}{\eta_0^2}\cos^2\varphi \sin^2\varphi\right]^2} , \end{aligned} \tag{150}$$

where $\eta_0 = w_0/D = \eta_c/\sqrt{2\pi}$. It is easy to check that (150) has the same asymptotic behaviour as (149). Another way to take the contribution of other levels into account is to consider them in the "picket-fence" model [Bunakov *et al* (1990) used it to find the distribution of a P-even, T-odd effect]. Within the latter all E_k levels except the nearest to E_i are assumed to be equidistant and separated by D spacing. This yields

$$f(\eta) = \int \Pi_k \left[\frac{e^{-w_i^2/2w_0^2}}{\sqrt{2\pi} w_0} dw_k\right] \delta\left(\eta - \sum_k \frac{w_k}{E_i - E_k}\right) P(\ldots, E_k, \ldots) \ldots dE_k \ldots \tag{151}$$

$$\to \frac{\sqrt{6}}{\pi^{3/2}\eta_0} \int_0^\infty \exp\left[-\frac{3\varepsilon^2\eta^2}{2\pi^2\eta_0^2\left(\varepsilon^2 + \frac{3}{\pi^2}\right)}\right] \frac{e^{-\pi\varepsilon^2} \varepsilon d\varepsilon}{\sqrt{\varepsilon^2 + \frac{3}{\pi^2}}} . \tag{152}$$

In Fig. 7 we compare distributions (149), (150), and (152). One can see that they differ only around the maximum and quickly achieve the same $1/\eta^2$ asymptotic behaviour as η increases. We should stress

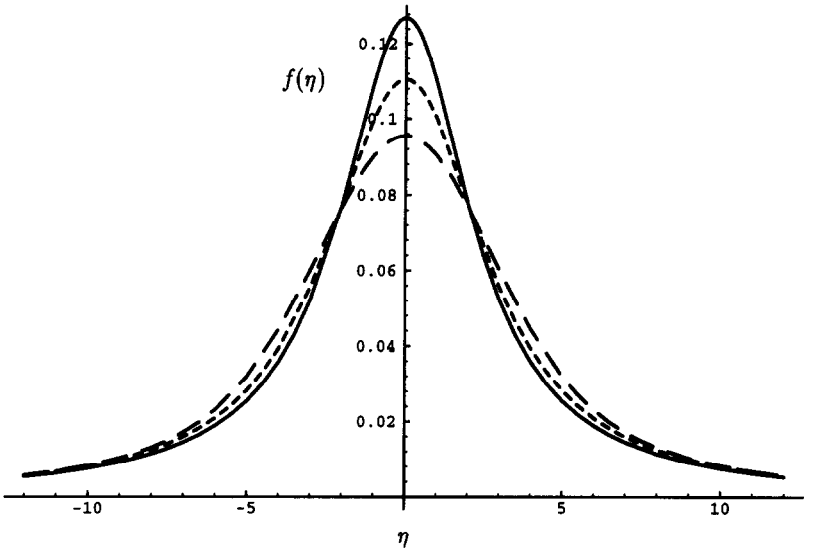

Figure 7: Probability densities for η in the nearest level [eq. (149), solid line], two neighbouring levels [eq. (150), short-dashed line], and "picket fence" [eq. (152), long-dashed line] models for $\eta_0 = 1$, $\eta_c = \sqrt{2\pi}$. Note the identical asymptotic behaviour of $f(\eta)$ at large η.

once more that the asymptotic behaviour of the probability density of x (138) or η is determined by the nearest-level mixing only.

Mathematical expressions describing real PNC effects usually contain products or ratios of several amplitudes. Therefore, the probability densities for these effects are different from eq. (149), even in the two-level approximation. For example, the difference between the capture cross sections for neutrons (protons, photons, etc.) of positive and negative helicity (7), or the photon polarization rotation (121), are proportional to the product of the two opposite parity capture amplitudes α and β (s-wave and p-wave neutrons, $E1$ and $M1$ photons, etc.), times the weak matrix element w divided by the energy denominator. In the two-level approximation the expression for the effect is

$$\phi = \frac{\alpha\beta w}{\varepsilon} = \frac{A}{\varepsilon}\,, \qquad A = \alpha\beta w\,. \tag{153}$$

Assuming that α, β, and w are independent Gaussian random variables, one can obtain the probability density for ϕ in the following form:

$$f_0(\phi) = \frac{2\eta_c\alpha_0\beta_0}{\pi^2}\int_0^\infty \frac{zK_0(z)dz}{(\eta_c\alpha_0\beta_0)^2z^2+\phi^2}\,\Bigg|_{\phi\to\infty} = \frac{1}{\pi}\,\frac{\phi_c}{\phi^2}\,, \tag{154}$$

where $K_0(z)$ is a modified Bessel function, and $\phi_c = 2\eta_c\alpha_0\beta_0/\pi = \sqrt{\frac{8}{\pi}}w_0\alpha_0\beta_0/D$. The asymptotic behaviour at $\phi \gg \phi_c$ coincides with (144), and of course, holds in the many-level case too.

The expression for a relative PNC effect, e.g., the spin asymmetry (8), looks like

$$p = \frac{\alpha}{\beta}\,\frac{w}{\varepsilon}\,. \tag{155}$$

It is a product of two factors (the kinematical factor $K = \alpha/\beta$, and the mixing coefficient $\eta = w/\varepsilon$). Each of them is distributed according to the Cauchy law [eq. (149)]. As a result the probability density for the relative effect p is

$$f_r(p) = \frac{1}{\pi^2}\,\frac{p_c}{p^2 - p_c^2}\ln\frac{p^2}{p_c^2}\,, \quad \text{where} \quad p_c = K_c\eta_c = \frac{\alpha_0}{\beta_0}\,\frac{w_0}{\varepsilon_0}\,. \tag{156}$$

The probability to find large values of p decreases very slowly, as $\ln p^2/p^2$, since there are two possibilities to obtain large p: $\beta \to 0$, or $\varepsilon \to 0$.

The distributions discussed above describe effects induced by mixing of states belonging to different manifolds, e.g., opposite parity states in the PNC or P,T-odd (violating both parity and time-reversal invariance) effects. However, some effects can be produced by mixing of states which have the same parity. The levels in this case repel each other, thus suppressing the probability to find large values of the effect. An example of such effect (T-odd and P-even fivefold correlation in neutron capture) was considered by Bunakov *et al* (1990). The probability density of the effect has the asymptotic form:

$$f_T(t)|_{t\to\infty} \sim \frac{\overline{A^2}}{D^2|t|^3}\,. \tag{157}$$

The variance of the distribution (157) is still infinite, however the relevant integral diverges very weakly, as $\ln t$ at $t \to \infty$. In the case of a finite level width Γ the variance was calculated in (Bunakov *et al* 1990). It is proportional to $\ln(D/\Gamma)$. It should be noted, however, that this purely "statistical" consideration may not be correct for the matrix element between close levels with identical exact quantum numbers due to existence of some approximate quantum numbers, e.g., the isospin $\langle T\rangle$, or the total orbital momentum $\langle L\rangle$.

4.2 PNC Effect Averaged over Many Resonances and the Role of Compound State Widths

As we have shown in the previous section, the probability densities $f(x)$ for PNC effects typically satisfy the following conditions:

$$f(x)|_{|x|\to\infty} = \frac{1}{\pi}\,\frac{x_c}{x^2}\,, \tag{158}$$

$$\int f(x)dx = 1\,,\ \overline{x} = \int xf(x)dx = 0\,. \tag{159}$$

Note that the second condition in (159) can always be achieved by subtracting the regular contribution $x \to x - \overline{x}$, and the corresponding integral exists only in the principle value sense. Suppose one knows the statistics of the on-resonance effects x_i. We need to find out, what is the size of effects one might expect measuring some averaged quantity X (136), or, in a more general form,

$$X = \sum_{i=1}^{n}\theta_i x_i\,, \quad \text{where} \quad \sum_{i=1}^{n}\theta_i = 1\,, \tag{160}$$

where θ_i are the weights which depend on the energy resolution function [$\theta_i = O(1/n)$]. If the variances σ_i^2 of $f_i(x_i)$ were finite the CLT would tell us that as $n \to \infty$ the distribution of X turns into a Gaussian one:

$$F_n(X) \longrightarrow \frac{1}{\sqrt{2\pi\langle\sigma^2\rangle_n}}\,\exp\left(-\frac{X^2}{2\langle\sigma^2\rangle_n}\right)\,, \quad \text{where} \quad \langle\sigma^2\rangle_n = \sum_{i=1}^{n}\theta_i^2\sigma_i^2 \sim O(1/n)\,, \tag{161}$$

producing typical effects X of about $\sigma_i/\sqrt{n}$, i.e., $\sqrt{n}$ times smaller than in a single-resonance measurement. However, the variance of the distribution (158) is infinite. Thus, the standard CLT is inapplicable, and the answer has quite a different form:

$$F_n(X)|_{n\to\infty} = \frac{1}{\pi}\,\frac{X_c}{X^2+X_c^2}\,, \quad \text{where} \quad X_c = \sum_{i=1}^{n}\theta_i x_{ci}\,. \tag{162}$$

The derivation of (162) is given in Appendix E together with the residual term which estimates the convergence of $F_n(X)$ to its limit. The most striking feature of $F_n(X)$ is that contrary to (161) the distribution (162) does not narrow as n increases. This means that in spite of the random signs of effects for different resonances one would obtain averaged PNC effects of about the same magnitude as those for individual resonances: $X_c \sim x_c$ [there is a certain suppression of the kinematical enhancement factor in some cases (sec. 4.3), but it has nothing to do with the statistical suppression due to the random sign of the effects for different resonances, which would take place if x_i had finite variance distributions].

To apply the CLT (162) to real physical effects we need statistical independence of the effects x_i for different resonances. Strictly speaking this is not true, because the energy levels are correlated. However, when the number of resonances n is large, and since the average is dominated by a few of them [see the reasoning after eq. (136)], it is quite improbable that these "important" ones are close to each other (when the level spacings D_+ and D_- in even and odd level sequences are different it is also "impossible"). Therefore, there is a small parameter of about $1/n$ which allows one to consider the effects for different resonances as independent variables.

Below we briefly discuss the limit theorem for some other distributions with infinite variances. The probability density for the relative PNC effect (156) displays the following asymptotic behaviour:

$$f_r(x)|_{x\to\infty} = \frac{1}{\pi^2}\,\frac{x_c}{x^2}\ln\frac{x^2}{x_c^2}\,, \qquad (x_c = p_c). \tag{163}$$

In this case the width of the distribution of the average effect X increases slowly ($\propto \ln n$) with n. With logarithmic accuracy

$$F_n(X) \simeq \frac{1}{\pi}\,\frac{X_c}{X^2+X_c^2}, \qquad X_c \simeq \frac{x_c}{\pi}\ln\frac{n^2X^2}{x_c^2}\,. \tag{164}$$

This means that the typical value of the average relative PNC effect increases with the number of resonances where the effect has been measured (a conclusion opposite to the standard CLT). This seems to happen in the present measurements of the PNC effects in neutron capture (Alfimenkov *et al* 1981, 1983, Masuda *et al* 1989, Bowman *et al* 1990, Frankle *et al* 1991). We should also mention the distributions of effects caused by mixing of levels repelling each other [see end of sec. 4.1, eq. (157)], where the asymptotic behaviour of the probability density is: $f(x) \sim x_c^2/|x|^3$. In this case the Fourier transform of the $F_n(X)$ probability density is

$$\tilde{F}_n(\omega) = \exp\left(-\frac{x_c^2\omega^2}{2n}\left[\ln\frac{2n}{x_c|\omega|} + \text{const}\right]\right)\,. \tag{165}$$

The difference with the standard CLT here is only the logarithmic term in the exponent. This term shows that the width of the distribution decreases as $\sqrt{\ln n/n}$ instead of the standard $1/\sqrt{n}$.

So far we neglected the widths of the compound states mixed by the weak interaction. It is easy to see that this supposition is crucial for the validity of eq. (162). When the finite widths are taken into account the mixing coefficient (137) can not be greater than $\sim w/\Gamma$, since Γ determines the smallest value of the denominator. This restriction becomes essential for the average effect X when the "probable" minimal interval $|E_+ - E_-| \sim D/n$ becomes of the order of Γ: $D/n \sim \Gamma$. In the many-decay-channel case the fluctuations of the compound state width are usually suppressed and the possible magnitude of the mixing coefficient is indeed limited. In the case of a single-decay-channel domination the fluctuations of the width are usually large. However, a simultaneous vanishing of the interval ε and the width Γ leading to a very large mixing is quite improbable. Therefore, in principle, finite widths make the variance of the probability distribution of the mixing coefficient finite. For small widths $\Gamma \ll D$ this variance is very large [$\propto (\Gamma D)^{-1}$ for mixing of opposite parity levels (Flambaum 1985), and $\propto \ln(D/\Gamma)$ for the same parity levels (Bunakov *et al* 1990)], and in practice it does not have any physical meaning, if the number of resonances involved is $n \ll D/\Gamma$ ($D/\Gamma \sim 300$ for compound states near the neutron threshold in non-fissionable nuclei). Indeed, the probability to find a pair of mixing levels separated by $\varepsilon \sim \Gamma$ interval is very small in this case ($\sim n\Gamma/D$), and the widths can be simply ignored. However, the widths must be taken into account for $n \gtrsim D/\Gamma$, or if one is interested in the probability of finding very large effects $|X| > X_c D/(\Gamma n)$.

Quantitatively the results for the finite width look as follows. The variance of x becomes finite and at $\Gamma \ll D$ it is given by

$$\overline{x^2} \simeq \frac{\pi \overline{A^2}}{D\Gamma} \,. \tag{166}$$

Of course, this means that the $1/x^2$ asymptotic behaviour of $f(x)$ is violated if finite Γ are taken into account, and there is a certain "cut-off" in $f(x)$ at large x. The variance of the average effect X (136) is now finite as well:

$$\langle X^2 \rangle_n \simeq \frac{\pi \overline{A^2}}{nD\Gamma} \,. \tag{167}$$

At $n \ll D/\Gamma$ its square root is much greater than X_c, the characteristic width of $F_n(X)$ (162): $X_c = x_c = \pi\overline{A}/D \sim \sqrt{\overline{A^2}/D^2}$. Thus, $F_n(X)$ retains its Cauchy form (162) for $|X| < \frac{D}{n\Gamma} X_c$. Therefore, as a manifestation of the finite state widths, we obtain the following interplay of the infinite-variance (162) and conventional (161) versions of the CLT for the probability density $F_n(X)$ of the average effect X:

$$\text{for } 1 \ll n \ll \frac{D}{\Gamma}: \quad F_n(X) = \frac{1}{\pi} \frac{X_c}{X^2 + X_c^2} \,, \qquad |X| < \frac{D}{n\Gamma} X_c \,, \qquad X_c = x_c = \frac{\pi \overline{|A|}}{D} \,, \tag{168}$$

$$\text{for } \quad n \gg \frac{D}{\Gamma}: \quad F_n(X) = \frac{\exp\left[-\frac{X^2}{2\langle X^2 \rangle_n}\right]}{\sqrt{2\pi \langle X^2 \rangle_n}} \,, \quad |X| \lesssim \sqrt{\langle X^2 \rangle_n} \,, \quad \langle X^2 \rangle_n = \overline{\frac{x^2}{n}} \simeq \frac{\pi \overline{A^2}}{nD\Gamma} \,. \tag{169}$$

4.3 PNC Effects Integrated over the Initial State Energy

Let us now show that real PNC effects averaged over the energy of the initial state can be indeed expressed in terms of the sum X (160) of individual resonance contributions. Such situation takes place when one cannot resolve individual compound resonances. In (Flambaum 1985) the mean square values of energy-averaged PNC effects were roughly estimated (the aim was to separate possible regular mechanisms of the effects). However, as has been shown above, when the number of resonances involved

is not too large: $n < D/\Gamma$, one has to consider the probability distribution of the effects, since the mean square value of the effect is too large [$\propto (D\Gamma)^{-1/2}$], and is not observable.

All PNC effects occur due to interference of some opposite parity amplitudes (s wave and p wave for neutrons, $E1$ and $M1$ for photons, etc.). The influence of energy averaging on the magnitude of a PNC effect depends on whether this interference happens in the capture channel or in the decay channel. Thus, we can divide all PNC effects into different classes.

PNC effects due to interference in the decay channel. In this case the consideration can be limited to one dominating capture amplitude (s wave for neutrons, $E1$ for photons, etc.). Examples of the corresponding PNC effects are: the $\boldsymbol{\sigma} \cdot \mathbf{p}_f$ correlation between the neutron spin and the momentum of the light fragment in nuclear fission, a similar correlation in the (n,γ) reaction, the circular polarization of the emitted γ quanta, and other correlations of the third class, according to the classification of Flambaum and Sushkov (1985). The amplitude for a reaction of this type which leads to some final state $|f\rangle$ looks like

$$\sum_s \frac{A_{fs}T_s}{E-E_s+\frac{i}{2}\Gamma_s} + \sum_{s,p} \frac{B_{fp}W_{ps}T_s}{(E-E_s+\frac{i}{2}\Gamma_s)(E-E_p+\frac{i}{2}\Gamma_p)} = \sum_s \frac{A_{fs}T_s}{E-E_s+\frac{i}{2}\Gamma_s}\left(1+\frac{1}{A_{fs}}\sum_p \frac{B_{fp}W_{ps}}{E-E_p+\frac{i}{2}\Gamma_p}\right), \tag{170}$$

where T_s is the capture amplitude, A_{fs} and B_{fp} are the decay amplitudes from the opposite parity compound states $|s\rangle$ and $|p\rangle$, and W_{ps} is the weak matrix element coupling these states. The relative magnitude of the PNC effect near an isolated s resonance is given by [compare with eq. (31)]

$$P = \mathrm{Re}\left(\frac{2}{A_{fs}}\sum_p \frac{B_{fp}W_{ps}}{E-E_p+\frac{i}{2}\Gamma_p}\right). \tag{171}$$

Here we do not specify any coefficients depending on the angular momenta of the resonances since they depend on the particular reaction under consideration. They can be found, e.g., in (Sushkov and Flambaum 1982, Flambaum and Sushkov 1984, 1985), see also Appendix A.

In order to find the integral value of the PNC effect the squared absolute value of the amplitude (170) has to be integrated over the energy E:

$$\int \theta(E)dE \left\{ \sum_{s,s'} \frac{A^*_{fs'}T^*_{s'}A_{fs}T_s}{(E-E_{s'}-\frac{i}{2}\Gamma_{s'})(E-E_s+\frac{i}{2}\Gamma_s)} + \left[\sum_{s,p,s'} \frac{A^*_{s'f}T^*_{s'}B_{fp}W_{ps}T_s}{(E-E_{s'}-\frac{i}{2}\Gamma_{s'})(E-E_s+\frac{i}{2}\Gamma_s)(E-E_p+\frac{i}{2}\Gamma_p)} + \text{c.c.} \right] \right\}, \tag{172}$$

where $\theta(E)$ is a smooth energy resolution function of the characteristic width Δ, normalized as $\int \theta(E)dE/D_s = 1$, so that $\sum_s \theta(E_s) = 1$. The term quadratic in W has been omitted from eq. (172). If $\Gamma \ll D$ the dominant contribution to the integral (172) is given by the diagonal terms $s = s'$. Assuming that the number of s-resonances inside the integration interval is large, $n \sim \Delta/D_s \gg 1$, and omitting some common factor we obtain the following result for the integral effect:

$$\sum_s \theta_s |A_{fs}|^2 |T_s|^2 + \left[\sum_{s,p} \theta_s \frac{A^*_{fs}B_{fp}W_{ps}|T_s|^2}{E_s-E_p+\frac{i}{2}(\Gamma_s+\Gamma_p)} + \text{c.c.} \right] = \overline{|A_{fs}|^2|T_s|^2}\,(1+X), \tag{173}$$

where $\theta_s = \theta(E_s)$, and X determines the relative magnitude of the integral effect:

$$X = \sum \theta_s x_s \,, \qquad x_s = \sum_p \mathrm{Re}\left[\frac{V_{ps}}{E_s - E_p + \frac{i}{2}(\Gamma_s + \Gamma_p)}\right] \,, \tag{174}$$

$$V_{ps} = \frac{2A^*_{fs}B_{fp}W_{ps}|T_s|^2}{\overline{|A_{fs}|^2|T_s|^2}} \,, \qquad \overline{|A_{fs}|^2|T_s|^2} = \sum_s \theta_s |A_{sf}|^2|T_s|^2 \,. \tag{175}$$

The squared amplitudes $|T_s|^2$ can be replaced by the capture widths $\Gamma_s^{(c)}$ (e.g., $\Gamma_s^{(n)}$, for the neutron capture), and $|A_{fs}|^2$ by the partial decay widths $\Gamma_s^{(d)}$:

$$\overline{|T_s|^2|A_{fs}|^2} = \sum_s \theta_s g \Gamma_s^{(c)} \Gamma_s^{(d)} \,,$$

where g is the statistical weight of the resonances. The value of V_{ps} is usually real (fission is an exception). Equation (174) shows that X is the weighted average of the single s-resonance contributions x_s [compare the expression for x_s with eq. (138); the width $\Gamma = \Gamma_s + \Gamma_p$ is introduced into it by $E_i \to E_i + i\frac{\Gamma}{2}$, and taking the real part]. Thus, the probability density of the integral PNC effect X at $n \ll D_s/\Gamma$ is given by [see eq. (168)]

$$f(X) \simeq \frac{1}{\pi} \frac{X_c}{X^2 + X_c^2}, \qquad X_c = \frac{\pi \overline{|V_{ps}|}}{D_p} \,. \tag{176}$$

Note that expression (174) for x_s differs from the single-resonance relative effect p (155) by the factor $|A_{fs}|^2|T_s|^2/\overline{|A_{fs}|^2|T_s|^2}$. The mean value of this factor is unity. However, the presence of the A_{fs} amplitude in the denominator of p [α in (155)] gives an extra possibility for p to be large [the $\ln(p^2/p_0^2)$ factor in the distribution (156)] and slightly changes the CLT. As a result the expected value of the average (integral) effect depends on the method of averaging. The distribution of the average over the single-resonance effects slowly widens with n [eq. (164)], whereas the distribution of the energy average tends to its limit (176).

PNC effects due to interference in the capture channel. Let us start from the calculation of a PNC effect in the total capture cross section: the difference of the cross sections for neutrons (protons, photons, etc.) of positive and negative helicity. The capture cross section $\sigma(E)$ is obtained from (19), (20):

$$\sigma(E) \propto \mathrm{Im}\left[\sum_s \frac{|T_s|^2}{E - E_s + \frac{i}{2}\Gamma_s} + \sum_p \frac{|T_p|^2}{E - E_p + \frac{i}{2}\Gamma_p} \pm \sum_{s,p} \frac{T_s^* W_{sp} T_p + T_p^* W_{ps} T_s}{(E - E_s + \frac{i}{2}\Gamma_s)(E - E_p + \frac{i}{2}\Gamma_p)}\right] \,. \tag{177}$$

If one neglects the kinematic dependence of the amplitudes T_s, T_p and integrates (177) over the energy interval $\Delta \gg D_s$, D_p, the third sum, which is responsible for the PNC effect, vanishes (the integration contour can be closed in the upper half of the complex plane leaving out all the poles of this term). It is easy to explain the reason for this vanishing. The expression in question has opposite signs at $E = E_s$ and $E = E_p$ and the contributions of s and p resonances cancel each other. However, the quantity measured experimentally is not the cross section itself, but the number of neutrons passed through the sample, or the neutron spin rotation (121), which is expressed in terms of $\mathrm{Re} f_{\mathrm{PV}}(0)$. In s resonances the attenuation length is too short for any neutrons to be detected in the end. Thus, the s-resonance contribution ($E = E_s$) is totally suppressed, and no cancellation happens.

Below we present some estimates for the magnitude of the energy-averaged PNC effect: the difference between the positive and negative helicity neutron numbers N_+ and N_-. The number of neutrons passed

through the sample of length l is $N = N_0 \exp(-\sigma n_0 l)$, where N_0 is the initial number of neutrons, and n_0 is the concentration of atoms in the sample. The neutron number difference then is

$$N_+ - N_- = N_0 \left(e^{-\sigma_+ n_0 l} - e^{-\sigma_- n_0 l}\right) \simeq -N_0 e^{-\sigma n_0 l}(\sigma_+ - \sigma_-) n_0 l \,, \tag{178}$$

where $\sigma = (\sigma_+ + \sigma_-)/2$ is the average cross section for neutrons with different helicities. The relative difference of the neutron numbers integrated over the energy distribution $\theta(E)$ of the projectiles is given by the ratio

$$\frac{N_+ - N_-}{N_+ + N_-} = -\frac{n_0 l \int (\sigma_+ - \sigma_-) e^{-\sigma n_0 l} \theta(E) dE}{2 \int e^{-\sigma n_0 l} \theta(E) dE} \,. \tag{179}$$

The difference $\sigma_+ - \sigma_-$ is large near p resonances only, where it is expressed in terms of the spin asymmetry P (8):

$$\sigma_+ - \sigma_- = 2 P_p \sigma_p(E) \,, \quad P_p \equiv \frac{\sigma_{p+} - \sigma_{p-}}{\sigma_{p+} + \sigma_{p-}} \simeq 2 \sum_s \frac{T_s}{T_p} \frac{W_{sp}}{E_s - E_p} \,, \tag{180}$$

where $\sigma_{p\pm}$ and $\sigma_p(E)$ are the p-wave capture cross sections dominating in σ at $E = E_p$. In the case of $\Gamma \ll D$ (well separated resonances) the total cross section can be presented as $\sigma = \sigma_0 + \sigma_p$, where σ_0 is the cross section far from the p resonance. The integral in the numerator of (179) is replaced by the sum over p resonances, the integral in each of its items being calculated over some energy interval Δ_p containing the resonance ($\Gamma_p \ll \Delta_p \ll D_p$):

$$\frac{N_+ - N_-}{N_+ + N_-} \simeq -\frac{n_0 l \sum_p P_p e^{-\sigma_0 n_0 l} \int\limits_{\Delta_p} \sigma_p(E) \theta(E) e^{-\sigma_p n_0 l} dE}{e^{-\sigma_0 n_0 l} \int \theta(E) dE} = -\sum_p P_p \frac{l}{l_0} \int\limits_{\Delta_p} \frac{\sigma_p(E)}{\sigma_0} \exp\left[-\frac{\sigma_p(E) l}{\sigma_0 l_0}\right] \theta(E) \frac{dE}{D_p}$$

$$\simeq \sum_p P_p \frac{l}{l_0} \frac{\pi \Gamma_p}{2 D_p} \frac{\sigma_p(E_p)}{\sigma_0} \exp\left[-\frac{\sigma_p(E_p) l}{\sigma_0 l_0}\right] \theta(E_p) \tag{181}$$

$$\equiv -\sum_p P_p q_p \theta_p \equiv \sum_p x_p \theta_p \,, \tag{182}$$

where q_p is defined by eqs. (181), (182), $\theta_p \equiv \theta(E_p)$, $x_p \equiv -P_p q_p$, $l_0 = 1/\sigma_0 n_0$ is the attenuation length far from the resonance, and the normalization $\int \theta(E) dE / D_p = 1$ has been used.

Now we can apply the CLT to the $X = \sum_p x_p \theta_p$ variable from eq. (182), where

$$x_p = -P_p q_p = \frac{A_p}{E_p - E_s} + \sum_s{}' B_{ps} \,, \tag{183}$$

$$q_p = \frac{\pi \Gamma_p}{2 D_p} Z_p \exp(-Z_p) \,, \quad Z_p = \frac{\sigma_p(E_p) l}{\sigma_0 l_0} \,. \tag{184}$$

The first term in the right hand side of (183) describes the mixing of the p resonance with the nearest s resonance [compare with eq. (138)], and produces the x^{-2} decrease of the corresponding probability density. The length of the sample l can be adjusted to achieve an optimal situation $\overline{Z_p} = 1$, $q_p = \pi \Gamma_p / (2 D_p e)$. In this case the magnitude of the PNC effect is $x_c \sim P_c \Gamma / D$ (P_c is a characteristic value of the single-resonance effect, Γ and D are the average width and spacing for the p resonances). Therefore, the PNC effect (178) in the integral spectrum is suppressed by a factor Γ/D, with respect to single-resonance effects, however, it does not decrease with the number n of resonances involved (poor energy resolution), as long as $n < D/\Gamma$. It is necessary to add that of course the magnitude of the relative effect (179), or P in (180), is limited: $|P| < 1$. Therefore, there is another boundary $\max|P| \sim n P_c < 1$

on the possible values of n in this case. Although, this limit is not important for the integral effect, where $x_c \sim 10^{-4}$, it can be essential if one calculates the average of the relative cross section differences P_p, which have typical values of about 10^{-2}. This gives the limit $n < 100$.

Integral PNC effect in elastic scattering and the "weak optical potential". This case is somewhat intermediate between those studied above. On the one hand, the corresponding PNC effect (e.g., the $\boldsymbol{\sigma} \cdot \mathbf{n}$ correlation, where $\boldsymbol{\sigma}$ is the incidental neutron spin, and $\mathbf{n}$ is the direction of the scattered neutron momentum) is due to interference of the final state amplitudes $[T_s Y_{00}(\vartheta, \varphi)$ and $T_p Y_{1m}(\vartheta, \varphi)]$. On the other hand, it is kinematically suppressed as T_p/T_s, since the s-wave scattering proportional to T_s^2 dominates. The scattering amplitude taking into account the s-wave capture is given by [eq. (20), Appendix A]

$$f(\vartheta) = f_0 - \frac{1}{2k}\left[\sum_s \frac{T_s^2}{E - E_s + \frac{i}{2}\Gamma_s} + \sum_{s,p} \frac{T^*_{p_{1/2}} W_{ps} T_s}{\left(E - E_s + \frac{i}{2}\Gamma_s\right)\left(E - E_p + \frac{i}{2}\Gamma_p\right)} (\boldsymbol{\sigma} \cdot \mathbf{n})\right] , \tag{185}$$

where the amplitudes are $T_s = \pm\sqrt{\Gamma_s^{(n)}}$, $T_p = \pm i\sqrt{\Gamma_p^{(n)}}$, and the simplest case of the zero-spin target is considered. For the longitudinally polarized neutrons $\boldsymbol{\sigma} \cdot \mathbf{n} = \cos\vartheta$. Folding the differential cross section with $\theta(E)$ energy distribution yields

$$\frac{d\sigma}{d\Omega} \to |f_0|^2 + \sum_s \theta_s \sigma_s(E_s) \frac{\pi\Gamma_s}{2D_s} \left\{1 + \sum_p \left[\frac{T^*_{p_{1/2}} W_{ps}}{T_s\left[E_s - E_p + \frac{i}{2}(\Gamma_s + \Gamma_p)\right]} + \text{c.c.}\right] \cos\vartheta\right\} . \tag{186}$$

The angular distribution of neutrons $W(\vartheta)$ is determined by the ratio of eq. (186) to its angular average. It is given by

$$W(\vartheta) = 1 + \frac{\sum_s \theta_s \sigma_s(E_s) \frac{\pi\Gamma_s}{2D_s} P_s}{|f_0|^2 + \sum_s \theta_s \sigma_s(E_s) \frac{\pi\Gamma_s}{2D_s}} \cos\vartheta , \tag{187}$$

where

$$P_s = 2\text{Re} \sum_p \frac{T^*_{p_{1/2}} W_{ps}}{T_s\left[E_s - E_p + \frac{i}{2}(\Gamma_s + \Gamma_p)\right]} \tag{188}$$

determines the effect for a given s resonance. Introducing the contribution of the s resonance to the energy averaged cross section $\sigma_s = \sigma_s(E_s)\pi\Gamma_s/(2D_s)$, we obtain

$$W(\vartheta) = 1 + \frac{\sum_s \sigma_s P_s \theta_s}{|f_0|^2 + \sum_s \sigma_s \theta_s} \cos\vartheta = 1 + \sum_s \frac{\sigma_s}{\overline{\sigma}} P_s \theta_s \cos\vartheta , \tag{189}$$

where $\overline{\sigma} = |f_0|^2 + \sum_s \sigma_s \theta_s$ is the sum of the potential cross section and the energy averaged resonance cross section, which are usually of the same order of magnitude. Thus, the angular dependence of $W(\vartheta)$ (189) is determined by the integral effect

$$X = \sum_s x_s \theta_s , \qquad x_s = \frac{\sigma_s}{\overline{\sigma}} P_s ,$$

which obeys the CLT (162). There is a certain kinematical suppression (T_p/T_s) for the effect in the s resonance, but, as in the case of capture, the effect does not decrease after averaging over the resonances.

Kinematical suppression takes place in the potential scattering as well (the PNC effect due to direct interaction of the neutron with the weak potential of the nucleus). However, the potential contribution

(valence mechanism) does not show statistical enhancement, and the resonant PNC effect dominates. Therefore, the PNC effect in the low-energy scattering should have giant fluctuations on the scale depending on the energy resolution (manifestation of the infinite-variance CLT). The magnitude of the statistically enhanced effect will be about $\sqrt{N} \sim 10^2 - 10^3$ times greater than the potential effect. As is known, the energy-averaged cross section $\overline{\sigma}$ can be obtained from the optical potential, since the fluctuations decrease as $1/\sqrt{n}$. Contrariwise, there is no "weak optical potential" for the PNC effects, since the size of the fluctuations is constant, and is much greater than the mean value (produced by the weak nucleon-nucleus potential).

PNC effects in the integral spectrum of final states in (n,γ) reaction. These effects were observed by Vesna *et al* 1982 and calculated by Bunakov *et al* 1984 and Flambaum and Sushkov 1985. However, in this case the statistical enhancement of mixing in the final states competes with the dynamical enhancement due to compound resonance mixing in the initial state [see diagrams (27) and eqs. (28), (29)], and the whole question deserves further investigation.

Concluding this section we should remind the reader that all PNC effects are of interference nature. The results obtained above show that because of the peculiar statistics the interference effects does not necessarily vanish upon averaging.

5 Is there a Limit for Enhancement?

When the number of excited particles increases the interval between the levels decreases exponentially. A natural question arises: can the magnitude of dynamical enhancement increase up to infinity? The common sense tells us that it is hardly possible, since we apparently do not observe large PNC effects in macroscopic bodies where the spectrum of states is "infinitely" dense. (Strictly speaking this argument is not correct since a macroscopic body is not in a stationary state and does not possess exact symmetries). However, one can consider a system of variable size, say, an atomic cluster, and try to follow what happens with the enhancement factor when the number of particles increases. There are several reasons which can limit the enhancement factor.

1. Widths of compound states. If the admixed state is quasistationary the energy denominator in the mixing coefficient is $E - E_s + i\Gamma_s/2$, and its magnitude can not be smaller than $\Gamma_s/2$. This is a natural limit of the enhancement for fissionable nuclei where the width is comparable with the level spacing D. The width also becomes important in any nuclear reaction at higher energies. However, in atomic systems the natural (radiative) width can be extremely small in comparison with the atomic energy unit.

2. "Spectator" degrees of freedom. There are certain degrees of freedom (vibrations, rotations) which do not participate in the weak interaction directly. However, these excitations have a very dense spectrum in molecules and clusters (recall that the rotational intervals in heavy molecules are $M_{\rm mol}/m_e \sim 10^5$ times smaller than the energy intervals between the electron states). At first sight one could conclude that only the interval between the electron states is important, and the interaction with rotations and vibrations (phonons) produces some effective width for electron states only, i. e., their contribution

to the enhancement is destructive. However, this is not true. The point is that one can construct an effective weak operator which mixes rotational or vibrational levels. For example, (Labzovsky 1978, Sushkov and Flambaum 1978, Flambaum and Khriplovich 1985) calculated the effective weak operator which mixes opposite parity rotational levels in diatomic molecules: $W_{\rm PNC} = \kappa(\mathbf{j}_e \times \mathbf{I}_n) \cdot \mathbf{A}_m$, where $\mathbf{j}_e$ is the electron angular momentum, $\mathbf{I}_n$ is the nuclear spin, and $\mathbf{A}_m$ is the direction of molecular axis. The effective interaction constant κ is proportional to the electron-nucleus PNC interaction. Note that only the nuclear-spin-dependent part of the weak interaction and the nuclear anapole moment (parity-nonconserving magnetic multipole) contribute to it. The situation is even simpler in the case of P,T-violation, where the effective interaction is $W^{\rm PT} = \lambda_e \mathbf{j}_e \cdot \mathbf{A}_m + \lambda_n \mathbf{I}_n \cdot \mathbf{A}_m$. The effective interaction constant λ_e (λ_n) is proportional to the P,T-odd electron (nucleon) electric dipole moment, or to the electron-nucleon (nucleon-nucleon) P,T-odd interactions. This effective interaction can mix very close opposite-parity rotational molecular levels, thus enhancing PNC and P,T-odd effects in molecules by 5 orders of magnitude in comparison with atoms.

The density of rotational and vibrational levels in complex molecules and clusters is very high even at low excitation energies (where the radiative width, proportional to ω^3, is negligibly small). Therefore, there is a possibility of very large enhancement factors. It would also be interesting to consider the enhancement of parity conserving effects: violation of the adiabatic approximation for the rotation (due to the Coriolis interaction) and for the vibration in the energy range of high electron level density.

3. Finite time of the process, collisional broadening, etc. These effects produce an effective width of the states and depend on particular experimental conditions.

4. Poor energy resolution. As it was shown in Section 4, the averaging of a "random" PNC effect by itself does not reduce the magnitude of typical enhancement. However, there could be some "kinematical" reasons for suppression. For example, the PNC effects are large in $M1$-electromagnetic transitions (due to the kinematical enhancement $E1/M1$), but the integrated photon-capture cross section is dominated by the $E1$-capture where the effects are suppressed by the factor of $M1/E1$. However, one can find effects which are not suppressed kinematically. In nuclear reactions these are PNC effects in fission, some effects in neutron radiative capture, etc. There is also an example of such effect in atomic physics: the P,T-odd rotation of the polarisation plane of light (optical activity) in a gas placed in a longitudinal electric field (Sushkov and Flambaum 1978, Barkov *et al* 1988). This effect is proportional to the P,T-violating electric dipole moment (similar to the Faraday rotation in magnetic field, where the effect is proportional to the magnetic moment).

6 Concluding Remarks

There are several mechanisms which enhance PNC and P,T-odd effects in complex systems:

1. Kinematical enhancement. The amplitude admixed by the weak interaction is substantially bigger than the main reaction amplitude (e.g., the admixed s-wave amplitude vs the main p-wave amplitude in neutron capture).

2. Dynamical enhancement. This enhancement is due to very small energy intervals between excited states in many-body systems. A naive estimate of this enhancement $\sqrt{N}$ (N is the number of principal components) is usually an order of magnitude greater than its true magnitude. The correct value should take into account particular dynamics of the system, e.g., the information about localization law for the components of the compound states, the properties of the perturbation operator (e.g., parity-violating operators in nuclei transfer particles from one shell to another), the single-particle occupation numbers, possible collective effects, etc.
3. Resonance enhancement. In the absence of kinematical enhancement in the capture channel of the reaction one can "come" very close to the admixed state energy. For example, in the case of PNC in nuclear fission the main neutron capture amplitude is the s wave. The energy dependence near an opposite parity (p-wave) compound resonance is given by $D/(E - E_p + \frac{i}{2}\Gamma_p)$. If the distance to the p-wave resonance is much smaller than the mean level spacing D between the compound states, we have resonance enhancement of up to D/Γ. This enhancement factor can be especially large for some PNC and P,T-odd effects in neutron radiative capture where the resonance width Γ is small.
4. Statistical enhancement.

   (a) Resonance statistical enhancement. As known the levels of two subsystems with different quantum numbers (say, opposite parities) do not repel each other. When one considers effects for n compound resonances there is a high probability that at least for one of them the distance to the nearest opposite-parity level will be very small $|E_s - E_p| \lesssim D/n$. This will make the contribution of this resonance about n times greater than the "typical" one.

   (b) Structural statistical enhancement. Relative values of resonant PNC effects usually contain ratios of the admixed amplitudes to the main one. Random fluctuations of the main (p-wave) amplitudes in the case of n resonances can make one of these amplitudes n times smaller than the r.m.s. one, producing the effect n times greater than the typical one.

   Statistical enhancement combined with dynamical and kinematical enhancement can produce maximal possible value of the effect (say, 100% parity nonconservation). Parity nonconservation at 10% level which corresponds to the total enhancement factor of 10^6 has been already observed in Dubna and Los Alamos. Statistical enhancement is very important when considering the effects averaged over many resonances. Because of this enhancement the values of the randomly fluctuating effect do not tend to zero (proportionally to $1/\sqrt{n}$ as prescribed by the standard Central Limit Theorem of the probability theory) for measurements including n resonances at once.

In this review we mostly considered nuclear physics applications. However, there are very interesting applications of perturbation enhancement to other systems and phenomena: violation of "non-relativistic" conservation laws in rare-earth and actinide atoms, violation of adiabatic approximation in molecules, parity violation in chemical reactions, enhancement of external noise and "violation" of quantum mechanics in atomic clusters, spin systems and mesoscopic systems, etc. For example, the idea of dynamical enhancement has been recently applied to such a "distant" physical phenomenon as Anderson localization. It was shown that the localization length in the two-body problem is strongly increased due to the enhancement of the interparticle interaction (Shepelyansky 1994, Sushkov 1994).

ACKNOWLEDGEMENTS

The authors would like to thank A. W. Thomas for suggesting the idea of this review, and M. B. Johnson, O. P. Sushkov and V. G. Zelevinsky for useful discussions. This work was supported by the Australian Research Council.

Appendices

A Calculation of Reaction Amplitudes

The rules for writing down reaction amplitudes near the neutron threshold have been formulated in (Flambaum and Sushkov 1984). Let $\mathbf{n}_k = \mathbf{k}/k$ be the direction of the neutron momentum $\mathbf{k}$, I the spin of the target nucleus, $\mathbf{J} = \mathbf{I} + \mathbf{j}$ the momentum of the compound resonance, α the polarization of the neutron, and $\mathbf{j} = \mathbf{l} + \mathbf{s}$ the momentum of the captured p-wave neutron. Then,

(i) The amplitude of neutron capture into the s resonance is

$$C^{JJ_z}_{II_z\frac{1}{2}\alpha}\gamma^{(n)}_s(E)\,. \tag{A1}$$

(ii) The amplitude of neutron capture into the p resonance is

$$\sum_{jj_zm} C^{JJ_z}_{II_zjj_z}C^{jj_z}_{1m\frac{1}{2}\alpha}\sqrt{4\pi}Y^*_{1m}(\mathbf{n}_k)i\gamma^{(n)}_{pj}(E)\,. \tag{A2}$$

Here $[\gamma^{(n)}_s(E)]^2 = \Gamma^{(n)}_s(E)$ is the s resonance neutron width, and $[\gamma^{(n)}_{pj}(E)]^2 = \Gamma^{(n)}_{pj}(E)$ is the neutron width corresponding to the emission of a neutron with momentum j ($\Gamma^{(n)}_p = \Gamma^{(n)}_{p_{1/2}} + \Gamma^{(n)}_{p_{3/2}}$).

(iii) The matrix element of the weak interaction between two compound states is $\langle s|W|p\rangle$. It is imaginary if we use the standard definition of the Y_{lm} functions.

(iv) The Green function of the compound nucleus is

$$\frac{1}{E - E_c + \frac{i}{2}\Gamma_c}\,. \tag{A3}$$

(v) The common factor for the scattering amplitudes is $-1/2k$.

The additional factor i in the p-wave capture amplitude is due to the phase of the free motion p wave. We consider scattering at $kR \ll 1$, therefore the potential scattering phase is zero. It is shown in (Flambaum and Sushkov 1984) that there is an additional phase factor $e^{i\phi}$ ($\phi \sim \delta\Gamma/D$, where $\delta\Gamma$ is the fluctuation of the total compound state width). However, this factor can be large only when the width fluctuations are large, e.g., if the fission channel is open. One can find the rules for the fission amplitudes in, e.g., (Sushkov and Flambaum 1981b, 1981c, 1982), and those for the emission (or absorption) of γ-quanta in (Blin-Style 1973, Flambaum and Sushkov 1985).

Let us illustrate the rules by writing several simple amplitudes. The forward elastic scattering amplitude near the s resonance is given by

$$f(0) = -\frac{1}{2k}C^{JJ_z}_{II_z\frac{1}{2}\alpha}\gamma^{(n)}_s(E)\frac{1}{E - E_s + \frac{i}{2}\Gamma_s}C^{JJ_z}_{II_z\frac{1}{2}\alpha}\gamma^{(n)}_s(E)\,. \tag{A4}$$

After summation over J_z and averaging over I_z one obtains the usual Breit-Wigner formula [the second term in the right hand side of eq. (20)] with $g = (2J+1)/2(2I+1)$. Similarly, for the p resonance

$$f(0) = -\frac{1}{2k} \sum_{\substack{jj_zm \\ j'j'_zm'}} C^{JJ_z}_{II_zj'j'_z} C^{j'j'_z}_{1m'\frac{1}{2}\alpha} \sqrt{4\pi} Y_{1m'}(\mathbf{n}_k)(-i)\gamma^{(n)}_{pj'}(E) \frac{1}{E - E_p + \frac{i}{2}\Gamma_p}$$
$$\times C^{JJ_z}_{II_zjj_z} C^{jj_z}_{1m\frac{1}{2}\alpha} \sqrt{4\pi} Y^*_{1m}(\mathbf{n}_k) i\gamma^{(n)}_{pj}(E) \tag{A5}$$

The expression obtained after summation over J_z and averaging over I_z

$$f(0) = -\frac{1}{2k} \frac{g\Gamma^{(n)}_p(E)}{E - E_p + \frac{i}{2}\Gamma_p} \tag{A6}$$

the expression coincides with the third term in the right hand side of eq. (20), $\Gamma^{(n)}_p = \gamma^{(n)2}_{p_{1/2}} + \gamma^{(n)2}_{p_{3/2}}$. Finally, the parity violating forward scattering amplitude [e.g., the fourth diagram in (21)] is given by

$$-\frac{1}{2k} C^{JJ_z}_{II_z\frac{1}{2}\alpha} \gamma^{(n)}_s(E) \frac{1}{E - E_s + \frac{i}{2}\Gamma_s} \langle s|W|p\rangle \frac{1}{E - E_p + \frac{i}{2}\Gamma_p} \sum_{jj_zm} C^{JJ_z}_{II_zjj_z} C^{jj_z}_{1m\frac{1}{2}\alpha} \sqrt{4\pi} Y_{1m}(\mathbf{n}_k) i\gamma^{(n)}_{pj}(E) \ . \tag{A7}$$

After summation over J_z, averaging over I_z, and adding the contribution of the third diagram in (21) we obtain

$$f_{\rm PV}(0) = \pm\frac{1}{2k} \frac{2g\gamma^{(n)}_s(E) i\langle s|W|p\rangle \gamma^{(n)}_{p_{1/2}}(E)}{(E - E_s + \frac{i}{2}\Gamma_s)(E - E_p + \frac{i}{2}\Gamma_p)} \ . \tag{A8}$$

in agreement with the last term in the right hand side of (20). The $\pm$ sign corresponds to the positive or negative helicities of the neutron.

B Correlations Between Eigenvectors and Superlocalization in the Random Separable Interaction Model

Assume that the off-diagonal matrix elements of the Hamiltonian matrix are separable:

$$H_{ij} = f v_i v_j + \epsilon_i \delta_{ij} \tag{B1}$$

where v_i are random variables, and ϵ_i are the basis state energies, $i = 1, N$. In this case the number of independent variables N is much smaller than the number of Hamiltonian matrix elements N^2 (as in a real physical system, see sec. 3.3). The Schrödinger equation $H\Psi_\lambda = E_\lambda \Psi_\lambda$, $\Psi_\lambda = \sum_i C^{(\lambda)}_i \Phi_i$ can be written in the matrix form: $\sum H_{ij} C^{(\lambda)}_j = E_\lambda C^{(\lambda)}_i$, which yields

$$C^{(\lambda)}_i = \frac{f q_\lambda v_i}{E_\lambda - \epsilon_i} \ , \tag{B2}$$

$$\text{where} \qquad q_\lambda = \sum_j C^{(\lambda)}_j v_j \ . \tag{B3}$$

Multiplying (B2) by v_i and summing over i gives the equation for the energy E_λ:

$$f \sum_i \frac{v_i^2}{E_\lambda - \epsilon_i} = 1 \ . \tag{B4}$$

The value of q_λ can be found from the normalization condition:

$$\sum_i C^{(\lambda)2}_i = q_\lambda^2 f^2 \sum_i \frac{v_i^2}{(E_\lambda - \epsilon_i)^2} = 1 \ . \tag{B5}$$

If v_i are independent random variables, $\overline{v_i v_j} = \overline{v_i^2}\delta_{ij}$, the signs of the coefficients $C_i^{(\lambda)}$ within one eigenstate are not correlated:

$$\overline{C_i^{(\lambda)} C_j^{(\lambda)}} = \left\langle \frac{q_\lambda^2 f^2 v_i v_j}{(E_\lambda - \epsilon_i)(E_\lambda - \epsilon_j)} \right\rangle \simeq \frac{q_\lambda^2 f^2}{(E_\lambda - \epsilon_i)^2} \overline{v_i^2} \delta_{ij} \,. \tag{B6}$$

The last equality is approximate since E_λ and q_λ^2 depend on v. However, they are even functions of v [see eqs. (B4), (B5)], while the coefficients C are odd functions of v [see eq. (B2)]. Thus, $\overline{C_i^{(\lambda)} C_j^{(\lambda)}} = 0$, if $i \neq j$. Consider now the correlator between two different eigenstates Ψ_λ and Ψ_μ:

$$\overline{C_i^{(\lambda)} C_i^{(\mu)}} = f^2 \left\langle \frac{q_\lambda q_\mu v_i^2}{(E_\lambda - \epsilon_i)(E_\mu - \epsilon_i)} \right\rangle \,. \tag{B7}$$

The signs of the normalization factors q_λ and q_μ are not fixed by eq. (B5) and we can always make them positive. In any case, physical effects can contain q_λ^2 only, since the compound state wave function always appears twice, say, in the capture amplitude and in the weak matrix element. Therefore, it is obvious that the correlator (B7) is not zero. Moreover, for close eigenstates ($E_\lambda \approx E_\mu$) the coefficients $C_i^{(\lambda)}$ and $C_i^{(\mu)}$ are almost equal, except for such i that $E_\lambda \leq \epsilon_i \leq E_\mu$, where their signs are opposite. Thus, the random separable interaction model (RSIM) gives very strong correlations between the eigenvectors which have close energies. This can result in strong correlations between "observable" effects induced by a weak perturbation.

Superlocalization of eigenstates in RSIM. Eigenvectors in the random matrix models or in real "chaotic" systems are characterised by large numbers of principal components N_c which dominate the normalization condition. Very often $N_c < N$, and it remains finite as N goes to infinity. N_c is related to the spreading width $\Gamma_{\rm spr}$ and the mean level spacing D as $N_c \sim \Gamma_{\rm spr}/D$. It is usually assumed that $\Gamma_{\rm spr}$ is determined by the strength of the residual interaction which mixes different components Φ_i. Surprisingly, this assumption is not valid in RSIM. The number of principal components is $N_c \sim 1$ for arbitrary strong interaction. Indeed,

$$C_i^{(\lambda)2} = \frac{q_\lambda^2 f^2 v_i^2}{(E_\lambda - \epsilon_i)^2} = \frac{q_\lambda^2 f^2 v_i^2}{D^2} \frac{1}{K^2} \,, \tag{B8}$$

where $K = (E_\lambda - \epsilon_i)/D$. The sum over i in the normalization condition (B5) converges as $\sum \frac{1}{K^2}$ and is dominated by few terms with $|K| \sim 1$ (see Flambaum 1995 for detailed discussion).

C All-Order IPNCI and Renormalization of the PNC and P,T-odd Interactions in Nuclei

Below we present the derivation of $V^{\rm IPNCI}$ and the analogous induced P,T-odd interaction $V^{\rm IPTI}$ based on the unitary transformation technique presented in (Flambaum and Vorov 1995a, 1995b). Consider the nuclear Hamiltonian $\hat{H}$ in the form

$$\hat{H} = \hat{H}_0 + \hat{V} + \hat{W} + \hat{F} \,, \tag{C1}$$

where $\hat{H}_0$ is the one-body Hamiltonian of the nucleons [see below eq. (82)], $\hat{V}$ is the residual two-body strong interaction, $\hat{W}$ is the PNC weak interaction (35), and $\hat{F}$ describes other possible interactions, e.g., coupling to an electromagnetic field (the hatted operators refer to the many-body system). Considering

the PNC interaction of valence nucleons one should distinguish the two contributions to it: the weak nuclear potential $\hat{w}$ (35) caused by averaging of the two-body interaction $\hat{W}$ over the nuclear core (this interaction mixes nucleon states from different shells), and the residual two-body weak interaction

$$:\hat{W}: \equiv \hat{W} - \langle \hat{W} \rangle_{\rm core} = \hat{W} - \hat{w} \ , \tag{C2}$$

which directly couples the nucleons in the valence shell. $:\hat{W}:$ and $\hat{w}$ are analogues of the residual strong interaction $\hat{V}$ and the strong nuclear potential $U(r)$.

Let us start with the case when $\hat{V}$ is switched off. Using (80), (81) and (82) one can show that in the constant-density approximation $w = i\xi\boldsymbol{\sigma}[H_0, \mathbf{r}]$, and the action of the weak perturbation of the single-particle orbital ψ_a is described as

$$\tilde{\psi}_\alpha = \psi_\alpha + \sum_\beta \psi_\beta \frac{\langle \psi_\beta | w | \psi_\alpha \rangle}{\epsilon_\alpha - \epsilon_\beta} = \psi_\alpha - \sum_\beta \psi_\beta \langle \psi_\beta | i\xi\boldsymbol{\sigma}\mathbf{r} | \psi_\alpha \rangle = (1 - i\xi\boldsymbol{\sigma}\mathbf{r})\psi_\alpha \simeq e^{-a}\psi_\alpha \ , \tag{C3}$$

where $a = i\xi\boldsymbol{\sigma}\mathbf{r}$. Accordingly, the matrix element of any operator $\hat{O}$, including the Hamiltonian, can be calculated by using the unperturbed wave functions Ψ and the transformed operator $\tilde{O}$:

$$\langle \tilde{\Psi}_\lambda | \hat{O} | \tilde{\Psi}_\mu \rangle = \langle \Psi_\lambda | e^{\hat{a}} \hat{O} e^{-\hat{a}} | \Psi_\mu \rangle \equiv \langle \Psi_\lambda | \tilde{O} | \Psi_\mu \rangle \simeq \langle \Psi_\lambda | \hat{O} + [\hat{a}, \hat{O}] | \Psi_\mu \rangle, \tag{C4}$$

where $e^{\hat{a}}$ is the operator of the corresponding unitary transformation with the one-body anti-Hermitian operator $\hat{a} = \sum_a i\xi_a \boldsymbol{\sigma}_a \mathbf{r}_a$. The correct choice of the transformation corresponds to the total compensation of the single-particle P-odd potential in the Hamiltonian: $e^{\hat{a}}\hat{H}e^{-\hat{a}}$: $\hat{w} + [\hat{a}, \hat{H}_0] = 0$. The effect of this potential is now included into the renormalized operators $\tilde{O}$ rather than the wave functions $\tilde{\Psi}$.

Let us switch on the strong interaction $\hat{V}$ and find the corresponding operator $e^{\hat{A}}$ (we will see below that the operator $\hat{A}$ differs from $\hat{a}$ mainly due to the renormalization of the weak interaction constants by the residual strong interaction $\hat{V}$). The transformed Hamiltonian looks like:

$$\tilde{H} = e^{\hat{A}}\hat{H}e^{-\hat{A}} = \hat{H}_0 + \hat{V} + \hat{w} + :\hat{W}: + \hat{F} + [\hat{A}, \hat{H}_0] + [\hat{A}, \hat{F}] + [\hat{A}, \hat{V}] \tag{C5}$$

where we have used the decomposition (C2) and neglected all terms above the first order in the weak interaction. To obtain the effective two-body P-odd interaction acting in the valence shells we should find the operator $\hat{A}$ which would compensate the single-particle P-odd contribution in $e^{\hat{A}}\hat{H}e^{-\hat{A}}$. The last term in (C5) is a two-body operator. Let us apply the decomposition (C2) to the last term in (C5): $[\hat{A}, \hat{V}] \equiv \langle [\hat{A}, \hat{V}] \rangle_{\rm core} + :[\hat{A}, \hat{V}]:$. The first, one-body term is the average over the paired nucleons, and the second one, $:[\hat{A}, \hat{V}]:$, which yields zero under such averaging, is the effective induced two-body interaction:

$$\hat{V}^{\rm IPNCI} \equiv :[\hat{A}, \hat{V}]: \ , \qquad \langle \hat{V}^{\rm IPNCI} \rangle_{\rm core} = 0 \ . \tag{C6}$$

If we impose the following compensation condition:

$$\hat{w} + [\hat{A}, \hat{H}_0] + \langle [\hat{A}, \hat{V}] \rangle_{\rm core} = 0 \ , \tag{C7}$$

the transformed Hamiltonian would take the form

$$\tilde{H} = \hat{H}_0 + \hat{V} + :\hat{W}: + \hat{V}^{\rm IPNCI} + \hat{F} + [\hat{A}, \hat{F}] \ , \tag{C8}$$

with no single-particle P-odd potential. Thus, there are three sources of the parity nonconservation in $\tilde{H}$ (C8):

Table 1: Comparison of the matrix elements of the induced parity-nonconserving interaction between the valence-shell orbitals with the matrix elements of the original two-body weak interaction in the Th-U region.

					Matrix elements [a] (eV)		
α	β	γ	δ	J	$V^{\rm IPNCI\ b}_{\alpha\beta\gamma\delta,J}$	$\tilde{V}^{\rm IPNCI\ c}_{\alpha\beta\gamma\delta,J}$	$W_{\alpha\beta\gamma\delta,J}$ [d]
$2g_{9/2}$	$1h_{9/2}$	$1h_{9/2}$	$1j_{15/2}$	3	0.067	0.082	0.009
$2g_{9/2}$	$1h_{9/2}$	$1h_{9/2}$	$1j_{15/2}$	4	0.033	0.062	0.001
$2g_{9/2}$	$1h_{9/2}$	$1h_{9/2}$	$1j_{15/2}$	5	0.035	0.048	0.012
$2g_{9/2}$	$1h_{9/2}$	$1h_{9/2}$	$1j_{15/2}$	7	0.029	0.043	0.016
$2g_{9/2}$	$1h_{9/2}$	$1h_{9/2}$	$1j_{15/2}$	8	0.043	0.082	0.001
$1i_{11/2}$	$1h_{9/2}$	$1h_{9/2}$	$1j_{15/2}$	3	0.144	0.184	0.007
$1i_{11/2}$	$1h_{9/2}$	$1h_{9/2}$	$1j_{15/2}$	5	0.130	0.165	0.016
$1i_{11/2}$	$1h_{9/2}$	$1h_{9/2}$	$1j_{15/2}$	7	0.131	0.166	0.032
$1i_{11/2}$	$1h_{9/2}$	$1h_{9/2}$	$1j_{15/2}$	9	0.172	0.218	0.027

[a] Given in the table are the absolute values of the matrix elements between pairs of neutron-proton single-particle states ($\alpha\beta$ and $\delta\gamma$) coupled into the total angular momentum J.
[b] The IPNCI (88), (89) obtained using the Landau-Migdal strong interaction (86).
[c] The IPNCI (C13) renormalized by the momentum-dependent component (C10) of the Landau-Migdal strong interaction.
[d] The initial two-body PNC interaction (35).

1. The commutator $[\hat{A}, \hat{F}]$ which gives a direct contribution of the PNC potential $\hat{w}$ to the matrix elements of the external field F: $\langle\Psi_\lambda|\hat{F} + [\hat{A}, \hat{F}]|\Psi_\mu\rangle = \langle\tilde{\Psi}_\lambda|\hat{F}|\tilde{\Psi}_\mu\rangle$.

2. The residual two-body weak interaction $:\hat{W}:$.

3. $\hat{V}^{\rm IPNCI}$, which plays the same role as $:\hat{W}:$, but is enhanced in comparison with $:\hat{W}:$ (see sec. 2.3 and below).

It is easy to check that if we use the Landau-Migdal interaction V (86), the operator A in the constant-density approximation is proportional to a:

$$A = i\tilde{\xi}\boldsymbol{\sigma}\mathbf{r}\ . \tag{C9}$$

Indeed, the commutator $[\hat{A}, V]$ would then give eq. (87) with ξ replaced by $\tilde{\xi}$. The average $\langle[\hat{A}, \hat{V}]\rangle_{\rm core}$ in the compensation equation (C7) is zero because of the spin-isospin structure of (87), and it would follow from the compensation equation that the interaction constants $\tilde{\xi}$ coincide with their "bare" values ξ (i.e., with those obtained without the strong interaction). Therefore, the $V^{\rm IPNCI}$ in this approximation is given by eq. (88), (89). The strength of this interaction was estimated analytically in eq. (90) to be $\sim A^{1/3}$ times greater than that of the original weak interaction W acting within the valence shell ($:\hat{W}:$). In Table 1 we present the matrix elements of $V^{\rm IPNCI}$ and W between the valence-shell orbitals calculated numerically by Flambaum and Vorov (1995a).

The fact that $\tilde{\xi} = \xi$ and the IPNCI above coincides with eq. (88) obtained by including the strong interaction in the lowest first order follows from the fact that the Landau-Migdal interaction (86)

does not renormalize the weak potential the nuclear weak potential w, unless momentum-dependent corrections to it are considered (Flambaum and Vorov 1994). The latter can be taken in the form

$$V_1 = \frac{C}{4p_F^2}(h_1 + h_1'\boldsymbol{\tau}_1\boldsymbol{\tau}_2)(\boldsymbol{\sigma}_1\boldsymbol{\sigma}_2)\{\{\delta(\mathbf{r}_1 - \mathbf{r}_2), \mathbf{p}_1\}, \mathbf{p}_2\} \ , \tag{C10}$$

which originates from the π-meson exchange contribution to the nucleon-nucleon interaction. Its constants are $h_1 = -0.5$, $h_1' = -0.26$ (Khodel and Saperstein 1982). Note, that only the terms contributing to the P-odd interaction renormalization are retained in (C10). Spin-independent contributions to V_1 responsible for, e.g., the mass renormalization, are supposed to be taken into account by the choice of the constants C, m, and h. Introducing the operator $\hat{A}$ in the same form (C9) into the compensation equation with $\hat{V} \to \hat{V} + \hat{V}_1$, one obtains from (C7):

$$w_a + \left[i\tilde{\xi}_a\boldsymbol{\sigma}\mathbf{r}, \frac{\mathbf{p}^2}{2m}\right] + K_a\{\boldsymbol{\sigma}\mathbf{p}, \rho(r)\} = 0 \ , \quad (a = p, n), \tag{C11}$$

where $K_a = -\frac{C}{2p_F^2}\left[\frac{Z}{A}(h_1 \pm h_1')\tilde{\xi}_p + \frac{N}{A}(h_1 \mp h_1')\tilde{\xi}_n\right]$, and $a = p(n)$ corresponds to the upper (lower) signs (see Appendix D). In the constant density approximation, all terms in eq. (C11) have the same operator structure and it is equivalent to an algebraic equation for the renormalized constants $\tilde{\xi}$. Since ξ_a and the weak-potential constants g_a are proportional to each other [eq. (81)] the solution of eq. (C11) is equivalent to the following renormalization of the constants $g_a \to \tilde{g}_a$:

$$\begin{aligned} \tilde{g}_p &= \tfrac{1}{D}\left\{g_p\left[1 + \tfrac{2N}{3A}(h_1 + h_1')\right] - \tfrac{2N}{3A}g_n(h_1 - h_1')\right\} \ , \\ \tilde{g}_n &= \tfrac{1}{D}\left\{g_n\left[1 + \tfrac{2Z}{3A}(h_1 + h_1')\right] - \tfrac{2Z}{3A}g_p(h_1 - h_1')\right\} \ , \end{aligned} \tag{C12}$$

where $D = \left[1 + \frac{2N}{3A}(h_1 + h_1')\right]\left[1 + \frac{2Z}{3A}(h_1 + h_1')\right] - \frac{4NZ}{9A^2}(h_1 - h_1')^2$ (Flambaum and Vorov 1994). Thus, the account of V_1 changes the IPNCI (88), (89) into

$$V^{\rm IPNCI} = \tilde{V}^{\rm IPNCI} + V_{\rm vel}^{\rm IPNCI} = 2(\tilde{\xi}_n - \tilde{\xi}_p)(h' - h)C\mathbf{r}_p(\boldsymbol{\sigma}_p \times \boldsymbol{\sigma}_n)\delta(\mathbf{r}_p - \mathbf{r}_n) + V_{\rm vel}^{\rm IPNCI} \ , \tag{C13}$$

where $\tilde{V}^{\rm IPNCI}$ has the form of (84) with the renormalized constants $\tilde{\xi}_p$, $\tilde{\xi}_n$. At $h_1, h_1' < 0$ (see above) the renormalized IPNCI is enhanced: $\tilde{\xi} \sim 1.4\xi$. Numerical values of the corresponding matrix elements are given in Table 1. Another calculation of the weak potential renormalization based on the $(\pi + \rho)$-exchange strong interaction is presented in Appendix D. It produces even larger values of the weak potential constants $\tilde{g}$, $\tilde{\xi}$. The second term in (C13) contains the velocity-dependent corrections:

$$\begin{aligned} V_{\rm vel}^{\rm IPNCI} = [\hat{A}, V_1] = -\frac{C}{4p_F^2}\Big\{&(\tilde{\xi}_n - \tilde{\xi}_p)(h_1 - h_1')(\tau_{1z} - \tau_{2z})\{\{\mathbf{r}_1 \cdot (\boldsymbol{\sigma}_2 \times \boldsymbol{\sigma}_1)\delta(\mathbf{r}_1 - \mathbf{r}_2), \mathbf{p}_1\}, \mathbf{p}_2\} \\ &+\Big[\Big[(\tilde{\xi}_n + \tilde{\xi}_p)(h_1 + h_1'\boldsymbol{\tau}_1\boldsymbol{\tau}_2) + \frac{1}{2}(\tilde{\xi}_n - \tilde{\xi}_p)(h_1 + h_1')(\tau_{1z} + \tau_{2z})\Big]\{\boldsymbol{\sigma}_1\mathbf{p}_1 + \boldsymbol{\sigma}_2\mathbf{p}_2, \delta(\mathbf{r}_1 - \mathbf{r}_2)\} \\ &\qquad + \frac{1}{2}(\tilde{\xi}_n - \tilde{\xi}_p)(h_1 - h_1')(\tau_{1z} - \tau_{2z})\{\boldsymbol{\sigma}_2\mathbf{p}_2 - \boldsymbol{\sigma}_1\mathbf{p}_1, \delta(\mathbf{r}_1 - \mathbf{r}_2)\}\Big]\Big\} \ , \end{aligned} \tag{C14}$$

where $C\tilde{\xi}/4p_F^2 = G\tilde{g}/(6\sqrt{2}m)$. One can see that $V_{\rm vel}^{\rm IPNCI}$ is not enhanced with respect to the two-body weak interaction W (35), except for the first term in the right hand side of (C14), which is the momentum-dependent correction to the IPNCI from eqs. (88), (89).

Using the same approach as above the induced P,T-odd interaction can be considered. The two-body weak P,T-odd interaction $W^{\rm P,T}$ can be presented in the form analogous to (35) [see, e.g., Flambaum *et al* (1986)]:

$$W_{ab}^{\rm PT} = \frac{G}{\sqrt{2}}\frac{1}{2m}[(\eta_{ab}\boldsymbol{\sigma}_a - \eta_{ba}\boldsymbol{\sigma}_b)\nabla_a\delta(\mathbf{r}_a - \mathbf{r}_b) + \eta_{ab}'(\boldsymbol{\sigma}_a \times \boldsymbol{\sigma}_b)\{\mathbf{p}_a - \mathbf{p}_b, \delta(\mathbf{r}_a - \mathbf{r}_b)\}] \ , \tag{C15}$$

Table 2: Single-particle matrix elements of the P-odd and P,T-odd nuclear potentials.

α	β	$\epsilon_\alpha - \epsilon_\beta$ (MeV)	$w_{\alpha\beta}$ (eV)	$w^{\rm PT}_{\alpha\beta}$ (eV)	$\tilde{w}^{\rm PT}_{\alpha\beta}$ (eV)
proton states					
$2p_{1/2}$	$3s^*_{1/2}$[a]	−8.44	$-0.500g_{pp} - 0.722g_{pn}$	$-0.066\eta_{pp} - 0.078\eta_{pn}$	$-0.044\eta_{pp} - 0.052\eta_{pn}$
$2d^*_{3/2}$	$3p_{3/2}$	−8.73	$-0.558g_{pp} - 0.803g_{pn}$	$-0.050\eta_{pp} - 0.073\eta_{pn}$	$-0.033\eta_{pp} - 0.048\eta_{pn}$
$1g_{9/2}$	$1h^*_{9/2}$	−11.05	$0.599g_{pp} + 0.842g_{pn}$	$0.112\eta_{pp} + 0.129\eta_{pn}$	$0.074\eta_{pp} + 0.086\eta_{pn}$
$1h^*_{9/2}$	$2g_{9/2}$	−9.42	$-0.575g_{pp} - 0.789g_{pn}$	$-0.055\eta_{pp} - 0.064\eta_{pn}$	$-0.037\eta_{pp} - 0.042\eta_{pn}$
neutron states					
$3p^*_{1/2}$	$4s_{1/2}$	−6.65	$-0.452g_{nn} - 0.660g_{np}$	$-0.035\eta_{nn} - 0.012\eta_{np}$	$-0.020\eta_{nn} - 0.007\eta_{np}$
$3p^*_{3/2}$	$2d_{3/2}$	7.78	$0.541g_{nn} + 0.778g_{np}$	$-0.071\eta_{nn} - 0.048\eta_{np}$	$-0.040\eta_{nn} - 0.027\eta_{np}$
$3p^*_{3/2}$	$3d_{3/2}$	−8.73	$0.446g_{nn} + 0.661g_{np}$	$0.060\eta_{nn} + 0.026\eta_{np}$	$0.033\eta_{nn} + 0.015\eta_{np}$
$2f^*_{5/2}$	$3d_{5/2}$	−6.63	$-0.539g_{nn} - 0.773g_{np}$	$-0.044\eta_{nn} - 0.017\eta_{np}$	$-0.024\eta_{nn} - 0.009\eta_{np}$

[a] Asterisks are used to mark the states closest to the Fermi energy.

where η_{ab}, η'_{ab} are the dimensionless constants which determine the scale of P,T-odd effects [very small, as predicted, e.g., by the Kobayashi-Maskawa model, see Sushkov *et al* (1984)]. Similarly to eq. (36) the P,T-odd potential of the nucleus is given by

$$w^{\rm PT}_a = \frac{G}{\sqrt{2}}\frac{\eta_a}{2m}\boldsymbol{\sigma}\nabla\rho(r)\,, \tag{C16}$$

where $\eta_p = \frac{Z}{A}\eta_{pp} + \frac{N}{A}\eta_{pn}$, $\eta_n = \frac{N}{A}\eta_{nn} + \frac{Z}{A}\eta_{np}$. Limits on these constants were obtained from atomic (Lamoreax *et al* 1987) and molecular (Cho *et al* 1991) electric dipole moment measurements [see calculations by Flambaum *et al* (1986)]. The matrix elements of the P,T-odd potential (C16) have the same selection rules as those of w:

$$\Delta l = \pm 1, \quad \Delta j = 0\,. \tag{C17}$$

Table 2 shows some of the matrix elements of $w^{\rm PT}$ (C16) and w (36) between the single-particle orbitals in ^{209}Pb calculated by Flambaum and Vorov (1995b). The numerical calculations were performed using the Woods-Saxon potential (91).

Table 2 shows that single-particle matrix elements of the P,T-odd potential are numerically suppressed (by about an order of magnitude) with respect to those of the P-odd potential, since $w^{\rm PT}$ is proportional to the derivative of the nuclear density and is large only near the nuclear surface. By analogy with w the single-particle states coupled by the P,T-odd potential usually belong to different nuclear shells and are separated by the energy of 5–10 MeV. Therefore, to study the effect of P,T-odd interaction within, say, valence shell one should consider the matrix elements of the two-body P,T-odd interaction (C15) directly coupling valence-shell orbitals. The effect of the one-body potential $w^{\rm PT}$ can be described by means of the induced P,T-odd interaction (IPTI). It can be derived similarly to the IPNCI.

The effect of the perturbation $w^{\rm PT}$ on the single-particle orbitals is now described as: $\tilde{\psi}_\alpha = e^{-a}\psi_\alpha$,

where

$$a = -\theta\boldsymbol{\sigma}\nabla\ , \qquad \theta = \frac{G\eta}{2\sqrt{2}m}\frac{\rho(0)}{U(0)} \simeq -2\times 10^{-8}\ \eta \times \text{fm}\ , \tag{C18}$$

[see eq. (D3)]. Introducing the transformation of operators $e^{\hat{A}}\hat{O}e^{-\hat{A}}$ and proceeding in a way similar to that for the P-odd interaction we arrive at the following effective P,T-odd operator:

$$\hat{V}^{\text{IPTI}} \equiv :[\hat{A},\hat{V}]:\ , \qquad \langle\hat{V}^{\text{IPTI}}\rangle_{\text{core}} = 0\ , \tag{C19}$$

and the compensation equation

$$\hat{w}^{\text{PT}} + [\hat{A},\hat{H}_0] + \langle[\hat{A},\hat{V}]\rangle_{\text{core}} = 0\ , \tag{C20}$$

which should determine the transformation operator $\hat{A}$, and thus, the IPTI (C19). The explicit expression for the IPTI can be obtained using the Landau-Migdal interaction (86). In this case A is proportional to a: $\hat{A} = -\sum_a \tilde{\theta}_a\boldsymbol{\sigma}_a\nabla_a$. Indeed, the commutator in (C20) yields:

$$\begin{aligned}[\hat{A},V] = &-C(f+f'\boldsymbol{\tau}_1\boldsymbol{\tau}_2)[\tilde{\theta}_1\boldsymbol{\sigma}_1\nabla_1\delta + \tilde{\theta}_2\boldsymbol{\sigma}_2\nabla_2\delta] - C(h+h'\boldsymbol{\tau}_1\boldsymbol{\tau}_2)[\tilde{\theta}_1\boldsymbol{\sigma}_2\nabla_1\delta + \tilde{\theta}_2\boldsymbol{\sigma}_1\nabla_2\delta]\\ &-iC(h+h'\boldsymbol{\tau}_1\boldsymbol{\tau}_2)(\boldsymbol{\sigma}_2\times\boldsymbol{\sigma}_1)\{\tilde{\theta}_1\nabla_1 - \tilde{\theta}_2\nabla_2, \delta(\mathbf{r}_1-\mathbf{r}_2)\}\ .\end{aligned} \tag{C21}$$

where we use the notation $\nabla_a\delta = \nabla_a\delta(\mathbf{r}_1-\mathbf{r}_2)$ $(a=1,2)$. Contrary to the case of the P-odd interaction, averaging (C21) over the core nucleons gives a nonzero contribution to eq. (C20), which now reads as eq. (D6) and produces the renormalized values of the P,T-odd potential constants $\tilde{\eta}_{p,n}$ [eq. (D7)]. One can see that the strong residual interaction reduces the values of the P,T-odd potential constants 1.5–2 times and, thus, further suppresses the size of its matrix elements ($\tilde{w}^{\text{PT}}_{\alpha\beta}$ in Table 2).

In principle, the commutator (C21) is the V^{IPTI} sought. It has the same operator structure as the original interaction W^{PT} (C15), and contrary to the V^{IPNCI}, is not enhanced with respect to it. Therefore, the P,T-odd interaction of nucleons in the valence shell is determined by the effective two-body interaction

$$\begin{aligned}W^{\text{PT}}_{\text{eff}} = W^{\text{PT}} + V^{\text{IPTI}} = \frac{G}{\sqrt{2}}\frac{1}{2m}\Big[&\big[(\eta_{ab}-\tilde{\eta}_b\tilde{C}h_{ab})\boldsymbol{\sigma}_a - (\eta_{ba}-\tilde{\eta}_a\tilde{C}h_{ab})\boldsymbol{\sigma}_b\big]\nabla_a\delta(\mathbf{r}_a-\mathbf{r}_b)\\ &-i(\boldsymbol{\sigma}_a\times\boldsymbol{\sigma}_b)\{(\eta'_{ab}+\tilde{\eta}_a\tilde{C}h_{ab})\nabla_a - (\eta'_{ab}+\tilde{\eta}_b\tilde{C}h_{ab})\nabla_b, \delta(\mathbf{r}_a-\mathbf{r}_b)\}\\ &+\tilde{C}(\tilde{\eta}_a\boldsymbol{\sigma}_a - \tilde{\eta}_b\boldsymbol{\sigma}_b)\nabla_a[\delta(\mathbf{r}_a-\mathbf{r}_b)f_{ab}(r_a)]\Big]\ ,\end{aligned} \tag{C22}$$

where $h_{pp} = h_{nn} = h + h'$, $h_{pn} = h_{np} = h - h'$, the constants $\tilde{\eta}_a$ and $\tilde{C}$ can be found in Appendix D [eq. (D7)], the strong interaction constants f_{ab} are defined in the same way as h_{ab}, and the fact that they depend on the radius has been taken into account.

D Renormalization of the Single-Particle P-odd and P,T-odd Potentials

This section is based on the work (Flambaum and Vorov 1994). Let us first consider the renormalization of the P,T-odd nuclear potential w^{PT}. Using the fact that the shape of the density $\rho(r)$ and the strong nuclear potential $U(\mathbf{r})$ are are similar, one can present the P,T-odd potential (C16) as

$$w^{\text{PT}} \simeq \frac{G\eta}{2\sqrt{2}m}\boldsymbol{\sigma}\nabla U(\mathbf{r}) = \theta\boldsymbol{\sigma}\nabla U(\mathbf{r})\ , \tag{D1}$$

where $\eta = \eta_p$ or η_n, and θ has been defined in (C18). The total single-particle potential acting on the nucleons is

$$U(\mathbf{r}) + w^{\text{PT}} = U(\mathbf{r}) + \theta\boldsymbol{\sigma}\nabla U(\mathbf{r}) \simeq U(\mathbf{r}+\theta\boldsymbol{\sigma})\ . \tag{D2}$$

Thus, it is obvious that $w^{\rm PT}$ perturbs the nucleon wave function ψ_α in the following way

$$\psi_\alpha \longrightarrow \tilde{\psi}_\alpha = \psi_\alpha(\mathbf{r}+\theta\boldsymbol{\sigma}) = (1+\theta\boldsymbol{\sigma}\nabla)\psi_\alpha(\mathbf{r}) = \psi_\alpha + \delta\psi_\alpha \ . \tag{D3}$$

Accordingly, the direct correction to the strong potential can be written as follows:

$$\delta U(1) = \sum_\alpha \left[\langle\delta\psi_\alpha(2)|V(1,2)|\psi_\alpha(2)\rangle + \langle\psi_\alpha(2)|V(1,2)|\delta\psi_\alpha(2)\rangle\right] \ , \tag{D4}$$

where $1(2) \equiv [\mathbf{r}_{1(2)}, \sigma_{1(2)}, \tau_{1(2)}]$ are nucleon variables (coordinate, spin and isospin), and the summation is carried out over the occupied nucleon states α. If the Landau-Migdal parametrization of the strong interaction (86) is used, only the direct terms should be considered. Equations (D4), (D3) and (86) than yield the following correction to the P,T-odd potential:

$$\begin{aligned} U^{\rm PT} &= -\sum_\alpha \int d^3r_2 \psi^\dagger_\alpha(\mathbf{r}_2)[\theta_2\boldsymbol{\sigma}_2\nabla_2, V(\mathbf{r}_1,\mathbf{r}_2)]\psi_\alpha(\mathbf{r}_2) \\ &= \sum_\alpha \theta_\alpha(h+h'\boldsymbol{\tau}_1\boldsymbol{\tau}_\alpha)\boldsymbol{\sigma}_1\nabla|\psi_\alpha|^2 = \gamma\boldsymbol{\sigma}_1\nabla\rho \ , \end{aligned} \tag{D5}$$

where $\gamma = C[\theta_p\frac{Z}{A}(h\pm h') + \theta_n\frac{N}{A}(h\mp h')]$ for protons (neutrons), $\rho = \sum_a |\psi_a|^2$, the proton and neutron densities are taken as $\rho_p = \frac{Z}{A}\rho$ and $\rho_n = \frac{N}{A}\rho$ respectively, and $\langle\boldsymbol{\sigma}_2\rangle_{\rm core} = 0$ (the potential considered is created by paired nucleons). Now the self-consistency equation $\tilde{w}_{\rm PT} = w^{\rm PT} + U^{\rm PT}$ should be solved to find the actual strength of the P,T-odd potential:

$$\tilde{\theta}\boldsymbol{\sigma}\nabla U = \theta\boldsymbol{\sigma}\nabla U + \tilde{\gamma}\frac{\rho(0)}{U(0)}\boldsymbol{\sigma}\nabla U \ . \tag{D6}$$

where the first term in the right hand side contains the "initial" values of the P,T-odd interaction constants η, whereas $\tilde{w}^{\rm PT} \propto \tilde{\theta}$ and $U^{\rm PT} \propto \tilde{\gamma}$ contain the "final", renormalized values $\tilde{\eta}$. The solution for the pair of simple linear algebraic equations for the constants $\tilde{\eta}$ is the following (Flambaum and Vorov 1994):

$$\begin{aligned} \tilde{\eta}_p &= \tfrac{1}{D}\left\{\eta_p\left[1+\tilde{C}\tfrac{N}{A}(h+h')\right] - \tilde{C}\tfrac{N}{A}\eta_n(h-h')\right\} \simeq \tfrac{\eta_p}{1.5} \ , \\ \tilde{\eta}_n &= \tfrac{1}{D}\left\{\eta_n\left[1+\tilde{C}\tfrac{Z}{A}(h+h')\right] - \tilde{C}\tfrac{Z}{A}\eta_p(h-h')\right\} \simeq \tfrac{\eta_n}{1.8} \ , \end{aligned} \tag{D7}$$

where $D = \left[1+\tilde{C}\frac{N}{A}(h+h')\right]\left[1+\tilde{C}\frac{Z}{A}(h+h')\right] - \tilde{C}^2\frac{NZ}{A^2}(h-h')^2$, $\tilde{C} = C\rho/|U| = 4\epsilon_F/3|U| = \frac{4}{3}(1+|\epsilon|/\epsilon_F)^{-1} \simeq 1$, and the well known relations have been used:

$$C = \frac{\pi^2}{p_F m} \ , \quad \rho = \frac{2p_F^3}{3\pi^2}, \quad \epsilon_F = \frac{p_F^2}{2m}, \quad |U| = \epsilon_F + |\epsilon|, \tag{D8}$$

where $|\varepsilon|$ is the nucleon separation energy.

Thus, the strong residual interaction reduces the values of the P,T-odd potential constants 1.5–1.8 times. Note that the response of the nucleus to the P,T-odd potential (C16), (D1) as a function of the interaction constants has poles ($D=0$) at $h = \tilde{C}^{-1} \simeq -1$ and $h' \simeq \tilde{C}^{-1} \simeq -1$ (for $N \simeq Z$). The positions of the poles differ from the instability points in the infinite Fermi system $h = h' = -1.5$ (see, e.g., Khodel and Saperstein 1982, Pines and Nozieres 1966), since the interaction (C16) does not exist in the infinite system ($w^{\rm PT} = 0$ at $\rho = {\rm const}$). It is interesting that the P,T-odd interaction induces a spin "hedgehog" ($\boldsymbol{\sigma} \propto \mathbf{r}$) in the nucleon spin distribution within a spherical nucleus (Flambaum 1994b;

such possibility was first noticed by R. M. Ryndin, see Khriplovich 1991). A simple calculation with the wave function (D3) gives the following proton and neutron spin distributions:

$$\boldsymbol{\sigma}_p(\mathbf{r}) = \theta_p \nabla \rho_p(\mathbf{r}), \quad \boldsymbol{\sigma}_n(\mathbf{r}) = \theta_n \nabla \rho_n(\mathbf{r}) \; . \tag{D9}$$

The interaction $U^{\rm PT}$ in eq. (D5) is, in fact, the strong interaction of the nucleon with the spin hedgehog $[Cg\boldsymbol{\sigma}_1\boldsymbol{\sigma}(\mathbf{r})]$.

Let us now consider the corrections to the weak P-odd potential w (36). In the constant nuclear density approximation its perturbation of the single-particle wave functions is described by eq. (C3), with ξ given by (81):

$$\delta\psi_\alpha = -i\xi\boldsymbol{\sigma}\mathbf{r}\psi_\alpha \; , \qquad \xi = \frac{Gg}{2\sqrt{2}}\rho_0 \; . \tag{D10}$$

In the general case (real density shape and the spin-orbit interaction taken into account) the correction to the wave function contains an extra spherically symmetric function $\phi_\alpha(r)$ (see, e.g., Khriplovich 1991):

$$\delta\psi_\alpha = -i\boldsymbol{\sigma}\mathbf{r}\phi_\alpha(r)\psi_\alpha(\mathbf{r}) \; . \tag{D11}$$

The P-odd weak interaction (36) also changes the spin distribution. It rotates the spin around vector $\mathbf{r}$ (see eq. (C3) by the angle ξr and creates a spin helix (Zeldovich 1957, see also Khriplovich 1991). However, after the summation over the paired nucleons of the core this spin structure disappears. As a result, the Landau-Migdal contact spin-dependent strong interaction (86) does not contribute to the renormalization of the weak potential [because of the factor i in eqs. (D10), (D11) the contributions of $\langle\delta\psi_\alpha(2)|V(1,2)|\psi_\alpha(2)\rangle$ and $\langle\psi_\alpha(2)|V(1,2)|\delta\psi_\alpha(2)\rangle$ cancel each other in (D4)]. This result looks natural since the only possible orientation of the spin in the spherical nucleus ($\boldsymbol{\sigma} \propto \mathbf{r}$) violates both P- and T-invariance and can not be produced by a T-even weak interaction (36). It also explains why the "all-order" treatment of $V^{\rm IPNCI}$ (Appendix C) gave the same result (84) as the first-order calculation in sec. 2.3.

The correlation which is actually produced by the P-odd weak interaction is $\boldsymbol{\sigma}\mathbf{p}$. To obtain such structure the contact strong interaction in (D4) must depend on both the spin and the momentum of the nucleons (another possibility is provided by a finite range exchange interaction considered below). Using the momentum-dependent component of the Landau-Migdal interaction (C10) one obtains from (D4), (D10):

$$\begin{aligned}\tilde{U} &= \sum_\alpha \int d^3r_2 \psi^\dagger_\alpha(\mathbf{r}_2)[i\xi_2\boldsymbol{\sigma}_2\mathbf{r}_2, V_1(\mathbf{r}_1,\mathbf{r}_2)]\psi_\alpha(\mathbf{r}_2) \\ &= -\frac{C}{2p_F^2}\sum_\alpha \xi_\alpha(h_1 + h_1'\tau_\alpha\boldsymbol{\tau}_2)\{\boldsymbol{\sigma}_1\mathbf{p}_1, |\psi_\alpha|^2\} = K(\boldsymbol{\sigma}_1\mathbf{p}_1\rho + \rho\boldsymbol{\sigma}_1\mathbf{p}_1) \; ,\end{aligned} \tag{D12}$$

where $K = -\frac{C}{2p_F^2}\left[\frac{Z}{A}(h_1 \pm h_1')\xi_p + \frac{N}{A}(h_1 \mp h_1')\xi_n\right]$ for protons (neutrons) respectively. The equation for the total P-odd nuclear potential is:

$$\tilde{w} = w + \tilde{U} \; , \tag{D13}$$

where $\tilde{w}$ and $\tilde{U}$ contain the renormalized constants $\tilde{\xi}$ ($\tilde{g}$), and w is the original P-odd potential (36) [compare with eq. (C11)]. Solving the corresponding pair of linear algebraic equations and using $Cpm/p_F^2 = 2/3$ one obtains the renormalized constants $\tilde{g}_p$, $\tilde{g}_n$ of the P-odd potential, eq. (C12). It

is worth noting that the poles ($D = 0$) in the response of a nucleus to the weak potential $w \propto \boldsymbol{\sigma}\mathbf{p}$ coincide with the boundary of stability of the Fermi liquid with the interaction (C10): $h_1 = h_1' = -1.5$ at $N = Z$ (boundaries of stability of the Fermi liquid with the Landau-Migdal interaction can be found, e.g., in Khodel and Saperstein 1982, Pines and Nozieres 1966). It looks natural, since the approximation $\rho = \text{const}$ has been used in the wave function (D10)[9].

The interaction V_1 with $h_1 = -0.5$, $h_1' = -0.26$ does not cause instability. However, it acts in the direction of the poles and increases the P-odd potential:

$$\tilde{g}_p = 1.3g_p + 0.18g_n, \quad \tilde{g}_n = 1.4g_n + 0.12g_p \ . \tag{D14}$$

Therefore, the Landau-Migdal interaction $V + V_1$ [eqs. (86), (C10)] does not produce critical changes in the values of the interaction constants of the P,T-odd and P-odd potentials. The corrections are of the same size as, e.g., the corrections to the Schmidt values of the magnetic moments. However, the Landau-Migdal interaction originates from the underlying $(\pi + \rho)$-exchange interaction which also generates tensor components. The account of the latter brings the nuclear matter much closer to the verge of instability against the P-odd perturbation.

The $(\pi + \rho)$-exchange strong interaction is given by

$$V^{\pi+\rho}(1,2) = -4\pi(\boldsymbol{\tau}_1\boldsymbol{\tau}_2)\left[\frac{f_\pi^2}{m_\pi^2}\frac{(\boldsymbol{\sigma}_1\mathbf{q})(\boldsymbol{\sigma}_2\mathbf{q})}{q^2+m_\pi^2} + \frac{f_\rho^2}{m_\rho^2}\frac{(\boldsymbol{\sigma}_1\times\mathbf{q})(\boldsymbol{\sigma}_2\times\mathbf{q})}{q^2+m_\rho^2}\right] , \tag{D15}$$

where $\mathbf{q}$ is momentum transferred, m_π (m_ρ) is the pion (ρ meson) mass, $f_\pi^2 = 0.08$ is the pion coupling constant, and f_ρ^2 is the ρ-meson constant ranging from 1.86 (weak coupling) to 4.86 (strong coupling) (see, e.g., Brown *et al* 1976, Speth *et al* 1977, Krewald *et al* 1988). When using $V^{\pi+\rho}$ one should add the exchange contributions to (D4). The single-particle matrix element of the induced P-odd potential $\langle\psi_\mu\tilde{U}\psi_\nu\rangle \equiv \tilde{U}_{\mu\nu}$ is then

$$\tilde{U}_{\mu\nu} = \sum_{\alpha,\,\beta}\left(A_{\alpha\beta}V^{\pi+\rho}_{\mu\beta\alpha\nu} - V^{\pi+\rho}_{\mu\alpha\beta\nu}A_{\beta\alpha}\right) - \sum_{\alpha,\,\beta}\left(A_{\alpha\beta}V^{\pi+\rho}_{\mu\beta\nu\alpha} - V^{\pi+\rho}_{\alpha\mu\beta\nu}A_{\beta\alpha}\right) \ , \tag{D16}$$

where $V^{\pi+\rho}_{\mu\alpha\beta\nu} = \int dr_1^3\ dr_2^3\ \psi_\mu^\dagger(1)\psi_\alpha^\dagger(2)V^{\pi+\rho}(1,2)\psi_\beta(2)\psi_\nu(1)$, $A_{\alpha\beta} = \langle\psi_\alpha|i\boldsymbol{\xi}\boldsymbol{\sigma}\mathbf{r}|\psi_\beta\rangle$, and $\sum_\alpha$ runs over the occupied nucleon states. Re-writing the first two (direct) terms as the commutator, we obtain:

$$\begin{aligned}\tilde{U}_{\mu\nu} = &\sum_\alpha\int dr_1^3\ dr_2^3\ \psi_\mu^\dagger(1)\psi_\alpha^\dagger(2)\left[i\xi_2\boldsymbol{\sigma}_2\mathbf{r}_2, V^{\pi+\rho}(1,2)\right]\psi_\alpha(2)\psi_\nu(1)\\ &-\sum_\alpha\int dr_1^3\ dr_2^3\ \psi_\alpha^\dagger(1)\psi_\mu^\dagger(2)\left(i\xi_1\boldsymbol{\sigma}_1\mathbf{r}_1V^{\pi+\rho}(1,2) - V^{\pi+\rho}(1,2)i\xi_2\boldsymbol{\sigma}_2\mathbf{r}_2\right)\psi_\alpha(2)\psi_\nu(1) \ .\end{aligned} \tag{D17}$$

In the coordinate representation the potential $V^{\pi+\rho}$ depends on $|\mathbf{r}_1 - \mathbf{r}_2|$ and its commutator with $A = i\xi_2\boldsymbol{\sigma}_2\mathbf{r}_2$ in (D17) is zero. On the contrary, the exchange terms are effectively momentum-dependent (due to the nonlocality of the potential) and yield a nonzero contribution to $\tilde{U}$. To calculate the latter, the exchange terms in (D16) should be reduced to the form of direct ones, which can be done by substituting $\mathbf{q} \to \mathbf{p}_1 - \mathbf{p}_2$ (the nucleons are on the Fermi surface) and performing the Fierz transformation of the spin and isospin tensor structures (see, e.g., Okun 1982). This yields

$$V^{\pi+\rho}_{\mu\beta\nu\alpha} = V'_{\mu\beta\alpha\nu} \equiv \int dr_1^3\ dr_2^3\ \psi_\mu^\dagger(1)\psi_\beta^\dagger(2)V'(1,2)\psi_\alpha(2)\psi_\nu(1) \ , \tag{D18}$$

[9]Zelevinsky (1993) independently obtained a similar result: the correction to the effective field $\boldsymbol{\sigma}\mathbf{p}$ diverges at the same point where the first harmonic of the Landau interaction $h_1(\boldsymbol{\sigma}_1\boldsymbol{\sigma}_2)(\mathbf{p}_1\mathbf{p}_2)$ leads to an instability of the Fermi liquid.

where

$$V'(1,2) = -2\pi\left(\frac{3}{2} - \frac{\boldsymbol{\tau}_1\boldsymbol{\tau}_2}{2}\right)\sum_{ij}[2\sigma_{1i}\sigma_{2j} + (1-\boldsymbol{\sigma}_1\boldsymbol{\sigma}_2)\delta_{ij}] \times\left[\frac{f_\pi^2}{m_\pi^2}\frac{(\mathbf{p}_1-\mathbf{p}_2)_i(\mathbf{p}_1-\mathbf{p}_2)_j}{(\mathbf{p}_1-\mathbf{p}_2)^2+m_\pi^2} + \frac{f_\rho^2}{m_\rho^2}\frac{(\mathbf{p}_1-\mathbf{p}_2)^2\delta_{ij}-(\mathbf{p}_1-\mathbf{p}_2)_i(\mathbf{p}_1-\mathbf{p}_2)_j}{(\mathbf{p}_1-\mathbf{p}_2)^2+m_\rho^2}\right]. \quad \text{(D19)}$$

By means of (D18) the integrand in the exchange terms in eqs. (D16), (D17) is reduced to the commutator $[i\xi_2\boldsymbol{\sigma}_2\mathbf{r}_2, V'(1,2)]$ and the meson exchange correction $\tilde{U}$ to the P-odd potential acting on the first nucleon is

$$\tilde{U}^{\pi+\rho} = -\sum_\alpha\langle\psi_\alpha(2)|[i\xi\boldsymbol{\sigma}_2\mathbf{r}_2, V'(1,2)]|\psi_\alpha(2)\rangle\ . \quad \text{(D20)}$$

Calculating the commutator in (D20) and using $[r_{2i}, p_{2j}] = i\delta_{ij}$, $\langle\sigma_{2i}\sigma_{2j}\rangle = \delta_{ij}$, one obtains

$$\tilde{U}^{\pi+\rho} = \sum_\alpha\langle\psi_\alpha(2)|K_\pi\boldsymbol{\sigma}_1(\mathbf{p}_1-\mathbf{p}_2)\left[\frac{1}{(\mathbf{p}_1-\mathbf{p}_2)^2+m_\pi^2} - \frac{(\mathbf{p}_1-\mathbf{p}_2)^2}{3[(\mathbf{p}_1-\mathbf{p}_2)^2+m_\pi^2]^2}\right]|\psi_\alpha(2)\rangle - \sum_\alpha\langle\psi_\alpha(2)|K_\rho\boldsymbol{\sigma}_1(\mathbf{p}_1-\mathbf{p}_2)\left[\frac{1}{(\mathbf{p}_1-\mathbf{p}_2)^2+m_\rho^2} - \frac{(\mathbf{p}_1-\mathbf{p}_2)^2}{2[(\mathbf{p}_1-\mathbf{p}_2)^2+m_\rho^2]^2}\right]|\psi_\alpha(2)\rangle\ , \quad \text{(D21)}$$

where $K_\pi = 6\pi(f_\pi^2/m_\pi^2)(3-\boldsymbol{\tau}_1\boldsymbol{\tau}_2)\xi_2$, and $K_\rho = 8\pi(f_\rho^2/m_\rho^2)(3-\boldsymbol{\tau}_1\boldsymbol{\tau}_2)\xi_2$. The expression (D21) can be evaluated using the Fermi-gas approximation to parametrize the density of the core nucleons $\sum_\alpha\psi_\alpha^\dagger(2)\psi_\alpha(2)$, as is often done in such calculations [e.g., obtaining the "bare" nucleon P-odd potential (Adelberger and Haxton 1985)]. Equation (D20) then yields

$$\tilde{U}^{\pi+\rho} = K^{\pi+\rho}2\rho_0\boldsymbol{\sigma}\mathbf{p}\ , \quad \text{(D22)}$$

where the constant $K^{\pi+\rho}$ for the proton and neutron has the following form:

$$K_p^{\pi+\rho} = q\left(\xi_p\frac{Z}{A} + 2\xi_n\frac{N}{A}\right),\quad K_n^{\pi+\rho} = q\left(\xi_n\frac{N}{A} + 2\xi_p\frac{Z}{A}\right),$$
$$q = 6\pi\left[\frac{f_\pi^2}{m_\pi^4}W_\pi\left(\frac{p_F}{m_\pi}\right) - \frac{4}{3}\frac{f_\rho^2}{m_\rho^4}W_\rho\left(\frac{p_F}{m_\rho}\right)\right], \quad \text{(D23)}$$

and the nonlocality factors W ($W_{\pi,\rho}\to 1$ for $m_{\pi,\rho}\to\infty$) are $W_\pi\left(\frac{p_F}{m_\pi}\right) = 0.11$, $W_\rho\left(\frac{p_F}{m_\rho}\right) = 0.69$. The nonlocality effect is stronger for the pion due to its smaller mass ($m_\pi = 0.7$ fm^{-1} compared to $p_F \simeq 1.3$ fm^{-1}, while $m_\rho = 3.7$ fm^{-1}). The above value of W_π is quite close to $W_\pi = 0.16$ obtained for the nonlocality factor for the "bare" weak potential obtained in α-cluster calculations (Flambaum *et al* 1984a,b, Dmitriev *et al* 1983, Flambaum *et al* 1985).

Introducing $\tilde{U}^{\pi+\rho}$ (D22) into eq. (D13) instead of $\tilde{U}$ one obtains the following renormalized constants of the P-odd potential:

$$\tilde{g}_p = \tfrac{1}{D}\left[g_p\left(1-\tfrac{N}{A}k\right) + 2\tfrac{N}{A}g_n k\right]\ ,$$
$$\tilde{g}_n = \tfrac{1}{D}\left[g_n\left(1-\tfrac{Z}{A}k\right) + 2\tfrac{Z}{A}g_p k\right]\ , \quad \text{(D24)}$$

where $k = 2q\rho m$, and the determinant D is equal to $D = \left(1-\frac{N}{A}k\right)\left(1-\frac{Z}{A}k\right) - 4\frac{NZ}{A^2}k^2$. The expression for q in eq. (D23) shows that the contribution of the ρ-meson exchange partially compensates the π-meson contribution, whereas the latter strongly pushes the solution towards the pole ($D = 0$). The condition $D = 0$ determines a curve (function of N/A) corresponding to the border of stability of

a nucleus against the P-odd perturbation. For real nuclei ($N/A \simeq 0.5$–0.6) the position of the pole corresponds to the critical value of $k = k_c \simeq 0.67$. The π-meson alone gives $k = k_\pi \simeq 1$ and produces an instability in the "shell-model" nucleus. The ρ-meson exchange reduces this value to $k = 0.4$ (strong ρ-meson coupling), which corresponds to enhancement factors $\tilde{g}_p/g_p = 1.6$, $\tilde{g}_n/g_p = 0.7$ (for $g_p = 4$ and $g_n \simeq 0$). Thus, g_n becomes comparable to g_p, even for a very small initial value of g_n. The weak ρ-meson coupling produces $k = 0.7 \simeq k_c$ ("infinite" enhancement). Of course, the accuracy of this calculation is not sufficient to give a definite answer in this situation, since only the linear response has been considered, and fine effects like smoothing of the pion in nuclear matter (Migdal 1967, Fayans *et al* 1979) have been neglected, to say nothing of the uncertainty in the π and ρ coupling constants. Nevertheless, the above calculation indicates that that there is a possibility of strongly enhanced ($D \simeq 0$) P-odd effects.

Interpretation of this fact which results mostly from the strong π-meson exchange contribution, is not straightforward. It is obviously related to the problem of stability of the nucleus against the tensor π-exchange interaction. This question has been widely discussed in the literature (see, e.g., Brown 1971, Speth *et al* 1977, Khodel and Saperstein 1982, Negele 1982, Osterfeld 1992, and references therein), in particular, in relation to the problem of π condensation in nuclei (see, e.g., Migdal 1967, Fayans *et al* 1979). The large enhancement factor is also naturally associated with the low-lying 0^- excitation (a node in D at finite frequency of the PNC field). The influence of the 0^- resonance on the PNC-effects was discussed by Kadmensky *et al* (1983), Auerbach and Bowman (1992) and Flambaum 1993. On the other hand, there is a recent evidence from $\pi-$nucleon scattering and deep inelastic scattering from nuclei that the formfactors of pion-nucleon interaction are probably very "soft" (cut-off parameter ~ 500 MeV) (Thomas 1983, Bertsch *et al* 1993 and references therein, Pearce 1994). This greatly suppresses the pion field at small distances. There are two direct consequences. Firstly, the original "bare" P-odd potential constant g_p may be reduced since the corresponding interaction contains two π-meson vertices at the basic level (whereas, g_n increased because the cancellation of the π- and ρ-meson contributions will no longer take place). Secondly, the renormalization of the P-odd potential by the residual strong interaction would be weaker. This will probably bring the renormalized constants $\tilde{g}_{p,n}$ back to the values (D14). Of course, it also makes the nucleus stable.

E Central Limit Theorem for Distributions with Infinite Variances

Suppose x_i ($i = 1, \ldots, n$) are independent random variables with probability densities satisfying conditions (158), (159). Let X be the weighted sum of x_i,

$$X = \sum_{i=1}^{n} \theta_i x_i \ , \quad \text{where} \quad \sum_{i=1}^{n} \theta_i = 1 \ . \tag{E1}$$

When the number of variables in the sum n increases, the weights behave as $\theta_i = O(1/n)$. Our aim is to find the distribution of X as $n \to \infty$.

It is convenient to present $f(x)$ in the form

$$f(x) = \frac{1}{\pi} \frac{x_c}{x^2 + x_c^2} + h(x) \ , \tag{E2}$$

$$\int_{-\infty}^{\infty} h(x)dx = \int_{-\infty}^{\infty} xh(x)dx = 0 \,, \tag{E3}$$

$$\sigma_2 \equiv \int_{-\infty}^{\infty} x^2 h(x)dx \,, \tag{E4}$$

where (E3) follows from (E2) and (159), since the first term in the right hand side of (E2) is normalized to unity. It is assumed that the integral (E4) for σ_2 converges. This condition is certainly fulfilled in all practical cases, where $h(x) \propto 1/x^4$ (the next term in the $1/x^2$ expansion). However, it is likely that the theorem can be proved without this restriction [compare with a very weak Liapounov condition required for the standard CLT (Ash 1970)]. Note that in principle all x_i can have different distributions $f_i(x)$, and consequently, different $x_c \equiv x_{ci}$ and $\sigma_2 \equiv \sigma_{2i}$.

Proceeding in a way similar to the proof of the standard CLT (see, e.g., Ash 1970) it is convenient to deal with the Fourier transforms of the probability densities:

$$\tilde{f}(\omega) \equiv \int_{-\infty}^{\infty} e^{-i\omega x} f(x)dx = e^{-x_c|\omega|} + \int_{-\infty}^{\infty} e^{-i\omega x} h(x)dx \,, \tag{E5}$$

$$\tilde{F}_n(\omega) = \int_{-\infty}^{\infty} e^{-i\omega X} \prod_{i=1}^{n} [f_i(x_i)dx_i] = \prod_{i=1}^{n} \tilde{f}_i(\theta_i\omega) \,. \tag{E6}$$

The Fourier transforms $\tilde{f}_i$ in (E6) are functions of $\theta_i\omega = O(1/n)\omega$. Being interested in the large-n limit we can expand the second term in the right hand side of eq. (E5) [with ω replaced by $\theta\omega$] in powers of $\theta\omega$:

$$\begin{aligned}\tilde{f}_i(\theta_i\omega) &= \exp(-x_{ci}\theta_i|\omega|) + \int_{-\infty}^{\infty} h_i(x)dx - i\theta_i\omega \int_{-\infty}^{\infty} xh_i(x)dx - \frac{1}{2}\theta_i^2\omega^2 \int_{-\infty}^{\infty} x^2 h_i(x)dx + O(\theta^3) \\ &= \exp\Big(-x_{ci}\theta_i|\omega| - \frac{1}{2}\theta_i^2\sigma_{2i}\omega^2\Big) + O(\theta^3) \,. \end{aligned} \tag{E7}$$

Let us introduce the weighted mean values of the distributions' parameters x_{ci} and σ_{2i} of the x_i random variables:

$$X_c = \sum_{i=1}^{n} \theta_i x_{ci} \,, \qquad \Sigma_2 = n\sum_{i=1}^{n} \theta_i^2 \sigma_{2i} \,, \tag{E8}$$

where the factor n in the definition of Σ_2 provides $\Sigma_2 = O(1)$ as $n \to \infty$. If all x_i are identically distributed, then $X_c = x_c$ and $\Sigma_2 \sim \sigma_2$. Using eqs. (E6), (E7), and (E8) one obtains

$$\begin{aligned}\tilde{F}_n(\omega) &= \exp\left(-X_c|\omega| + \frac{\Sigma_2\omega^2}{2n}\right) + O(1/n^2) = \left(1 - \frac{\Sigma_2\omega^2}{2n}\right) e^{-X_c|\omega|} + O(1/n^2) \\ &= \left(1 - \frac{\Sigma_2}{2n}\frac{\partial^2}{\partial X_c^2}\right) e^{-X_c|\omega|} + O(1/n^2) \,. \end{aligned} \tag{E9}$$

$F_n(X)$ is obtained as the inverse Fourier transform of (E9):

$$F_n(X) = \frac{1}{\pi}\,\frac{X_c}{X^2 + X_c^2} - \frac{\Sigma_2}{2n}\frac{\partial^2}{\partial X_c^2}\left(\frac{1}{\pi}\frac{X_c}{X^2 + X_c^2}\right) + O(1/n^2) \,. \tag{E10}$$

As $n \to \infty$ only the first term in the right hand side of eq. (E10) survives

$$F_n(X)|_{n\to\infty} = \frac{1}{\pi}\,\frac{X_c}{X^2 + X_c^2} \,. \tag{E11}$$

This is the form of the CLT for distributions with $1/x^2$ asymptotic behaviour. Note that if all $f_i(x_i)$ are Cauchy distributions [eq. (149)], then $h(x) = 0$, $\Sigma_2 = \sigma_2 = 0$, and $F_n(X)$ is also a Cauchy distribution for any (finite) n. If all x_i are distributed identically and $\theta_i = 1/n$ the theorem proved is a particular case of the Levy-Khintchine theorem (see, e.g., Gnedenko and Kolmogorov, 1954), which specifies the limit distribution for a sum of independent random variables with $f(x) \propto 1/|x|^\mu$ $(x \to \infty)$, $1 < \mu < 3$.

References

Abov, Yu. G. and P. A. Krupchitskii (1976) *Usp. Fiz. Nauk.*, **118**, 141 [*Sov. Phys. Usp.*, **19**, 75].

Abov, Yu. G., O. N. Ermakov, I. L. Karpikhin, P. A. Krupchitsky, G. A. Lobov, V. L. Perepelitsa, V. I. Petrushin and A. N. Starodumov (1989) *Phys. Lett. B*, **217**, 225.

Adelberger, E. G. and W. C. Haxton (1985) *Ann. Rev. Nucl. Part. Sci.*, bf 35, 501.

Alfimenkov, V. P., S. B. Borzakov, Vo Van Thuan, Yu. D. Mareev, L. B. Pikelner, A. S. Khrykin and E. I. Sharapov (1981) *Pis'ma Zh. Eksp. Teor. Fiz.*, **34**, 308 [*JETP Lett.*, **34**, 295].

Alfimenkov, V. P., S. B. Borzakov, Vo Van Thuan, Yu. D. Mareev, L. B. Pikelner, A. S. Khrykin and E. I. Sharapov (1983), *Nucl. Phys. A*, **398**, 93.

Alfimenkov, V.P. (1984) *Usp. Fiz. Nauk*, **144**, 361 [*Sov. Phys. Usp.*, **27**, 797].

Andreev, V. N., M. M. Danilov, O. N. Ermakov, V. G. Nedopekin and V. I. Rogov (1978) *Pis'ma Zh. Eksp. Teor. Fiz*, **28**, 53 [*JETP Lett.*, **28**, 50].

Ash, R. B. (1970) *Basic Probability Theory.* John Wiley & Sons Inc., New York.

Auerbach, N (1992) *Phys. Rev. C*, **45**, R514.

Auerbach, N. and J. D. Bowman (1992) *Phys. Rev. C*, **46**, 2582.

Auerbach, N. and B. A. Brown (1994) *Phys. Lett. B*, **340**, 6.

Auerbach, N. (1994) *Nucl. Phys. A*, **557**, 443.

Auerbach, N., J. D. Bowman and V. Spevak (1994) Preprint NUCL-TH-9408027, Los Alamos Preprint Library.

Bengtsson, R., I. Ragnarsson, S. Aberg, A. Gyurkovich, A. Sobiczevski and K. Pomorski (1987) *Nucl. Phys. A*, **473**, 77.

Benkoula, H., T. C. Cavignac, T. L. Charvet, D. H. Koang and B. Vignon (1977) *Phys. Lett. B*, **71**, 287.

Bertsch, G. F., L. Frankfurt and M. Strikman (1993) *Science*, **259**, 773.

Blin-Stoyle, R. J. (1960) *Phys. Rev.*, **120**, 181.

Blin-Stoyle, R. J. (1973) *Fundamental Interaction and The Nucleus.* North Holland, Amsterdam.

Bohr, A. and B. Mottelson (1969) *Nuclear Structure*, Vol. 1. Benjamin, New York.

Bohr, A. and B. Mottelson (1974) *Nuclear Structure*, Vol. 2. Benjamin, New York.

Bouchad, J. P. and A. Georges (1990) *Phys. Rep.*, **195**, 127.

Bouchiat, C. and C. A. Piketty (1991) *Z. Phys. C*, **49**, 91.

Bowman, J.D., C. D. Bowman, J. E. Bush, P. P. J. Delheij, C. M. Frankle, C. R. Gould, D. G. Haase, J. Knudson, G. E. Mitchell, S. Penttila, H. Postma, N. R. Robertson, S. J. Seestrom, J. J. Szymanski, V. W. Yuan and X. Zhu (1990) *Phys. Rev. Lett*, **65**, 1192.

Bowman, J. D., G. T. Garvey, C. R. Gould, A. C. Hayes and M. B. Johnson (1992) *Phys. Rev. Lett.*, **68**, 780.

Brody, T. A., J. Flores, J. B. French, P. A. Mello, A. Pandey and S. S. M. Wong (1981) *Rev. Mod. Phys.*, **53**, 385.

Brown, G. E. (1971) *Rev. Mod. Phys.*, **43**, 1.

Brown, G. E., S.-O. Backman, E. Oset and W. Weise (1976) *Nucl. Phys. A*, **286**, 191.

Barkov, L. M., M. S. Zolotarev and D. A. Melik-Pashaev (1988) *Pis'ma Zh. Eksp. Teor. Fiz.*, **48**, 134 [*JETP Lett.*, **48**].

Bunakov, V. E. and V. P. Gudkov (1981) *Z. Phys. A*, **303**, 285.

Bunakov, V. E. and V. P. Gudkov (1983) *Nucl. Phys. A*, **401**, 93.

Bunakov, V. E., V. P. Gudkov, S. G. Kadmensky, L. A. Lomachenkov and V. I. Furman (1984) *et al Yad. Fiz.*, **40**, 188 [*Sov. J. Nucl. Phys.*, **40**, 119].

Bunakov, V. E., E. D. Davis and H. A. Weidenmüller (1990) *Phys. Rev. C*, **42**, 1718.

Camarda, H. S. and P. D. Georgopulos (1983) *Phys. Rev. Lett.*, **50**, 492.

Casati, G., L. Molinari and F. Izrailev (1990) *Phys. Rev. Lett.*, **64**, 1851.

Cho, D., K. Sangster and E. A. Hinds (1991) *Phys. Rev. A*, **44**, 1783.

Ćwiok, S., W. Nazarevicz, J. X. Saladin, W. Plociennik and A. Johnson (1994) *Phys. Lett. B*, **322**, 304.

Danilyan, G. V., V. V. Novitsky, V. S. Pavlov, S. P. Borovlev, B. D. Vodennikov and V. P. Dronyaev (1976) *Pis'ma Zh. Eksp. Teor. Fiz*, **24**, 380 [*JETP Lett.*, **24**, 344].

Danilyan, G. V., B. D. Vodennikov, V. P. Dronyaev, V. V. Novitsky, V. S. Pavlov and S. P. Borovlev (1977) *Pis'ma Zh. Eksp. Teor. Fiz*, **26**, 197 [*JETP Lett.*, **26**, 186].

Desplanques, B., J. F. Donoghue and B. R. Holstein (1980) *Ann. Phys. (N.Y.)*, **124**, 449.

Dmitriev, V. F., V. V. Flambaum, O. P. Sushkov and V. B. Telitsin (1983) *Phys. Lett. B*, **125**, 1.

Dubovik, V. M. and S. V. Zenkin (1986) *Ann. Phys.*, **172**, 100.

Ericson, T. E. O. (1966) *Phys. Lett.*, **23**, 97.

Ericson, T. and T. Mayer-Kuckuk (1966) *Annu. Rev. Nucl. Sci.*, **16**, 183.

Fayans, S. A., E. E. Saperstein and S. V. Tolokonnikov (1979) *Nucl. Phys. A*, **326**, 463.

Feshbach, H. (1958) *Ann. Phys.*, **5**, 357.

Feshbach, H. (1962) *Ann. Phys.*, **19**, 287.

Feynman, R. P. and M. Gell-Mann (1958) *Phys. Rev.*, **109**, 193.

Flambaum, V. V. and I. B. Khriplovich (1980) *Zh. Eksp. Teor. Fiz.*, **79**, 1656 [*Sov. Phys. JETP*, **52**, 835].

Flambaum, V. V. and O. P. Sushkov (1980) *Phys. Lett. B*, **94**, 277.

Flambaum, V. V. and I. B. Khriplovich (1985) *Phys. Lett. A*, **110**, 121.

Flambaum, V. V. and O. P. Sushkov (1984) *Nucl. Phys. A*, **412**, 13.

Flambaum, V. V., I. B. Khriplovich and O. P. Sushkov (1984a) Preprint 84-89. INP, Novosibirsk.

Flambaum, V. V., I. B. Khriplovich and O. P. Sushkov (1984b) *Phys. Lett. B*, **146**, 367.

Flambaum, V.V. (1985) *Yad. Fiz.*, **42**, 578 [*Sov. J. Nucl. Phys.*, **42** 366].

Flambaum, V.V. and O. P. Sushkov (1985) *Nucl. Phys. A*, **435**, 352.

Flambaum, V. V., V. B. Telitsin and O. P. Sushkov (1985) *Nucl. Phys. A*, **444**, 611.

Flambaum, V. V., I. B. Khriplovich and O. P. Sushkov (1986) *Nucl. Phys. A*, **449**, 750.

Flambaum, V. V. (1992) *Phys. Rev. C*, **45**, 437.

Flambaum, V. V. (1993) Talk at 85th Nobel Symposium (Saltjobaden, June 1992). *Physica Scripta*, **T46**, 198.

Flambaum, V.V. and O. K. Vorov (1993) *Phys. Rev. Lett.*, **70**, 4051.

Flambaum, V. V. (1994a) In: *Time Reversal and Parity Violation in Neutron Reactions* (C. R. Gould, J. D. Bowman and Yu. P. Popov, ed.), p. 39. World Scientific, Singapore.

Flambaum, V. V. (1994b) *Phys. Lett. B*, **320**, 211.

Flambaum, V. V. (1995) Submitted to Phys. Rev. E.

Flambaum, V.V. and O. K. Vorov (1994) *Phys. Rev. C*, **49**, 1827.

Flambaum, V. V., A. A. Gribakina, G. F. Gribakin and M. G. Kozlov (1994) *Phys. Rev. A*, **50**, 267.

Flambaum, V. V. and G. F. Gribakin (1994) *Phys. Rev. C*, **50**, No.6.

Flambaum, V. V. and V. G. Zelevinsky (1994) Preprint MSUCL-963; submitted to Phys. Lett. B.

Flambaum, V. V. and O. K. Vorov (1995a) *Phys. Rev. C*, **51**, No.2.

Flambaum, V. V. and O. K. Vorov (1995b) *Phys. Rev. C*, **51**, in press.

Forte, M. (1978) In: Higher Energy Polarised Beams (Ann Arbor, 1977), Proceedings of the Workshop on Higher Energy Polarized Proton Beams (A. D. Kirsch and A. Salthouse, ed.), AIP Conf. Proc. No. 42, Chap. 2, p. 86. AIP, New York.

Forte, M., B. R. Hechel, N. F. Ramsey, K. Green, G. L. Greene, T. Byrne and T. M. Pendlebury (1980) *Phys. Rev. Lett.*, **45**, 2088.

Frankle, C. M., J. D. Bowman, J.E. Bush, P. P. J. Delheij, C. R. Gould, D. G. Haase, J. N. Knudson, G. E. Mitchell, S. Penttilä, H. Postma, N. R. Robertson, S. J. Seestrom, J. J. Szymanski, S. H. Yoo, V. W. Yuan and X. Zhu (1991) *Phys. Rev. Lett*, **67**, 564.

French, J. B., V. K. B. Kota, A. Pandy and S. Tomsovic, (1988) Ann. Phys. (N.Y.), **181**, 235.

Gnedenko, B. V. and A. N. Kolmogorov (1954) *Limit Distributions for Sums of Independent Random Variables.* Addison-Wesley, Cambridge, MA.

Gribakina, A. A., V. V. Flambaum and G. F. Gribakin (1995) Submitted to Phys. Lett. A.

Gudkov, V. P. (1993) *Phys. Rev. C*, **47**, 372.

Haas, R., L. B. Leipuner and R. K. Adair (1959) *Phys. Rev.*, **116**, 1221.

Haxton, W. C., E. M. Hanley and M. I. Musolf (1989) *Phys. Rev. Lett.*, **63**, 949.

Horoi, M., V. G. Zelevinsky and B. A. Brown (1994) Submitted to Phys. Rev. Lett.

Hussein, M. S., A. K. Kerman and C-Y Lin (1994) Preprint CTP#2296, Massachussets Institute of Technology.

Johnson, M. B., J. D. Bowman and S. H. Yoo (1991) *Phys. Rev. Lett.*, **67**, 310.

Johnson, M. B. and J. D. Bowman (1995) *Phys. Rev. C*, **51**, 999.

Jolos, R.V. and P. von Brentano (1994) *Phys. Rev. C*, **49**, R2301.

Kabir, P. K. (1982) *Phys. Rev. D*, **25**, 2013.

Kadmensky, S. G., V. P. Markushev and V. I. Furman (1983) *Yad. Fiz.*, **37**, 581 [*Sov. J. Nucl. Phys.*, **37**, 345].

Karl, G. and D. Tadic (1977) *Phys. Rev. C*, **16**, 1726.

Karmanov, V. A. and G. A. Lobov (1969) *Pis'ma Zh. Eksp. Teor. Fiz.*, **10**, 332 [*JETP Lett.*, **10**, 212].

Khodel, V.A. and E. E. Saperstein (1982) *Phys. Rep.*, **92**, 183.

Khriplovich, I. B. (1991) *Parity Nonconservation in Atomic Phenomena.* Gordon and Breach, New York.

Koonin, S. E., C. W. Johnson and P.Vogel (1992) *Phys. Rev. Lett.*, **69**, 1163.

Krewald, S., K. Nakayama and J. Speth (1988) *Phys. Rep.*, **161**, 103.

Labzovsky, L. N. (1978) *Zh. Eksp. Teor. Fiz.*, **75**, 856 [*Sov. Phys. JETP*, **48**, 434].

Lamoreax, S. K., J. P. Jacobs, B. R. Heckel, F. J. Raab and E. N. Fortson (1987) *Phys. Rev. Lett.*, **59**, 2275.

Landau, L. D. (1957) *Zh. Eksp. Teor. Fiz.*, **32**, 405 [*Sov. Phys. JETP*, **5**, 336].

Landau, L. D. (1958) *Zh. Eksp. Teor. Fiz.*, **35**, 97 [(1959) *Sov. Phys. JETP*, **8**, 70].

Leander, G. A., R. K. Sheline, P. Möller, P. Olanders, I. Ragnarsson and A. J. Sierk (1982) *Nucl. Phys. A*, **388**, 452.

Lewenkopf, C. H. and H. A. Weidenmüller (1992) *Phys. Rev. C*, **46**, 2601.

Lobov, G. A. (1970) *Izv. Akad. Nauk SSSR (Ser. Fiz.)*, **34**, 1141.

Lobov, G. A. (1980) *Izv. Akad. Nauk SSSR (Ser. Fiz.)*, **44**, 2364.

Mahaux, C. and H. A. Weidenmüller (1966) *Phys. Lett.*, **23**, 100.

Martin, W. S., R. Zalubas and L. Hagan (1978) *Atomic Energy Levels - The Rare-Earth Elements*, Natl. Bur. Stand. Ref. Data Ser. Natl. Bur. Stand. (U.S.), NBS-60, Washington.

Masuda, Y., T. Adachi, A. Masaike and K. Morimoto (1989) *Nucl. Phys.*, **A504**, 269.

McKellar, B. H. J. (1968) *Phys. Rev. Lett*, **21**, 1822.

Migdal, A. B., (1967) *Theory of Finite Fermi Systems and Applications to Atomic Nuclei.* John Wiley & Sons, New York.

Moldauer, P. A. (1968), *Phys. Rev.*, **165**, 1136.

Mughabhab, S. F., M. Divadeenam and N. E. Holden (1981) *Neutron Cross Sections*, Vol. 1,2. Academic Press, New York.

Nazarevicz, W. (1990) *Nucl. Phys. A*, **520**, 333.

Negele, J. W. (1982) *Rev. Mod. Phys.*, **54**, 913.

Noguera, S. and B. Desplanques (1986) *Nucl. Phys. A*, **457**, 189.

Okun, L. B. (1982) *Leptons and Quarks.* North Holland Publishing Co., Amsterdam.

Osterfeld, F., (1992) *Rev. Mod. Phys.*, **64**, 491.

Otsuka, T. (1986) *Phys. Lett. B*, **182**, 256.

Pashkevich, V. V. (1971) *Nucl. Phys. A*, **169**, 275.

Pearce, B. C. (1994) In: *The 15th Nuclear and Particle Physics Conference, Abstracts of Talks*, p. 53. Griffith University, Brisbane.

Petukhov, A.K., G. A. Petrov, S. I. Stepanov, D. V. Nikolaev, K. Zvedkina, V. I. Petrova and V. A. Tyukavin (1979) *Pis'ma Zh. Eksp. Teor. Fiz*, **30**, 470 [*JETP Lett.*, **30**, 439].

Pines, D. and P. Nozieres (1966) *The Theory of Quantum Liquids.* Benjamin, New York.

Shapiro, I. S. (1968) *Usp. Fiz. Nauk.*, **95**, 647 [(1969) *Sov. Phys. Usp.*, **11**, 582].

Shepelyansky (1994) *Phys. Rev. Lett.*, **73**, 2607.

Speth, J., E. Werner and W. Wild (1977) *Phys. Rep.*, **33**, 127.

Stodolsky, L. (1980) *Phys. Lett. A*, **96**, 127.

Stodolsky, L. (1982) *Nucl. Phys. B*, **197**, 213.

Sushkov, O. P. and V. V. Flambaum (1978) *Zh. Eksp. Teor. Fiz.*, **75**, 1208 [*Sov. Phys. JETP*, **48**, 608].

Sushkov, O. P. and V. V. Flambaum (1980a) *Pis'ma Zh. Eksp. Teor. Fiz.*, **32**, 377 [*JETP Lett.*, **32**, 353] (detailed version of this work in Preprint INP 80-148, Novosibirsk).

Sushkov, O. P. and V. V. Flambaum (1980b) *Yad. Fiz.*, **31**, 55 [*Sov. J. Nucl. Phys.*, **31**, 28].

Sushkov, O. P. and V. V. Flambaum (1981a) In: *16th LINP Winter School, Proceedings*, p. 200. LINP, Leningrad.

Sushkov, O. P. and V. V. Flambaum (1981b) *Yad. Fiz.*, **33**, 59 [*Sov. J. Nucl. Phys.*, **33**, 31].

Sushkov, O. P. and V. V. Flambaum (1981c) *Yad. Fiz.*, **33**, 629 [*Sov. J. Nucl. Phys.*, **33**, 329].

Sushkov, O. P. and V. V. Flambaum (1982) *Usp. Fiz. Nauk*, **136**, 3 [*Sov. Phys. Usp.*, **25**, 1].

Sushkov, O. P., V. V. Flambaum and I. B. Khriplovich (1984) *Zh. Eksp. Teor. Fiz.*, **87**, 1521 [*Sov. Phys. JETP*, **60**, 873].

Sushkov, O. P. (1994) Private communication.

Thomas, A. W (1983) *Phys. Lett. B*, **126**, 97.

Tests of Time Reversal Invariance in Neutron Physics (1987) (N. R. Robertson, C. R. Gould, and J. D. Bowman, eds.), World Scientific, Singapore.

Time Reversal Invariance and Parity Violation in Neutron Reactions (1994) (C. R. Gould, J. D. Bowman and Yu. V. Popov, eds.), World Scientific, Singapore.

Urin, M. H. and O. N. Vyazankin (1991) *Phys. Lett. B*, **269**, 13.

Vesna, V. A., V. A. Knyazkov, E. A. Kolomensky, V. M. Lobashev, A. N. Pirozhkov, L. A. Popeko, L. M. Smotritskii, S. M. Solovyev and N. A. Titov (1980) *Pis'ma Zh. Eksp. Teor. Fiz*, **31**, 704 [*JETP Lett.*, **31**, 663].

Vodennikov, B. D., G. V. Danilyan, V. P. Dronyaev, V. V. Novitsky, V. S. Pavlov and S. P. Borovlev (1978) *Pis'ma Zh. Eksp. Teor. Fiz*, **27**, 68 [*JETP Lett.*, **27**, 62].

Wigner, E. P. (1955) *Ann. Math.*, **62**, 548.

Warburton, E. K. and B. A. Brown (1992) *Phys. Rev. C*, **46**, 923.

Zaretsky, D. F. and V. I. Sirotkin (1983) *Yad. Fiz.*, **37**, 607 [*Sov. J. Nucl. Phys.*, **37**, 361].

Zaretsky, D. F. and V. I. Sirotkin (1987) *Yad. Fiz.*, **45**, 1302 [*Sov. J. Nucl. Phys.*, **45**, 808].

Zeldovich, Ya. B. (1957) *Zh. Eksp. Teor. Fiz.*, **33**, 1531 [(1958) *Sov. Phys. JETP*, **6**, 1184].

Zelevinsky, V. G. (1993) private communication.

Zelevinsky, V. G. (1994) Talk at Program INT-94-2 "Applications of Chaos in Many-Body Quantum Physics", Seattle.